

Chapter One

1.0 Introduction

1.1 General Information

South Africa like many other countries, is witnessing a rapid growth in the construction industry, involving the use of natural resources for the development of infrastructures. This growth is jeopardized by the lack of natural resources that are available. Natural resources are depleting worldwide, while at the same time the generated wastes from the industry are increasing substantially (Al-Jabri, 2009).

Slag, the glassy materials left when metals are either hydrometallurgically or pyrometallurgically extracted from their ores, in the metallurgical industries have previously been considered a waste product (Gorai *et al.*, 2002). Waste from extractive industries are therefore to be properly managed, in order to ensure in particular the long term stability of disposal facilities, to prevent or minimise any water and soil pollution arising from acid or alkaline drainage and the leaching of heavy metals (European Commission, 2012). Current management options of slags are recycling and recovering of metal, production of value added products and the disposal in slag dumps, stockpiles or tailing dams.

Over the years, rigorous environmental impacts have been associated with copper tailings dam failure. According to Grimalt *et al.*, (1999) approximately 2 million m³ of mud containing heavy metals were spread over 4286 ha of land and surface water during the 1998 Aznalcollar tailings pond failure in Spain. Lungu (2008) also highlighted that, the year 2000 tailings spillage of Nchanga Copper Processing Plant in Zambia released high concentrations of heavy metals into the nearby surface water, thereby contaminating the local source of water supply. Similar contamination of the Katamanda River in Lubumbashi, Democratic Republic of Congo, was also observed by Mutombo *et al.*, (2011). According to the authors, metallic trace elements such as Cu, Co, Cd, Pb, and Zn are frequently dispersed into the Katamanda River due to an

adjacent heap of slag tailings produced by Electronic Foundry Panda copper plant (FEP) in Lubumbashi.

Industrial waste and by-products such as coal fly ash, pulverized fuel ash, blast furnace slag and silica fume have been successfully used in the construction industry as either binders or partial replacement of fine or coarse aggregates in concrete. Researchers across the world are developing waste management strategies for specific needs which are sustainable and environmentally friendly.

1.2 Justification

Although there are numerous studies that assess the suitability of copper slag as firstly, a replacement of Portland cement (as a binder) and secondly, aggregates in concrete; many of these studies have focussed on the strength properties with little emphasis on the durability. Nevertheless, only limited research has been carried out in sub-Saharan Africa concerning the incorporation of copper slag in concrete. This research was performed in order to generate specific experimental data on the potential use of copper slag as a cement replacement in concrete; and to assess its suitability as a concrete fine aggregate.

Utilisation of copper slag in concrete has the dual benefit of eliminating the costs of disposal and lowering the cost of the concrete production in construction; especially, in regions where a considerable amount is produced. This will lead to sustainable concrete design and a greener environment.

1.3 Aim and Objectives

The aim of the research report is to assess the performance and durability of copper slag as partial replacement of Portland cement (PC) in concrete. Based on the above, the specific objectives are:

1. Assessment of the physical characteristics of granulated copper slag as a comparison to conventional fine aggregates (sand) used in concrete production.
2. Investigation of the chemical oxides and mineralogical composition of copper slag, as well as, the total threshold leaching characteristics to check the limit of trace metals present in the slag.
3. Evaluation of the compressive strength development of pulverised copper slag as partial replacement of Portland cement using three different curing methods.
4. Determination of the flexural strength development of pulverised copper slag concrete cured in water.
5. Assessment of the long term durability performances of pulverised copper slag as partial replacement of cement in concrete.

1.4 Scope

The study builds on and contributes to the development of new, environmentally friendly binders in concrete. In this study, the effect of using copper slag in improving the strength and durability of concrete properties was thoroughly investigated.

Pulverised copper slag was added to Portland cement paste and concrete in varying proportions ranging from 0; 2.5; 5; 10 and 15% replacing Portland cement by weight. Prior to pulverizing the copper granules into powder, the granulated copper slag was assessed for its physical characteristics i.e. aggregate grading, water absorption and relative density, as a comparison to conventional fine aggregates (sand) used in concrete production.

1.5 Limitations

This research study is limited to only un-reinforced concrete specimens. Curing of the concrete samples was only considered up to 90 days due to limited time frame.

Assessment of the durability of the concrete specimen for carbonation depth was also not studied. Production of concrete with granulated copper slag as partial replacement of sand was excluded due to limited quantity of the slag and this is highly recommended for further studies.

1.6 Structure of Research Report

The research report is organized into five chapters. Chapter one describes the motivation for the development and use of copper slag in concrete technology. Chapter two reviews the literature on the history and reaction mechanisms of pozzolans and slags as cementitious material. The hydration mechanism of Portland cement, the use of copper slag in concrete technology and various durability tests performed on concrete were thoroughly reviewed in chapter two. Chapter three is a description of the materials and experimental methods, while the results are analysed and discussed in Chapter four. Chapter five presents the summary, conclusions and recommendations, followed by the list of references. Lastly, detailed experimental results are recorded in the appendix.

Chapter Two

2.0 Literature Review

2.1 Introduction

Many studies have been done by various researchers from all over the world on the use of copper slag in concrete structural material applications. The literature survey covers Portland cement hydration characteristics, the advantages of using pozzolans, fly ash and steel slag in conventional concrete. The chemical composition, mineralogical phases, leaching characteristics, physical characteristics and mechanical strength of copper slag concrete are thoroughly reviewed. Moreover, the literature review covers the utilisation of copper slag in concrete production both as a binder and replacement of aggregates (fine and coarse) in concrete technology.

The investigation will follow with a look at the effects of different curing methods on the compressive strength of concrete. It will further include assessment of the various concrete durability tests such as, oxygen permeability index, water sorptivity and chloride conductivity in accordance with the draft South African National Standards (SANS); and then sodium sulphate attack.

2.1.1 Cement

Cements are adhesive materials which have the ability of bonding particles of solid matter into a compact whole (Soroka, 1979). This broad definition encompasses a wide variety of adhesive materials. However, for engineering purposes it is restricted to calcareous cements that contain compounds of lime as their main principal constituent. The main raw materials used in producing Portland cement are the oxides: lime (CaO), produced by heating calcium carbonate; silica (SiO₂), found in natural rocks and minerals; alumina (Al₂O₃), found in clay minerals; and ferric oxide (Fe₂O₃), found in clays.

Cement as a binder is a vital element in concrete and the quality of concrete depends on the cement or binder, the aggregate, the mix design and the handling involved in making, placing and subsequent curing. The performance of cement used in concrete is influenced by its chemical composition. A typical chemical composition of South African Portland cement clinker is shown below in Table 2.1.

Table 2.1: Typical Composition of South African Portland Cement Clinker (Addis, 2001)

Chemical Oxides	CaO	SiO ₂	Al ₂ O ₃	Fe ₂ O ₃	MgO	Na ₂ O + 0.658 K ₂ O
% by mass in cement	63-68	19-24	4-7	1-4	0.5-3.5	0.2-0.8

2.1.2 Compounds Composition of Cement

There are four main compounds present in ordinary Portland cement clinker, namely: tricalcium silicate (C₃S), dicalcium silicate (C₂S), tricalcium aluminate (C₃A) and tetra calcium aluminoferrite (C₄AF). These compounds are formed from the following oxide reactions under equilibrium conditions (Bogue, 1947).

- Fe₂O₃ reacts with Al₂O₃ and CaO to produce $4CaO.Al_2O_3.Fe_2O_3$ (C₄AF)
- The remaining Al₂O₃ reacts with CaO to produce $3CaO.Al_2O_3$ (C₃A)
- The remaining CaO reacts with SiO₂ to first form $2CaO.SiO_2$ (C₂S) and
- Excess CaO reacts further with C₂S to produce $3CaO.SiO_2$ (C₃S).

Following the aforementioned reactions, any CaO uncombined at this point remains as CaO (free lime) in the cement. In addition, the cement clinker also consists of minor compounds such as MgO, TiO₂, K₂O and Na₂O; which are usually present in minor quantities. K₂O and Na₂O referred to as alkali metals are also of interest because they are found to react with some aggregates and cause deterioration of concrete (Neville, 1981). The quantity of these alkali metals present in cement is therefore important for the durability performances of concrete in structural applications.

C₃S is more reactive than C₂S under hydraulic condition and therefore dominates the first four weeks of hydration; after which C₂S becomes a part of the hydration process (Javed *et al.*, 1985). C₃S and C₂S are the chemical compounds which mostly determine the physical engineering properties of the concrete. However, C₃A has important influence on the long term durability performance of the concrete structure since it is particularly vulnerable to sulphate attack. Typical compound composition of South African Portland cements is shown in Table 2.2.

Table 2.2: Typical Compound Composition of South African Portland Cements (Addis, 2001)

Hydration Compounds	Common Names	Formula	Acronym	Percentage by weight
Tricalcium silicate	Alite	$3CaO SiO_2$	C ₃ S	45-60
Dicalcium silicate	Belite	$2CaO SiO_2$	C ₂ S	10-35
Tricalcium aluminate	Aluminate	$3CaO Al_2O_3$	C ₃ A	4-10
Tetracalcium aluminoferrite	Ferrite	$4CaO Al_2O_3 FeO_3$	C ₄ AF	5-10
Magnesium oxide	Periclase	MgO	M	0.3-4.0
Gypsum	-	$CaSO_4 2H_2O$	-	3.5-7
Calcium oxide	Lime	CaO	C	0.3-2.5

2.1.3 Hydration of Cement

Hydration is the reaction of cement compounds, tricalcium silicate (C₃S) and dicalcium silicate (C₂S) with water (H₂O) to give calcium hydroxide Ca(OH)₂ and calcium silicate hydrate (C-S-H) as products (Soroka, 1979). Hydration of calcium aluminate in the presence of gypsum produces ettringite and monosulphate after further hydration. Gypsum is added to cement to extend the setting time.

The hydration processes of the different compounds are shown in equations 2.1 to 2.4. The reactions are generally exothermic in nature, generating heat into their immediate surroundings. The setting and hardening of cement paste is due to the formation of C-S-H gel during hydration (Soroka, 1979).

cement before it sets. The ettringite is converted to monosulphate and hydration continues until stable hydrate is formed (Soroka, 1979).

Concrete exposed to sulphate solution after the hardening process causes the formation of delayed ettringite. Delayed ettringite formation (DEF) leads to cracking and expansion of concrete and facilitates the deterioration mechanism of the concrete in structural applications. The fourth compound, C_4AF reacts with gypsum to form iron-substituted ettringite (Sha *et al.*, 1999).

2.1.4 Heat of Hydration of Portland Cement

The hydration process of cement is exothermic, i.e. heat is released as the reaction progresses. This property is used in laboratories to monitor the hydration process by using a special calorimeter. The calorimeter records the rate of heat conduction needed to keep the temperature constant. The results often presented as the calorimetric curve were first explained by Forrester (1970).

A typical calorimetric curve for the hydration of Portland cement is shown in Figure 2.1. As seen on the graph, the hydration process is divided into five stages according to their different characteristics of heat release.

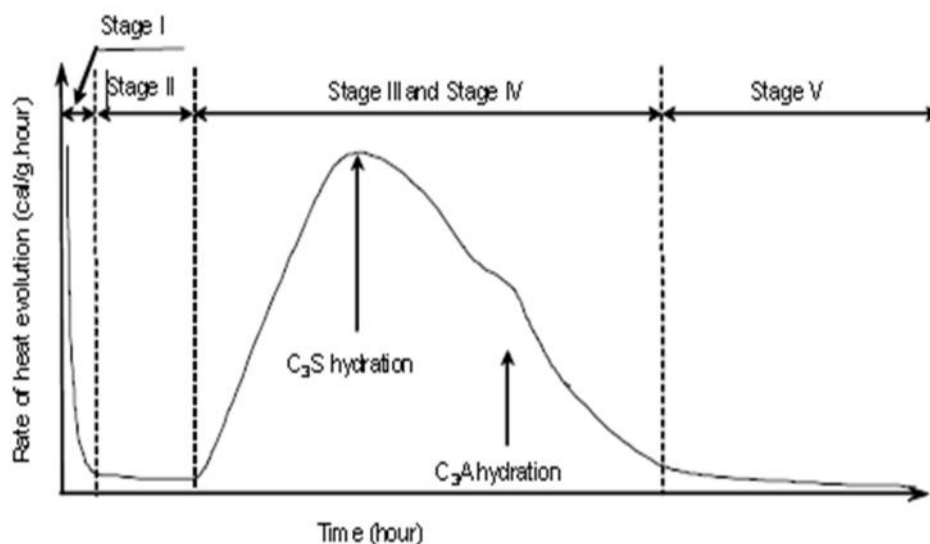


Figure 2.1: The Heat evolution curve of Portland cement (Forrester, 1970)

Almost immediately on adding water, some of the clinker sulphates and gypsum dissolve producing an alkaline, sulphate-rich solution. Immediately after mixing, the C_3A phase (the most reactive of the four main clinker minerals) reacts with the water to form an aluminate-rich gel (Stage I on the heat evolution curve above). The gel reacts with sulphate in solution to form small, rod-like crystals of ettringite.

C_3A reaction with water is strongly exothermic, but does not last for long, typically only a few minutes. If the cement is rich in Potassium (K), syngenite (K_2CS_2H) can form in this stage, causing false set (Chen, 2006).

The hydration process of Portland cement is marked by an obvious dormant period (Stage II in Figure 2.1). During the dormant period, which lasts typically for a few hours, the hydration progresses at a very low rate and no significant strength is gained. The amount of heat released by the cement hydration is also greatly reduced (Forrester, 1970).

The first half part of the dormant period corresponds to when the concrete can be placed. This dormant period is important because during this period the concrete can be transported and shaped on the construction site. As the dormant period progresses the paste becomes too stiff to be worked with (Forrester, 1970).

At the end of the dormant period, the alite and belite in the cement start to react, with the formation of calcium silicate hydrate ($C-S-H$) and calcium hydroxide ($C-H$). These correspond to the main period of hydration (Stage III), during which time concrete strengths increase. The individual grains react from the surface inwards, and the anhydrous particles become smaller. C_3A hydration also continues, as fresh crystals become accessible to water (Forrester, 1970).

After the acceleration period follows the deceleration and steady state period (Stage IV and V), during which the hydration rate is relatively slow. The strength of the

concrete keeps increasing and the heat released is much reduced compared to that of the acceleration period (Forrester, 1970).

2.2 Pozzolans and Binding Materials

Taylor (1991) explains that, the word pozzolan is derived from Pozzuoli, where the Romans found a volcanic ash from Mount Vesuvius that would form cement, with hydraulic properties when mixed with lime putty. Kumar *et al.* (1993) defined pozzolan as any siliceous or alumina-siliceous material that, in finely divided form and in the presence of moisture chemically reacts with the calcium hydroxide released by the hydration of Portland cement to form calcium silicate hydrate and other cementitious compounds.

Pozzolan is also defined by Baronia and Binda (1994) as materials which, though not cementitious in themselves, contain constituents which will combine with lime at ordinary temperature. In the presence of water, the pozzolan will then form stable insoluble compounds possessing cementitious properties.

Pozzolans are generally categorized as supplementary cementitious materials or mineral admixtures. According to Komar (1973) and Spence (1980), binding materials have been identified and utilised as early as 3000 B.C. Stronger binders have been obtained artificially by burning substances, with gypsum and lime being among the first in this group. According to Lea (1970), more than 2000 years ago the Greeks and Romans built structures that are still surviving to date. These structures took the advantage of the pozzolan-lime reaction.

2.2.1 Types of Pozzolans

Pozzolans are classified as either natural or artificial. Day and Shi (1994) classify natural pozzolans as those present on the earth's surface such as diatomaceous earth, volcanic ash, opaline shale, trass, pumicite and tuffs. Natural pozzolans require further processing such as calcining (burning), grinding and drying.

ASTM C618-99 classifies artificial pozzolans as the by-products of industrial and agricultural processing found in large quantities, such as rice husk ash, burnt clay, burnt gaize, shales, moler, bauxite, etc. They are burnt or calcined at higher temperature to bring them to their active form. Artificial pozzolans are also produced when pulverized coal is burnt in electric power plants called fly ash. The glassy (amorphous) spherical particulates are the reactive pozzolanic portion.

2.2.2 Pulverised Fly Ash (PFA)

Fly ash, also known as pulverised fuel ash, is produced from burning pulverized coal in electric power generating plants. During combustion, mineral impurities in the coal (clay, feldspar, quartz, and shale) fuse in suspension and float out of the combustion chamber along with exhaust gases (Siddique and Khan, 2011). As the fused material rises, it cools and solidifies into spherical glassy particles called fly ash. It is a fine-grained, powdery material that is collected from the exhaust gases by electrostatic precipitators or bag filters (Siddique and Khan, 2011).

Depending upon the collection system, varying from mechanical to electrical precipitators or bag houses and fabric filters, approximately 85–99% of the ash from the flue gases is retrieved in the form of fly ash. Fly ash accounts for 75–85% of the total coal ash, and the remainder is collected as bottom ash or boiler slag (Siddique and Khan, 2011).

The spherical shape of fly ash often helps to improve the workability of the fresh concrete, while its small particle size also plays as filler of voids in the concrete, hence to produce dense and durable concrete (Hardjito *et al.*, 2005).

2.2.3 Classification of Fly Ash

ASTM C618-99 categorizes natural pozzolans and fly ashes into the following three categories: Class F, Class C and Class N.

Class F fly ashes are low in CaO and are normally produced from burning. Anthracite or bituminous coal falls in this category. This class of fly ash exhibits pozzolanic property but rarely, if any, self-hardening property. They are predominantly 70% non-crystalline silica which is the determining factor for pozzolanic activity. Their crystalline minerals are generally composed of quartz, hematite, mullite and magnetite (Roy *et al.*, 1984).

Class C fly ashes are generally produced from lignite or sub-bituminous coal. This class of fly ash has both pozzolanic and varying degree of self-cementitious properties. Most Class C fly ashes contain more than 15% CaO. Other Class C fly ashes may also contain as little as 10% CaO. Class C fly ashes contain predominantly calcium aluminosilica glass which is highly reactive. A crystalline phase in Class C ash includes quartz, lime, mullite, gehlenite, anhydrite and cement materials such as C₃A, C₂S and C₄A₃S (Siddique and Khan, 2011).

Class N raw or calcined natural pozzolans such as some diatomaceous earths, opaline chert and shale, stuffs, volcanic ashes and pumice are included in this category. Moreover, calcined kaolin clay and laterite shale also fall in this category of pozzolans (Siddique and Khan, 2011).

2.2.4 Mineralogy Characteristics of Fly Ash

X-ray diffraction study of the crystalline and glassy phases of a fly ash is known as mineralogical analysis. Mineralogical characterization determines the crystalline phases that contain the major constituents of fly ash. Generally, fly ashes have 15–45% crystalline matter (Siddique and Khan, 2011).

The high-calcium ashes (Class C) contain larger amounts of crystalline matter ranging between 25 and 45%. Although high-calcium Class C ashes may have less glassy or amorphous material, they do contain certain crystalline phases such as anhydrite (CaSO₄), tricalcium aluminate (3CaO·Al₂O₃), calcium sulpho-aluminate

(CaS.Al₂O₃) and very small amount of free lime (CaO) that participate in producing cementitious compounds (Siddique and khan, 2011).

Anhydrite (CaSO₄) is formed from the reaction of CaO, SO₂ and O₂ in the furnace or flue and increases with subsequent increase in SO₃ and CaO contents. Anhydrite plays a significant role in fly ash hydration behaviour by reacting with tricalcium aluminate and other soluble aluminates to produce ettringite and calcium sulphoaluminate hydrate (Siddique and khan, 2011).

Table 2.3: Requirements for Fly Ash and Natural Pozzolans for Use as Mineral Admixtures in Portland Cement Concrete (ASTM C618-99)

Requirements	Fly Ash Classification		
	N	F	C
Chemical requirements SiO ₂ + Al ₂ O ₃ + Fe ₂ O ₃ min (%)	70	70	70
SO ₃ , max (%)	4.0	5.0	5.0
Loss of ignition, max (%)	10	6.0	6.0
Physical requirement amount retained when wet sieved on 45µm sieve, max (%)	34	34	34
Pozzolanic activity index, with Portland cement at 28 days, min (%) of control	75	75	75
Pozzolanic activity index with lime at 7 days, min (MPa)	5.5	5.5	-
Water requirement, max (%) of control	115	105	105
Autoclave expansion or contraction, max (%)	0.8	0.8	0.8
Specific gravity, max variation from average	5	5	5
Percentage retained on 45-µm sieve, max variation, percentage points from average	5	5	5

Tricalcium aluminate (3CaOAl₂O₃) is one of the most important crystalline phases to identify and quantify fly ash because it contributes to ettringite formation, also in self-hardening reactions and disruptive sulphate reactions in hardened concrete (Siddique and khan, 2011).

Periclase is the crystalline form of magnesium oxide (MgO). The presence of MgO in fly ash affects the soundness of the resulting concrete through its expansive hydration to brucite, Mg (OH)₂ (Siddique and khan, 2011).

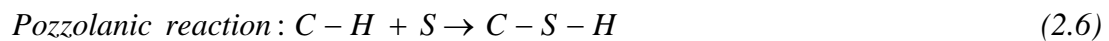
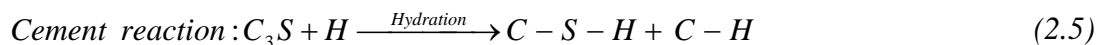
Crystalline iron oxide, ferrite spinel and/or hematite are also generally found in all fly ashes. In most of fly ashes, about 0.33–0.50% of iron is present as crystalline oxide. The reactivity of fly ash however, is dependent on the glassy phases of Fe₂O₃ (Siddique and khan, 2011).

2.2.5 Reaction Mechanism of Fly Ash

Setting or hardening of Portland cement concretes occurs due to the hydration reaction between water and cementitious compounds present in the cement; which give rise to several types of hydrates e.g. calcium silicate (*C-S-H*), calcium aluminate hydrate (*C-A-H*) and calcium hydroxide (*C-H*) (Siddique and khan, 2011).

The adhesive and cohesive properties of the gel bind the aggregate particles. When fly ash is incorporated into concrete, the calcium hydroxide (*C-H*), a by-product liberated during hydration of ordinary Portland cement reacts slowly with the amorphous alumino-silicates, the pozzolanic compounds present in the fly ash. The products of these reactions, termed as pozzolanic reaction products are time dependent, but are basically of the same type and characteristics as the products of the cement hydration (Siddique and khan, 2011).

Thus, additional cementitious products become available, conveying additional strength to concrete. The following equations illustrate the pozzolanic reaction of fly ash with lime to produce additional calcium silicate hydrate (*C-S-H*) binder (Siddique and khan, 2011).



2.2.6 Uses of Fly Ash in Cement Concrete

Utilization of fly ash in cement or concrete can be categorized based on the volume of its usage (Siddique and khan, 2011).

- **High Volume Uses:**

High volume utilization of fly ash includes, structural fills used in construction of embankments, dams, dikes and levees and also as sub-base and base courses in roadway construction (Siddique and khan, 2011).

- **Medium Volume Uses:**

This includes the use of fly ash as raw material in cement production, admixture in blended cements, as partial replacement of cement or as a mineral admixture in concrete. In addition, coal ash (including fly ash) may be used as partial replacement of fine aggregate in concrete for production of light weight aggregates and many other applications (Siddique and khan, 2011).

- **Low Volume Uses**

This includes the coal ash utilization in high value added applications such as metal extractions. High value metal recovery of Aluminium (Al), Gold (Au), Silver (Ag), Vanadium (Va) and Strontium (Sr) fall in this category. Fly ash has potential uses for producing light weight refractory material and exotic high temperature resistant tiles (Siddique and khan, 2011).

2.2.7 Advantages of Using Fly Ash

The objective of using fly ash in concrete is to achieve one or more of the following benefits: reducing the cement content to reduce costs; improving workability; obtaining reduced heat of hydration (especially in mass concreting); attaining required levels of strength in concrete at ages beyond 56 days; increasing the durability performances of concrete; as land fill in land reclamations for residential and commercial developments; as filler in asphalt, etc. (Siddique and khan, 2011).

2.3 Ground Granulated Blast Furnace Slag (GGBS)

Ground granulated blast furnace slag (GGBS) is a by-product from the blast furnaces used to make iron. Blast-furnaces are fed with controlled mixture of iron ore, coke and limestone; and operated at a temperature of about 1500°C.

When iron-ore, coke and limestone melt in the blast furnace, two products are formed (molten iron and molten slag). The molten slag is lighter and floats on the top of the molten iron. The molten slag comprises mostly silicates and alumina from the original iron ore, combined with some oxides from the limestone (Siddique and khan, 2011).

- **Granulated slag:**

The process of granulating the slag involves cooling of the molten slag through high pressure water jets (Siddique and khan, 2011). This rapidly quenches the slag and forms granular particles generally not bigger than 5 mm. The rapid cooling prevents the formation of larger crystals and the resulting granular material comprises around 95% non-crystalline calcium-aluminosilicates. The granulated slag is further processed by drying and then grinding in a rotating ball mill to a very fine powder, which is then called GGBS (Chen, 2007).

- **Pelletized slag:**

The pelletized slag is produced by partially cooling the slag with water, and then tossing it into air. The pellets contain much less glass content when compared to granulates; as low as 50%. Pelletized slag is commonly used as concrete aggregate and as raw material in cement production (Chen, 2006).

- **Air-cooled slag:**

Air-cooled slag is formed by allowing the slag to solidify slowly in air, and sometimes followed by accelerated cooling with a water spray. The air-cooled slag is hard and dense, normally used for road bases, railway ballast, asphalt paving and used as concrete aggregate (Chen, 2006).

GGBS can be used as a direct replacement for ordinary cement on one-to-one basis by weight. Replacement rates for GGBS vary from 30% up to 85%. Generally 50% is used in most applications. Higher replacement rates up to 85% are used in special applications like aggressive environments and to reduce the heat of hydration in mass concrete. GGBS can be used at replacement levels of 70% in lean mix concrete (Siddique and khan, 2011).

2.3.1 Chemical Composition of Ground Granulated Blast Furnace Slag (GGBS)

Blast furnace slag is a non-metallic product, consisting essentially of silicates and alumino-silicates of calcium and other bases. Slag is made up of both glassy and crystalline phases. The glassy nature is responsible for its cementitious properties (Siddique and khan 2011).

In GGBS, the glass content is between 85% and 90% and comprises mainly of CaO, SiO₂, Al₂O₃, and MgO. It has similar chemical constituents as ordinary Portland cement, but in different proportions. Typical Chemical Composition of GGBS, reported by some authors is given in Table 2.4

Table 2.4: Typical Chemical Composition of GGBS

Composition	Mantel (1991)	Tasong <i>et al.</i> (1999)	Oner <i>et al.</i> (2007)	Hui-Sheng <i>et al.</i> (2009)
SiO₂	36.6	35.34	39.18	36.39
Al₂O₃	13.2	11.59	10.18	13.76
Fe₂O₃	0.60	0.35	2.02	2.44
CaO	33.0	41.99	32.82	30.13
MgO	10.7	8.04	8.52	9.36
Mn₂O₃	1.20	0.45	-	-
SO₃	2.50	1.23	-	1.30

2.3.2 Reactivity of Ground Granulated Blast Furnace Slag (GGBS)

ASTM C 989 is the standard for evaluating the cementitious potential of slags. The factors that determine the cementitious properties are; chemical composition of the slag, alkali concentration of the reacting system, glass content of the slag, fineness of

the slag and cement, as well as, the temperature variations during the early phases of the hydration process.

Cheron and Lardinois (1968) defined the hydraulic activity index of a slag as represented by equation 2.7 below. Slag hydraulic activity indices between 1.65 and 1.85 are considered normal for reactivity:

$$\text{Hydraulic activity index} = \frac{\text{CaO} + 0.5\text{Al}_2\text{O}_3 + 1.4\text{MgO}}{\text{SiO}_2 + \text{Al}_2\text{O}_3} \quad (2.7)$$

2.3.3 Classifications of Ground Granulated Blast Furnace Slag (GGBS)

ASTM C 989 characterises three strength grades of slag depending upon their respective mortar strengths when blended with an equal mass of Portland cement.

The classifications are; Grades 120, 100 and 80, based on the slag-activity index expressed as the ratio of the average compressive strength of the slag mortar cubes to the compressive strength of reference cement mortar cubes without slag, shown in equation 2.8.

$$\text{Slag activity index (\%)} = \frac{SP}{P} \times 100 \quad (2.8)$$

Where;

SP represents the average compressive strength of the slag mortar cubes.

P is the compressive strength of reference cement mortar cubes without slag.

Grades 100 and 120 are the most commonly used as admixtures in concrete. Table 2.5 summarises the criteria for ASTM C 989 classification of GGBS.

Table 2.5: ASTM C 989 Minimum Slag Activity Index Criteria for Classification of GGBS

Days Index	Grade Type	Average of Five Consecutive Samples	Average of individual sample
7 Days	Grade 80	-	-
	Grade 100	75	70
	Grade 120	95	90
28 Days	Grade 80	75	70
	Grade 100	95	90
	Grade 120	115	110

2.3.4 Hydration Mechanism of Ground Granulated Blast Furnace Slag (GGBS)

The hydration mechanism of the combination of GGBS and Portland cement is slightly more complex than that of a Portland cement alone. This reaction involves activation of the GGBS by alkalis and sulphates to form its own hydration products.

These hydration products combine with the Portland cement to form further hydrates which have a pore blocking effect. The result is a hardened cement paste made of very small gel pores. Generally, the rate of strength development is slower than that of cement mortar (Siddique and khan, 2011).

The resulting hardened cement paste using GGBS is also more chemically stable. It contains much less free lime, which in concrete made with Portland cement leads to the formation of further reaction products such as ettringite or efflorescence. In addition, GGBS contains no C_3A , making GGBS concrete much less reactive to sulphates (Siddique and khan, 2011).

When GGBS is used in concrete, the resulting hardened cement paste produced has smaller gel pores and fewer larger capillary pores, than is the case with concrete made with normal Portland cement. This finer pore structure gives GGBS concrete a much lower permeability, and makes an important contribution to the greater durability of the resultant concrete produced (Siddique and khan, 2011).

2.3.5 Advantages of Using Ground Granulated Blast Furnace Slag (GGBS)

The incorporation of GGBS in cement and concrete results in an improved workability and compaction characteristics, increased pump-ability, increased strength, enhanced durability, reduced permeability, greater resistance to chloride penetration, greater resistance to sulphate attack, greater resistance to alkaline silica reaction (ASR), low heat of hydration for mass concrete applications, improved surface finish, enhanced architectural appearance, suppresses efflorescence, enhancement of the life cycle of concrete structures, reduction in maintenance and repair costs, reduced lifetime construction costs etc. Production of GGBS involves very low carbon dioxide (CO₂) and sulphur dioxide (SO₂) emissions and mono nitrogen oxides (NO_x).

2.4 Copper

Copper is a chemical element in the periodic table that has the symbol Cu (Latin: cuprum) and atomic number 29. It is a ductile metal with excellent electrical conductivity, and finds extensive use as an electrical conductor, as a building material, and as a component of various alloys.

Copper is a reddish-coloured metal, with a high electrical and thermal conductivity, silver is the only pure metal to have a higher electrical conductivity at room temperature. Copper has its characteristic colour because it reflects red and orange light and absorbs other frequencies in the visible spectrum, due to its band structure. This can be contrasted with the optical properties of silver, gold and aluminium (Copper Development Agency (CDA), 2012).

Copper is malleable and ductile, a good conductor of heat and, when very pure, a good conductor of electricity. It is used extensively, in products such as: copper wire, electromagnets, electrical machine, especially in electromagnetic motors and generators. Moreover copper is used for plumbing, doorknobs and other fixtures in

houses, roofing, guttering and rainspouts on buildings. In cookware, such as frying pans, knives, forks, spoons (CDA, 2012)

2.4.1 Copper Mining in Southern Africa

The Democratic Republic of Congo (DRC) is potentially one of the richest mining countries in Africa, based on its vast resources of copper, cobalt and diamonds. Most mining activities are concentrated in the southern and eastern parts of the country, where the famous Copper Belt extends into Zambia from the Democratic Republic of Congo near Lubumbashi. The Copper Belt is one of the world's greatest metallogenic regions.

Metal extractive companies include former state mining company Gecamines, STL, Electric foundry Panda (FEP) and FELCO among others are located in Lubumbashi, Democratic Republic of Congo (Kitobo and Ilunga, 2012). Lubumbashi has a great deposit of slag which is being re-mined by STL Company. In Likashi, a city in the Katanga province of DRC, two types of slag are produced by Electric foundry FEP Panda and gypsum waste by Shituru (Kitobo and Ilunga, 2012).

Zambia generates about 3.3% of the total world's copper and is ranked seventh in the world for copper production. The Southern African nation is also the world's second largest producer of cobalt, producing 19.7% of global total. It also has significant quantities of selenium and silver, with more than 300 gold occurrences and produces some platinum group elements; an important by-products of the copper mining and processing (Global Business Report, 2012).

Zambia has a long history with copper production beginning as early as the 1930's. In 1990, after years of losses, the Zambian government privatized its copper mines, and the economic growth has been increasing in the country since 2004, largely due to high copper prices and foreign investment (Global Business Report, 2012). There is an estimated 2 billion Mega tonnes of total mineral resource on the Zambian Copper Belt. Zambia's economy is heavily reliant on mining, particularly its copper and

cobalt minerals and the mining sector contributes approximately \$822 million to the country's total exports (Global Business Report, 2012).

Palabora Mining Company Limited (Palabora) is a member of the Rio Tinto group of companies, situated in the Ba-Phalaborwa area of Limpopo province in South Africa. Palabora operates a large block cave copper mine and smelter complex. It is South Africa's only producer of refined copper Palabora Company 2011. The company produces about 80,000 tonnes of refined copper per year, supplying most of South Africa's copper needs and exporting the balance. The refinery produces continuous cast rod for the domestic market and cathodes for export. Useful by-product metals and minerals include zirconium chemicals, magnetite and nickel sulphate, as well as, small quantities of gold, silver and platinum.

2.4.2 Production of Copper slag

Copper slag is produced either by hydrometallurgically or pyrometallurgically production of copper from copper ores and contains materials like iron, alumina, calcium oxide, silica etc. (Gorai *et al.*, 2002). The pyrometallurgically method is the only method applicable to ores containing copper-iron-sulphide minerals (such as chalcopyrite and chalcobornite), which are the most abundant. The waste material produced by the hydrometallurgical method is not considered as a slag.

In copper ore the oxides and sulphides combine covalently to form Cu-Fe-O- phase in the absence of silica. Because of the low copper content of the ores (of the order of 0.5%), copper extraction is achieved in several steps during the smelting operation. Initially a copper concentrate (25-40% Cu) is obtained by fine grinding and separation by flotation. The copper concentrate is smelted at a temperature of 1250°C with the aim of obtaining an intermediate product, called matte.

The matte is further converted to copper metal by removing parts of the iron and sulphur by blowing oxygen onto the molten matte (Gorai *et al.*, 2002). More silica flux is added to facilitate the removal of iron oxides under the form of a converter

slag. Certain amount of lime and alumina are added to stabilize the slag structure. The molten slag is discharged from the furnace between 1000 – 1300 °C. When liquid slag is cooled slowly, it forms a dense, hard crystalline product; whereas quick solidification by pouring molten slag into water gives amorphous granulated slag (Gorai *et al.*, 2002). Table 2.6 shows a typical oxide composition of copper slag obtained from different regions of the world.

Table 2.6: Typical Chemical Composition of Copper Slag from Different Regions

NO	Origin of Copper slag	Fe (%)	SiO ₂ (%)	CaO (%)	MgO (%)	Al ₂ (%)	S (%)	Cu (%)
1	Iranian National Copper Industries Company	44.78	40.79	5.24	1.16	3.78	1.06	-
2	Etibank Ergani Copper Plant, Turkey	39.65	31.95	3.95	2.82	2.40	-	1.01
3	Kure Copper Slag	47.8	26.10	0.70	1.00	6.80	1.50	0.82
4	Copper Queen, Prince, USA	34.62	27.16	17.42	3.51	14.70	0.33	1.64

1-Marghussian *et al.*, (1999) 2-Kiyak *et al.*, (1999) 3-Yucel *et al.*, (1999) 4-Mobasher *et al.*, (1996)

2.4.3 Mineralogical Composition of Copper Slag

Microscopic observations conducted by Kiyak *et al.*, (1999), indicate most of the copper slag are well crystallised. In addition to iron oxides, other oxides such as silica, alumina, lime and magnesia constitute 95% or more of the total oxides. The X-ray diffraction pattern shows 2FeOSiO₂, Fe₃O₄ and Ca (Fe, Mg) (SiO₃)₂ as the main phases present in copper slag (Kiyak *et al.*, 1999).

Najimi *et al.*, (2011) also demonstrated that, the mineralogical compounds of copper slag are pyroxene (CaZnSi₂O₆), fayalite (SiO₄Fe₂), anorthite (CaAl₂Si₂O₈), quartz (SiO₂) and magnetite (Fe₃O₄) similar to the main compounds of copper slag used in

various researches, such as fayalite, magnetite and quartz (Alp *et al.*, 2008; Arino and Mobasher, 1999; Mobasher *et al.*, 1996; Moura *et al.*, 1999; Sanchez de Rojas *et al.*, 2008; Tixier *et al.*, 1997).

As the metals are most stable in oxide and silicate forms, construction material produced from copper slag have least possibility of corroding (Gorai *et al.*, 2002).

2.4.4 Physical and Mechanical Characteristics of Copper Slag

Some physical and mechanical properties of copper slag are shown in Table 2.7. Air-cooled copper slag has a black colour and glassy appearance. The specific gravity varies with iron content, from as low as 2.8 to as high as 3.8. The unit weight of copper slag is comparably higher than that of conventional aggregate and the water absorption capacity of the copper slag material is typically very low (0.13%).

Table 2.7: Typical Physical and Mechanical Properties of Copper Slag

Appearance	Black, glassy, more vesicular when granulated
Unit weight	2800 -3800 ($\frac{\text{kg}}{\text{m}^3}$)
Water absorption,%	0.13
Bulk density	2300 – 2600 ($\frac{\text{kg}}{\text{m}^3}$)
Conductivity	500 $\mu\text{s/cm}$
Sp. gravity	2.8 - 3.8
Hardness	6-7 Moh
Moisture	< 5%
Abrasion loss,%	24.1
Sodium sulphate soundness loss, %	0.90
Angle of internal friction	40-50

Emery (1986), Hughes and Haliburton (1973), Das *et al.*, (1993) and Feasby (1975)

Granulated copper slag is more porous and therefore, has lower specific gravity and higher water absorption capacity than air-cooled copper slag. Granulated copper slag is made up of regularly shaped, angular particles, mostly between 4.75 and 0.075 mm in size, similar to the particle size range for conventional fine aggregates for concrete (Emery 1986; Hughes and Haliburton 1973).

2.4.5 Copper slags as Fine and Coarse Aggregates Replacement in Concrete

A study carried out by Central Road Research Institute (CRRI), India has shown that copper slag can be used as a partial replacement for sand as fine aggregate in concrete up to 40% in pavement grade concrete without any loss of cohesiveness and the compressive and flexural strength of such concretes is about 20% higher than that of conventional cement concretes of the same grade (IS, 1987).

Caliskan *et al.*, (2004) conducted a comprehensive investigation on the compressive strength of normal strength concrete containing copper slag coarse aggregate and showed that the compressive strength of copper slag coarse aggregate concrete was slightly higher than that of limestone aggregate concrete.

Concrete mixtures containing different levels percentage replacements by silica fume ranging from 0%, 6% 10% and the use of copper slag aggregate replacing limestone aggregate was monitored by Khanzadi and Behnood (2007). The use of copper slag aggregate compared to limestone aggregate resulted in a 28-day compressive strength increase of about 10–15%, and a split tensile strength increase of 10–18%. It was concluded from the results of the study that, using copper slag as coarse aggregate in high-strength concrete is technically possible and useful.

Al-Jabri *et al.*, (2009) prepared eight concrete mixtures with different proportion of copper slag ranging from 0 to 100% as replacement of fine aggregate. The results indicate that, there is a slight increase in high performance concrete (HPC) density of nearly 5% with the increase of copper slag content, whereas the workability increased rapidly with increases in copper slag percentage. Addition of up to 50% of copper slag as sand replacement yielded comparable strength with that of the control mix.

Wei Wu *et al.*, (2010) examined the microstructures of control concrete and copper slag reinforced concrete with various contents of copper slag as replacement of sand. The experiment was investigated with Scanning Electron Microscope (SEM) and the dynamic mechanical properties of copper slag reinforced concrete were studied using

a 50-mm diameter split Hopkinson pressure bar system. The outcome of the results suggested that, the dynamic compressive strength of copper slag reinforced concrete was generally improved with substitution amounts of copper slag up to 20%, compared with the control concrete, beyond which the strength reduced.

Another research study was conducted by Wei Wu *et al.*, (2010) to investigate the mechanical properties of high strength concrete incorporating copper slag as a fine aggregate. The workability and strength characteristics were assessed through a series of tests on six different mixing proportions at 20% incremental copper slag by weight replacing sand, from 0 to 100%. The results indicated that, the strength of the concrete with less than 40% copper slag replacement was higher than or comparable to that of control specimens. The microscopic view also demonstrated limited differences between the control concrete and slag concrete with less than 40% content.

Al-Jabri *et al.*, (2009) performed another thorough investigation on the performance of high strength concrete (HSC) made with copper slag as a fine aggregate at constant workability and to study the effect of superplasticizer addition on the properties of high strength concrete (HSC) made with copper slag. The results signified that, the water demand reduced by almost 22% at 100% copper slag replacement compared to the control mixture. Nonetheless, the strength and durability of high strength concrete were generally improved with the increase of copper slag content in the concrete mixture. The strength and durability characteristics of high strength concrete were adversely affected by the absence of the superplasticizer from the concrete paste.

M20 grade concrete was assessed for various proportions of copper slag replacing sand, ranging from 0, 20, 40 and 60% by Brindha *et al.*, (2010). Another mix design replacing cement ranging from 0, 5, 15 and 20% and combination of (60% sand + 40% copper slag for fine aggregate and 85% cement + 15% copper slag for cement) in concrete was cast and cured in water. The results of the compressive, split tensile

strength test indicated that, the strength of concrete increases proportionally with percentage increase of slag replacing up to 40% of the sand and 15% of the cement.

An experimental procedure to investigate the effect of using copper slag and ferrous slag as partial replacement of sand was studied by Sudarvizhi and Ilangovan (2011). The results indicate that workability increases with an increase in copper slag and ferrous slag percentage. The highest compressive strength obtained was 46 MPa (for 100% replacement) and the corresponding strength for the control mix was 30 MPa.

Copper slag as substitution of fine aggregate in reinforced concrete slender columns was exploited by Alnuaimi (2009). 20 columns measuring 150x150x 2500 mm were tested for monotonic axial compression load until failure. The concrete mixture included ordinary Portland cement (OPC), fine aggregate of size 10 mm substituted with copper slag and coarse aggregate. The results showed that the replacement of up to 40% of fine aggregate with copper slag caused no major changes in concrete strength, column failure load, or measured flexural stiffness (EI).

Onuaguluchi and Ozgur (2012) pursued an investigating study of the consistency, hardened and toxic metal immobilization properties of concrete containing copper tailings as an additive. The author's objectives were to compare the effect of copper tailings on the strength across two series of concrete with 0.57 and 0.5, water to binder ratios. The authors concluded a potential use of copper tailings in concrete to about 5%.

Ayano and Sakata (2000) critically reviewed the characteristics of copper slag and its effects on the engineering properties of cement, mortars and concrete. They reported that the shrinkage of specimens containing copper slag fine aggregate was similar to that of specimens without copper slag.

Hwang and Laiw (1989) also reported that the amount of bleeding of mortar made with copper slag is comparatively less than that using natural sand. However, the

heavy specific weight and the glass-like smooth surface properties of the irregular grain shape of the copper slag aggregates were effective for the control of concrete bleeding.

2.4.6 Copper Slag as Portland Cement Replacement in Concrete

The effect of the incorporation of the copper slag in cement was measured by Sanchez de Rojas *et al.*, (2004). Hydrated calcium aluminates phases were analysed using scanning electron microscopy (SEM) and X-ray diffraction (XRD) techniques. The authors concluded that, the replacement of 30% cement by copper slag reduces the flexural and compressive strength in a similar way to fly ash; however, after 28 days, the reduction becomes less.

Tixier *et al.*, (1996) reported on the hydration reactions of copper slag used as Portland cement replacement by weight up to 15%, through semi quantitative X-ray diffraction. Samples of copper slag and hydrated lime were used to test the pozzolanic properties of the slag. In addition, the porosity was examined using mercury intrusion porosimetry. The outcome shows a decrease in capillary porosity as opposed to the gel porosity which increased. A significant increase in the compressive strength for up to 1 year was also observed.

Arino and Mobasher (1999) studied the effect of ground copper slag on the strength and fracture of cement-based materials up to 15% by weight of ground copper slag replacing Portland cement. The strength and fracture toughness of concrete samples were studied using closed-loop controlled compression and Three-point bending fracture test. Test results were used to construct the resistance curve (R-Curve) response of the specimens describing the dependence of fracture toughness on the stable crack length. The conclusion made was, the use of ground copper slag increased the strength significantly.

Mobasher and Devaguptapu (1996) studied the activation of pozzolanic reactions using up to 1.5% hydrated lime. The hydration reactions and porosity were monitored

using quantitative x-ray diffraction (QXRD) respectively. Results indicate a significant increase in the compressive strength for up to 90 days of hydration and a decrease in the capillary porosity measured using mercury intrusion porosimetry.

Al-Jabri *et al.*, (2006) undertook another study on the effect of copper slag (CS) and cement by-pass dust (CBPD) addition on concrete properties. In addition to the control mixture, two different trial mixtures were prepared using different proportions of copper slag and cement by-pass dust. One mixture consisted of 5% copper slag substitution for Portland cement. The other mixture consisted of 13.5% CS, 1.5% CBPD and 85% Portland cement. Three water-to-binder (w/b) ratios of 0.5, 0.6 and 0.7 were studied.

The experimental outcome showed that 5% copper slag substitution for Portland cement gave a similar strength performance as the control mixture, especially at low w/b ratios. Higher copper slag (13.5%) replacement yielded lower strength values. The results also demonstrated that the use of copper slag & cement by-pass dust as partial replacements of cement has no significant effect on the modulus of elasticity of concrete, especially at small quantities substitution.

2.4.7 Other Useful Applications of Copper Slag

A research study intend to establish the level of catalytic activity of flash smelting furnace slag and converter slag in reactions complete oxidation was carried out by Mihailova *et al.*, (2011). The analysis of the samples of slag was conducted using scanning electron microscopy, element distribution mapping, electron micro analysis and BET surface area. The catalytic activities of the samples were measured in two types of reaction oxidation of carbon monoxide and oxidation of toluene. The results of the study demonstrated that copper slag samples show relatively high catalytic activity in oxidation reaction.

The determination of the proportions of copper slag and Portland cement in blended cement in terms of the cement chemistry ternary phase diagram was critically

research by Marku and Vaso (2010) with the sole objective of finding the intersection between the line connecting the cement and the slag composition and the boundary line of calcium hydroxide stability field. The outcome suggested that, the increase of copper slag amount in cementing material decreases the mechanical strengths of hardened mortars especially in the early ages. However, the by-product of the melting copper slag plant can be used successfully as Portland cement substitute in the cement industry.

The potential use of flotation waste from copper slag as iron source in the production of Portland cement clinker was thoroughly exploited by Alpha (2008). The results show that, the chemical compositions of all the clinker products including those of flotation wastes of copper slag are typical of a Portland cement clinker. The mechanical performances of the standard mortars prepared from the flotation waste from copper slag clinkers were found to be similar to those from the iron ore clinkers with the desired specifications for the industrial cements.

A research study focussed on the effect of copper slag on the strength characteristics of cement-treated Singapore marine clay by varying the percentage of copper slag at 100% water content and constant workability of cement-clay mix was examined by Chew and *et al.*, (2009). The results illustrate that when the workability of cement-treated clay with and without copper slag is kept constant, the unconfined compressive strength at 28 days curing time is observed to be constant. Therefore to suggest that copper slag can be used in treating soft marine clay with less amount of cement and yet no reduction in strength is achieved.

Moura *et al.*, (1999) used the copper slag from Bahia, Brazil as construction materials and observed that, the physical characteristic of the material was equivalent to the traditional ones or even better. Copper slag can be a potential alternative to the admixtures used in concrete and mortars.

One province in China published technical guidelines for the use of copper slag as sand for mortars and concrete (SPCSA, 1999); while other provinces are developing the specifications for its inclusion in concrete.

2.5 Curing of Concrete

Curing is the process used for promoting the hydration of cement and consists of a control of temperature, moisture movement from and into the concrete; with the aim of keeping the concrete saturated or as nearly saturated as possible until the originally water-filled space in the fresh cement paste has been filled to the desired extent by the products of cement hydration (Neville, 1981).

Proper curing reduces the rate of moisture loss and provides a continuous source of moisture required for the hydration that reduces the porosity and provides a fine pore size distribution in concrete (Alamri, 1988).

Curing may be applied in a number of ways and the most appropriate means of curing may be dictated by the site or the construction method. It may be either after it has been placed in position (or during the manufacture of concrete products), thereby providing time for the hydration of the cement to occur (Curing of concrete, 2006).

Curing is designed primarily to keep the concrete moist, by preventing the loss of moisture from the concrete during the period in which it is gaining strength. Curing may be applied in a number of ways and the most appropriate means of curing may be dictated by the site or the construction method (Curing of concrete, 2006).

Since the hydration of cement does take time and days, curing must be undertaken for a reasonable period of time if the concrete is to achieve its potential strength and durability. Curing may also encompass the control of temperature since this affects the rate at which cement hydrates. Curing period may depend on the properties required of the concrete, the purpose for which it is to be used and the ambient conditions i.e. the temperature and relative humidity of the surrounding atmosphere.

Methods of curing concrete fall broadly into the following categories:

- Those that minimise moisture loss from the concrete, for example by covering it with a relatively impermeable membrane.
- Those that prevent moisture loss by continuously wetting the exposed surface of the concrete.
- Those that keep the surface moist and at the same time, raise the temperature of the concrete, thereby increasing the rate of strength gain. This method is typically used for precast concrete products (Curing of Concrete, 2006).

The durability of concrete is affected by a number of factors including its permeability and absorptivity. These factors are related to the porosity of the concrete and whether the pores and capillaries are discrete or interconnected (Curing of Concrete, 2006).

Whilst the number and size of the pores and capillaries in cement paste are related directly to its water-cement ratio, they are also related to the extent of water curing. Over time, water curing causes hydration products to fill, either partially or completely, the pores and capillaries present to help reduce the porosity of the concrete paste (Curing of Concrete, 2006).

2.5.1 Effect of Curing on Conventional Concrete

Experimental studies by Gonnerman and Shuman (1928), and Price (1951), show that concrete continuously cured in air had lower compressive strength compared to water cured concrete at all the required age of testing.

Additionally, Guneyisi *et al.*, (2005) reported a compressive strength loss of 10-20% of concrete cubes air cured compared to cubes that were wet cured. Compressive strength losses were also recorded at ages of 28, 90 and 180 days for cubes air cured compared to wet cured cubes. Wet curing was reported to be more effective in

improving the compressive strength at later ages for higher water to cement (w/c) ratio specimen than lower w/c ratio specimens.

Soroka and Baum (1994) concluded that, at 28 days the compressive strength of concrete cube specimens continuously wet cured was 40% higher than those uncured and at 90 days, specimens continuously moist cured had compressive strength 20% higher than those of uncured cubes.

The effect of curing period and curing delay on the properties of concrete in hot weather was studied by Al-Ani *et al.*, (1998). The authors reported that wet burlap curing method was an effective technique for maintaining the moisture in concrete for curing. However, they recommended a minimum of 3 days of wet burlap curing for rich mixes, whereas 7 days for lean mixes.

Soroka *et al.*, (1998) conducted a similar study on the effect of steam curing on the late strength of concrete with cement content ranging from 150 to 400 kg/m³. The delay in pouring the concrete was between 30–60 minutes, the curing period varied from 2 to 5 hours and the curing temperature ranged from 60 to 80°C, the results showed that steam curing adversely affected the late strength of concrete. However, under short curing periods and moderate temperatures this negative effect was primarily due to lack of supplementary wet curing and due to physical factors, such as increased porosity, internal cracking and the heterogeneity of the paste.

2.5.2 Effect of Curing on Different Concrete Admixtures

An investigation report on the performance of slag, fly ash, and silica fume concretes were studied by Ramezaniapour and Malhotra (2005) under four different curing regimes, moist curing, curing at room temperature after demoulding, curing at room temperature after two days of moist curing, and curing at 38°C and 65% relative humidity. The results indicate the reduction in moist-curing period results in lower strengths, higher porosity and more permeable concretes. The strength of the concretes containing fly ash or slag appears to be more sensitive to poor curing than

to control concrete, with the sensitivity increasing with the increasing amounts of fly ash or slag in the mixtures.

Experiments conducted by Grafe *et al.*, (1984) on the influence of curing on the gas permeability of concrete prepared with different types of cement indicated that ground granulated blast furnace slag (GGBS) and pulverised fly ash (PFA) cement concrete had greater permeability than Portland cement concrete, when specimens were cured only for 1 day. However, conclusion made was that, with prolonged sealed curing, mixes prepared with blended cements performed better than Portland cement with the same water–cement ratio.

An experimental study on the effect of air curing, water curing and steam curing on the compressive strength of Self-compacting concrete was done by Bingol *et al.*, (2003). Self-compacting concrete was produced by using silica fume instead of cement by weight, in the ratios of 5%, 10% and 15%, and fly ash in the ratios of 25%, 40% and 55%. The authors concluded that, mineral admixtures had a positive effect on the self-settlement properties and the highest compressive strength was observed in the concrete specimens with using 15% silica fume and curing for 28 days in water. Air curing caused compressive strength losses in all groups. Nonetheless, relative strengths of concretes with mineral admixtures were determined to be higher than concretes without admixtures at steam curing conditions.

The effect of curing on the strength development of both OPC and fly ash cement concretes was investigated by Haque (1990). The 90-day compressive strength of OPC and fly ash cement concrete was reported to be 67% and 50% of continuously fog cured concrete specimens. However, 7 days prior curing improved these values to 95% and 82% of the fully cured concrete

Khan and Ayers (1995) suggested that, a minimum period of curing should be optimized in terms of several properties, such as strength, permeability and the movement of aggressive gases and/or liquids from the environment. The authors

experimental results showed that, the minimum period of curing required for Portland cements, fly ash and the silica fume concrete mixtures were 3, 3.75, and 6.5 days, respectively and proved that concretes prepared with mineral admixtures are more sensitive to water curing than Portland cement concretes.

2.6 Concrete Durability

The permeation properties are the key factors controlling the durability of concrete. Aggressive agents such as: water, oxygen and chloride will permeate and deteriorate the concrete either by reacting with the other aggressive agents which are already contained in the concrete or by corroding the reinforcement which in turn will cause cracking of the concrete member. Durable concrete must be dense and impermeable to liquids and gases. It should possess high intrinsic resistance to external penetration of ionic species such as sulphates and chloride (Osborne, 1999).

Ho (2003) defined permeation properties of concrete as the ease with which fluids, both liquids and gases, can enter into, or move through concrete. Long *et al.* (2001) categorised the main transport processes, which describe the movement of aggressive substances through concrete into three types, absorption, permeability and diffusion.

- **Absorption:**

Absorption or sorption is a movement of the liquids in the pores of hardened cement paste under capillary suction in ambient conditions where concrete takes in liquid by capillary suction to fill the pore space available. The capillary suction occurs in dry or partially dry concrete, where the liquids fill the available pore spaces. This type of permeation is particularly relevant to coastal structures, where chloride salts (carried by wind) are deposit on concrete surfaces and dissolved by rain to form chloride ions which are then absorbed into the concrete leading to deterioration (Long *et al.*, 2001).

- **Permeability:**

Permeability is where a fluid passes into concrete under the action of a pressure gradient. The rate of flow follows Darcy's law for laminar flow through a porous

medium. It depends on the pressure gradient and size of interconnected pores in the cement paste. For flow to occur, the concrete has to be in its saturated conditions with relevant pores being continuous. Permeability is a relevant property to be measured in assessing the durability and serviceability of structures like dams, foundations and underground structures, where they are in constant contact with water (Long *et al.*, 2001).

- **Diffusion:**

Diffusion is where a liquid, gas or ion migrates through concrete, due to a concentration gradient. In addition to the concentration gradient and the sizes of capillary pores, the rate of diffusion is influenced by the type of penetrating substance and the chemical properties of the concrete (Long *et al.*, 2001).

Diffusion of gases is very slow in saturated concrete and therefore, the property is most relevant to concrete in above-ground structures such as buildings and bridges, where concrete is partially dry. For the durability of submerged or underground structures, the diffusion of chloride and sulphate ions should be considered (Long *et al.*, 2001).

Durability of concrete is of great concern to researchers because it determines the service life of concrete structures. Many structural failures can be traced to poor durability development of concrete with time. Enhancing concrete durability has been widely discussed in a number of publications (Tarun *et al.*, 1994; Osborne, 1999; Bai *et al.*, 2002; Canan, 2003; Courard *et al.*, 2003; Tsivilisa *et al.*, 2003). One of the important factors that have gained attention of researchers in improving concrete durability is the use of cement extenders or pozzolans in concrete mixtures.

2.6.1 Oxygen Permeability Test

Permeation describes the process of movement of fluids through the pore structure under an externally applied pressure whilst the pores are saturated with the particular

fluid (Alexander *et al.*, 1999). Permeability is therefore a measure of the capacity for concrete to transfer fluids by permeation.

The permeability of concrete is dependent of microstructure, the moisture condition of the material and the characteristics of the permeating fluid (Alexander *et al.*, 1999).

The falling head gas permeameter use the permeability of the oven dried concrete core samples to oxygen gas, determined by measuring the pressure decay with time (from an initial value of 100 KPa). The pressure decay curve measured either directly from gauges or using data logging from transducers is converted to a linear relationship by plotting the logarithm of the ratio of pressure heads versus time.

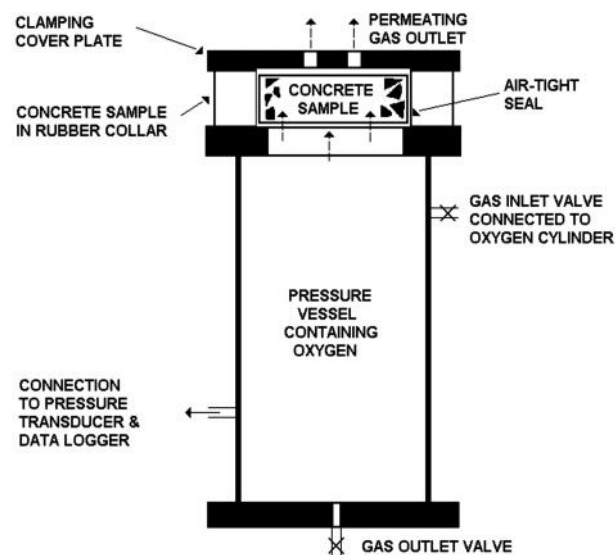


Figure 2.2: A setup of oxygen permeability apparatus (Alexander *et al.*, 1999)

The oxygen permeability index test (OPI) is sensitive to the amount and continuity of larger pores and voids where most of the flow will occur due to poor compaction and bleeding. The OPI is the negative logarithm of the Darcy coefficient of permeability and values generally range from 8 to 11. The higher the permeability index the less permeable the concrete, which enhances durability performances.

2.6.2 Water Sorptivity Test

Absorption is the process whereby fluid is drawn into a porous, unsaturated material under the action of capillary forces (Alexander *et al.*, 1999). The capillary suction is dependent on the pores geometry and the saturation level of concrete. Water absorption caused by wetting and drying at the concrete surface is an important transport mechanism but becomes less significant with depth. The water sorptivity test measures the rate of movement of a water front through the concrete under capillary suction (Alexander *et al.*, 1999).

Sorptivity is particularly sensitive to the micro-structural properties of the near-surface zone of concrete and therefore reflects the nature and effectiveness of curing. Generally, a lower water sorptivity index enhanced the potential durability of the concrete and the values vary from approximately $5 \text{ mm/h}^{0.5}$ for well-cured grade M30-50 concretes to $15\text{-}20 \text{ mm/h}^{0.5}$ for poorly cured grade M20 concretes (Alexander *et al.*, 1999). A set up of the water sorptivity test shown in Figure 2.3

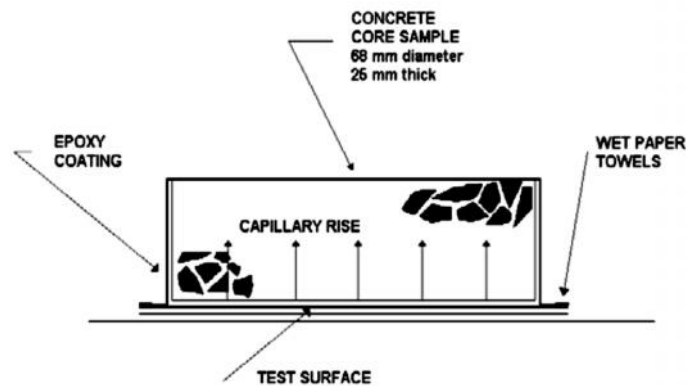


Figure 2.3: A setup of water sorptivity test apparatus (Alexander *et al.*, 1999).

2.6.3 Chloride Ingress into Concrete

The movement of chloride ions in concrete pore solution is somewhat different from that in a pure solution as the pore structure of concrete develops additional resistance to ionic movement (Alexander *et al.*, 1999).

Diffusion as defined in section 2.6 takes place in completely saturated conditions which differs from sorptivity, where the transport process occurs in an unsaturated condition. Although diffusion is not the only processes influencing the penetration of aqueous ions into the concrete, most of theories regarding the chloride ingress are based on diffusion (Alexander *et al.*, 1999).

The accepted method of modelling the chloride ingress due to diffusion is by using Fick's first law (Crank, 1975). The chloride conductivity test measures the conductive ionic flux through a concrete disc under a potential difference, and is related to the chloride diffusion properties of the concrete.

The apparatus consists of a two-cell conduction rig, each cell containing a 5 M NaCl solution so that there is no concentration gradient across the sample and chloride migration is due to conduction from the applied potential difference as shown in Figure 2.4. The concrete disc is pre-conditioned by vacuum saturation with a 5 M NaCl solution.

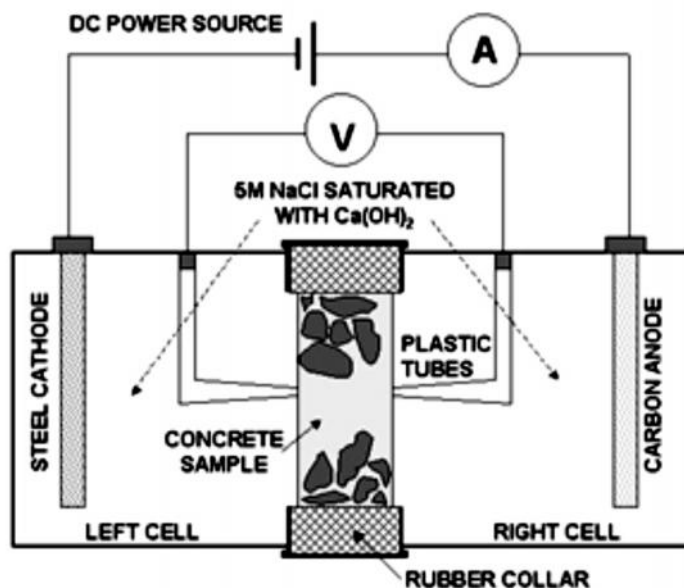


Figure 2.4: A setup of chloride conductivity test apparatus (Alexander *et al.*, 1999).

2.6.4 Implications of Durability Results

According to Alexander *et al.*, (1999), the suggested ranges of index values for durability classification of concrete for three index tests are shown in Table 2.8

Table 2.8: Suggested Ranges for Durability Classification Using Index Values

Durability Class	OPI (Log Scale)	Water Sorptivity (mm/hr ^{0.5})	Chloride Conductivity (mS/cm)
Excellent	> 10.0	< 6.0	< 0.75
Good	9.5–10.0	6.0–10.0	0.75–1.50
Poor	9.0–9.5	10.0–15.0	1.50–2.50
Very poor	< 9.0	>15.0	> 2.50

2.6.5 Sulphate Attack

Sulphate attack can be defined as the deterioration of concrete as a result of physical-chemical interaction between minerals in hydrated Portland cement paste and sulphate from the environment (Mehta *et al.*, 1992). The interaction causes expansion, cracking, spalling or even disintegration of concrete. It may be noted that, attack of the same nature can also occur when there is reaction between cement constituents and internal sulphate. The common feature is the appearance of excess sulphate bearing phases, ettringite in the deterioration.

Sulphate attack can also lead to leaching of calcium compounds, degradation of calcium silicate hydrate (*C-S-H*) and the overall deterioration of cement paste matrix (Nabil, 2006). One of the most severe conditions for durability of concrete is sulphate or acid environment caused by industrial wastes or chemical residues at reclaimed grounds (Hanifi and Orhan, 2006).

Several studies have been performed to investigate ways of increasing concrete resistance to sulphate attack through incorporation of extenders (pozzolans) in mortars and concrete mixes (Torri *et al.*, 1995; Osborne, 1999; Rodriguez-Camacho and Uribe-Afif, 2002; Courard *et al.*, 2003; Nabil, 2006).

Consumption of calcium hydroxide produced during hydration by cement extenders and C₃A presence due to reduced quantity of cement content when cement extenders are incorporated will improve the resistance of concrete to sulphate attack (Rodriguez-Camacho *et al.*, 2002; Salah 2007). This originates from reduction of gypsum (CaSO₄.2H₂O) and ettringite (C₆AS₃H₃₂) formation within the cementitious system.

2.6.5.1 Internal and External Sulphate Attack

Internal sulphate attack occurs when deterioration of concrete is caused by sulphate that has been introduced with cementitious materials and/or with aggregates. External sulphate attack is caused by sulphates from ground water, soils, solid industrial waste and fertilizers, atmospheric SO₂, or liquid industrial wastes.

The ready availability of these sulphates causes damage to concrete, depending on its concentration and solubility, the transport of water and environmental conditions (Skalny *et al.*, 1976; Torres *et al.*, 2003; Senhadji *et al.*, 2005).

Both forms of sulphate attack are manifested by expansion, cracking and sometimes spalling of concrete. According to Omar (2002), formation of gypsum and ettringite are characteristics of sulphate attack. Gypsum formation results in the deterioration of hydrated cement paste, which is characterized by softening of the cement matrix and causes reduction in cross-sectional area of the structural component and strength, due to loss of cohesiveness of the cement hydration products.

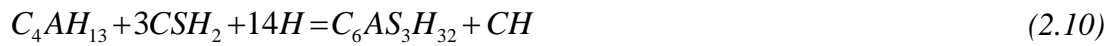
Ettringite formation results in expansion and cracking, when reactive hydrated aluminate phases are attacked by sulphate ions.

2.6.5.2 Effect of Cement type

The different forms of sulphate attack can be affected by the cement type. Sulphate ions can be introduced to concrete mix from internal sources. Cement type with high content of tricalcium aluminate (C₃A) will exhibit low resistance to sulphate attack. If

the C_3A content of cement is more than 5%, most of the alumina it contained will be in the form of mono-sulphate hydrate, $C_3A.CS.H_{18}$ or $C_3A.CS.H_{12}$. If the C_3A content is more than 8%, the hydration product will also contain hydro garnet, $C_3A.CH.H_{18}$ or $C_3A.CH.H_{12}$.

Alumina containing hydrates will be converted to ettringite, which generates excessive expansion in hardened concrete, when cement paste comes in contact with sulphate ions in the presence of moisture. The reactions that result are shown in equations (2.9) and (2.10).



High content of C_3S in cement is essential for early strength development. It also produces high quantities of calcium hydroxide as a by-product of hydration. CH in concrete will aid gypsum formation when exposed to sulphate ions (Al-Dulaijan *et al.*, 2003).

2.6.5.3 Effect of Sulphate Type and Concentration on Concrete

Concrete deterioration due to sulphate attack tends to increase with increase in the concentration of sulphate solution to some extent (Omar, 2002) but beyond 0.5 % of $MgSO_4$ or 1 % of Na_2SO_4 , the rate of increase in the intensity of the attack becomes smaller (Neville, 1981).

In the case of Na_2SO_4 attack, formation of sodium hydroxide ($NaOH$) is a by-product of the reaction causing continuation of high alkalinity in the system. This is essential for the stability of the ettringite and reduces sulphate attack.

On the other hand, in the case of $MgSO_4$ attack, gypsum formation is simultaneously accompanied by the formation of magnesium hydroxide ($Mg(OH)_2$), which is insoluble and causes reduction in the alkalinity of the system. In the absence of

hydroxyl ions in the solution, *C-S-H* is no longer stable and is also attacked by the sulphate solution (Kumar *et al.*, 1993). The attack by magnesium sulphate is therefore more severe on concrete.

2.6.5.4 Effect of Pozzolans on Sulphate Attack

The reaction between calcium hydroxide and pozzolans to form secondary calcium-silicate-hydrate (*C-S-H*) helps in increasing the resistance of concrete structures to sulphate attack in the following ways (Omar, 2002; Al-Dulaijan *et al.*, 2003; Sideris *et al.*, 2006)

- Consumption of calcium hydroxide reduces the formation of gypsum.
- Replacement of cement quantity with pozzolan, leads to reduction in C_3A content.
- Secondary *C-S-H* formation in the cement paste matrix produces a coating around the reactive phases, thereby hindering formation of secondary ettringite.
- Formation of secondary *C-S-H* results in a more dense and impermeable concrete, reducing the ingress of sulphate ions.

2.7 Hazardous Waste

A hazardous waste is a waste with a chemical composition or other properties that make it capable of causing illness, death, or some other harm to humans and other life forms when mismanaged or released into the environment (EPA, 2005).

The Environmental Protection Agency (EPA) of the United States of America (USA) created hazardous waste identification regulations that outline a process to determine whether any particular material is a hazardous waste for the purposes of Resource Conservation and Recovery Act (RCRA) (EPA, 2005).

2.7.1 Classification of Hazardous Waste

In California and other States of the United States of America (USA), there are both Federal and State regulations governing hazardous waste determination. A waste is considered hazardous by exhibiting any of the four characteristics: Ignitability, Corrosivity, Reactivity or Toxicity (EPA, 2005).

- **Ignitability:**

Ignitable wastes are wastes that can readily catch fire and sustain combustion. Many paints, cleaners, and other industrial wastes pose such a fire hazard. Most ignitable wastes are liquid in physical form. Many wastes in solid or no liquid physical form (e.g. wood and paper) can also readily catch fire and sustain combustion. Ignitable wastes carry the waste code D001 and are among the most common hazardous wastes (EPA, 2005).

- **Corrosivity:**

Corrosive wastes are acidic or alkaline (basic) wastes which can readily corrode or dissolve flesh, metal, or other materials. They are also among the most common hazardous waste streams. Waste sulphuric acid from automotive batteries is an example of a corrosive waste. Corrosive wastes carry the waste code D002 (EPA, 2005).

- **Reactivity:**

A reactive waste is one that readily explodes or undergoes violent reactions. Common examples are discarded munitions or explosives. Wastes exhibiting the characteristic of reactivity are assigned the waste code D003 (EPA, 2005).

- **Toxicity:**

The leaching of toxic compounds or elements into groundwater drinking supplies from wastes disposed of in landfills is one of the most common ways; a general population can be exposed to the chemicals found in industrial wastes (EPA, 2005). Toxicity characteristic of a waste is further explained below.

2.7.2 Toxicity Characteristics of Waste

The Environmental Protection Agency (EPA) developed a characteristic designed to identify wastes likely to leach dangerous concentrations of certain known toxic chemicals into groundwater in order to predict whether any particular waste is likely to leach chemicals into groundwater in the absence of special restrictions on its handling.

The EPA has designed a laboratory procedure that replicates the leaching process and other effects that occur when wastes are buried in a typical municipal landfill. This laboratory procedure is known as the Toxicity Characteristic Leaching Procedure (TCLP) (EPA, 2005). The EPA used groundwater modelling studies and toxicity data for a number of common toxic compounds and elements to set these threshold concentration levels. Much of the toxicity data were originally developed under the Safe Drinking Water Act (EPA, 2005).

In 1990, the U.S. Environmental Protection Agency (EPA) promulgated a rule to revise the existing toxicity characteristics which are used to identify wastes that are hazardous and thus subject to regulation under Subtitle C of the Resource Conservation and Recovery Act (RCRA) (Bricka, 1992).

2.7.2.1 Total Threshold Limit Concentration (TTLC)

The Total Threshold Limit Concentration (TTLC) is the maximum concentration allowed for a waste in solid or powdered form to be considered possibly non-hazardous (EPA 2005).

Total Threshold Limit Concentration analysis determines the total concentration of each target analytes in a sample. Samples are analysed by EPA 7420 for lead and by EPA 6010 for other metals. When any target analytes exceeds the TTLC limits the waste is classified as hazardous and its waste code is determined by the compounds that failed the TTLC test (Micro Analytical Laboratories, 2013)

The results of TTLC can be used to determine if analysis for Soluble Threshold Limit Concentration (STLC) level is necessary by comparing 10 times the STLC limit to TTLC results. A factor of ten is considered to compensate for a 1:10 dilution factor that is present in one analysis but not the other. If the TTLC results do not exceed 10 times the STLC limit then normally no further analysis is required (Micro Analytical Laboratories, 2013)

2.7.2.2 Soluble Threshold Limit Concentration (STLC)

The Soluble Threshold Limit Concentration (STLC) is the maximum concentration allowed for a waste in liquid form to be considered possibly non-hazardous (EPA 2005).

This analysis determines the amount of each analyte that is soluble in the "Waste Extraction Test" (WET) leachate. This Waste Extraction Test (WET) leachate procedure is used for solid samples or for samples containing <0.5% solids. The sample is stirred by measuring 10 times its weight in a 0.2M sodium citrate buffer for 48 hours. This leachate is then analysed to determine the soluble concentrations (Micro Analytical Laboratories, 2013)

Total threshold limit concentration and Soluble threshold limit concentration are intended to simulate the conditions that may be present in a landfill where water may pass through the landfill waste and travel into the groundwater, carrying the soluble materials with it. When a waste is analysed and the concentration of a substance is found to lie between the accepted Total Threshold Limit Concentration (TTLC) and Soluble Threshold Limit Concentration (STLC) values for a particular substance, further analysis may be required (EPA 2005).

2.7.2.3 Toxicity Characteristic Leaching Procedure (TCLP)

This analysis is similar to the Waste Extraction Test (WET) and determines the soluble portion of the analytes. The alkalinity of the sample is first determined in order to know which of the two different extraction fluids should be used. Samples

with a low alkalinity use extraction fluid made of sodium acetate solution with a pH of 4.93.

Samples with a high alkalinity use extraction fluid made of dilute acetic acid solution with a pH of 2.8. The sample is then tumbled in the appropriate extraction fluid for 18 hours (Micro Analytical Laboratories, 2013)

2.7.2.4 Inductively Coupled Plasma (ICP)

Inductively coupled plasma-atomic emission spectrometry (ICP-AES) is an instrument used to determine the trace elements in a solution. With the exception of groundwater samples, all aqueous and solid matrices such as waste, soils, sediments, paint chips, dust wipes, air and other solid wastes need acid digestion prior to analysis (EPA, 2005).

Inductively coupled plasma-atomic emission spectroscopy (ICP-AES) is also applicable to all of the elements shown in Table 2.9. For analysis, samples are nebulized and the resulting spray is transported to the plasma torch. Element-specific atomic line emission spectra are produced by a radio-frequency inductive coupled plasma.

The spectra are dispersed by a grating spectrometer, and the intensities of the lines are monitored by ultra violet (UV) and visible solid state detectors (Segmented Array Charge-coupled Device Detectors (Micro Analytical Laboratories, 2013)

2.7.3 Leaching Characteristic of Metallurgical Slags in Concrete

One potential concern for slag materials used in concrete is their heavy metal content and leaching characteristics. A slag has to be characterized, irrespective of whether the material will be utilized or landfilled (Tossavainen, 2005).

Slags that are to be used especially in road-making have to fulfil the requirements of mechanical and environmental properties according to specified standards (Tossavainen, 2005)

Lind (2002) has shown that blast furnace slag, aside from the fact that it leaches less than rock materials, reduces the impact on the environment by sorption of metals on the slag.

Togerö (2004) investigated the leaching of substances and metals from a reference concrete, GGBS and fly ash concrete. The author concluded that, concrete type does not necessarily change the leaching behaviour in short-term tests; however, more research on the long-term binding of substances in cement-based materials is needed.

A similar research work by Alter (2005) and Shi *et al.*, (2008) confirmed that, the amounts of leached elements of copper slag are significantly lower than the regulatory levels determined by the United States Environmental Protection Agency (EPA).

Zain *et al.*, (2004) also reported that, cement mortar made by incorporating waste copper slag up to 10% replacement by weight of Portland cement, is safe with respect to leachability of heavy metal similar to Table 2.9; the authors used direct air-acetylene flame atomic absorption spectrometer method to determine the concentration of the respective ions in the leachability test.

Sanchez de Rojas *et al.*, (2004), showed that the copper slag incorporation into cement mortar does not cause an increase in leached elements and therefore their application in conventional concrete production posed moderate environmental threat.

Table 2.9: List of Inorganic Substance and Their Soluble Threshold Limit Concentration

Substance	STLC (mg/L)	TTLIC (mg/kg)	Range of STLC values for which further testing must be done	TLCP (mg/L)
Antimony	15	500	150 mg/kg	-
Arsenic*	5	500	50 mg/kg	5
Barium*	100	10,000	1000 mg/kg	100
Beryllium	0.75	75	7.5 mg/kg	-
Cadmium*	1	100	10 mg/kg	1
Chromium*	5	2,500	50 mg/kg	5
Cobalt	80	8,000	800 mg/kg	-
Copper	25	2,500	250 mg/kg	-
Lead*	5	1,000	50 mg/kg	5
Mercury*	0.2	20	2 mg/kg	0.2
Molybdenum	350	3,500	3,500 mg/kg	-
Nickel	20	2,000	200 mg/kg	-
Selenium*	1	100	10 mg/kg	1
Thallium	7	700	70 mg/kg	-
Vanadium	24	2,400	240 mg/kg	-
Zinc	250	5,000	2,500 mg/kg	-

*TLCP Metals (Source:<http://www.northcoastlabs.com/services-analysis-testing/hazardouswaste.php>)

Chapter Three

3.0 Materials and Experimental Procedure

3.1 Materials

3.1.1 Portland Cement

Type 1 Portland cement with strength class of 52.5 MPa at 28-days water curing (CEM I, 52.5N) procured from local cement manufacturing company called PPC (Ltd), was used for this study. PPC (Ltd) type 1 cement is among the most widely used cements in the construction industry in South Africa, made from high quality raw materials (limestones and clays or shales).

The limestone enters the kiln, which consist of a slowly rotating tube set at a slight angle with an operating temperature usually in the order of 900-1500°C. The product of the limestone burning process called clinker is air cooled and inter-ground with 5% gypsum to control the flash setting of the cement (Mantel, 1991). Grinding was carefully controlled to ensure consistent performance in the 52.5 N strength classes of cement type in accordance with SANS 50197-1 for common cements (Mantel, 1991).

The properties of the cement conforms to the requirement of SANS 50197-1 and both the chemical oxide and mineralogy composition of the copper slag examined using the X-ray fluorescence (XRF) techniques and X-ray diffraction (XRD) pattern respectively are shown in chapter four. The total trace metal constituents of the copper slag was analysed using the Inductively Coupled Plasma Emission Spectroscopy (ICP-AES) in accordance with EPA methods 200.7 and 200.8. The physical property of the granulated slag is also tabulated in chapter four, Table 4.3.

3.1.2 Fine and Coarse Aggregates

Granite aggregates are crushed hard rock of granular structure, being the most common on Earth. Granite rock comes from magma that erupted on the ground surface and then hardened (Lafarge, 2013). Good properties of granite stones make it

the most popular building material and in terms of its technical characteristics. Coarse granite aggregates between 18-20mm and fine granite aggregates between 75 μ m – 4.75mm particle sizes procured from Afrisam South Africa were used for this experimental work.

The sampling of aggregates were done in accordance with BS EN 932-1: 1997 and the particle size distribution curve for both granulated copper slag, coarse and fine aggregates used for this experiment are shown in Figure 4.2 in accordance with SABS 829:1994. All the aggregates used for this experiment were air dried under standard laboratory temperature. For gradation of aggregates using standard SABS sieves, samples were placed in a suitable basin and dried in an oven at a temperature not exceeding 110°C in accordance with SABS 829:1994.

3.1.3 Copper Slag

The copper slag used for this research work was brought from Katanga Province, Democratic Republic of Congo. Katanga is a province with several mining companies producing copper and cobalt. These companies include Electric Foundry of Panda (FEP), Electric Foundry of Kolwezi (FELCO) and STL Company all located in Lubumbashi.



Figure 3.1: Granulated Copper Slag



Figure 3.2: Pulverised Copper Slag

The physical appearance of the copper slag is black, glassy and granular in nature with similar particle size range like sand, mostly between 4.75 and 0.075 mm in size. The relevant chemical compositions such as its oxide constituents and physical characteristics were determined and given in Table 4.1 and 4.3 respectively and are thoroughly discussed in chapter four.

3.1.4 Mixing Water

Water of drinking standard at room temperature was used for all concrete mixes and also for curing of all concrete specimens. Similarly for the durability test and other test performed involving water, the water used was of the same quality standard. A constant water to cement ratio, mix proportion was maintained for all concrete batches and is represented in Table 3.1.

3.2 Physical Test Procedure for Cement and Pulverised copper slag

3.2.1 Milling of Copper Slag

Two batches of the copper slag are each weighed to an approximate maximum value of 4 kg on an electronic beam balance. The weighed samples were then placed into the grinding chamber of a two feed pot milling machine. Prior to placement of the slag into the pot chamber, 30 kg weight of steel balls were simultaneously placed in the grinding chamber of each cylinder compartment or pot.

The two cylinders were tightly closed and the mill was set to a rotation speed of about 14000 rev/min. The mill ran for approximately 5 ± 1 hours, afterwards the pulverized slag was removed and tested for surface area and fineness using the Blaine permeability apparatus and steel mesh sieves respectively. The milling process was repeated until the desired fineness was achieved.

The Blaine permeability apparatus and the stainless steel sieves of sizes 45, 90 and 212 μ m are shown in Figures 3.4 and 3.3 respectively.

3.2.2 Fineness Test Using Sieve Analysis

25 g of the pulverize copper slag was carefully placed in a 45 μm sieve to avoid losses, the sieve was fitted with the lid and agitated by swirling until no more fine material passed through in accordance with EN 196-6. The residue was removed, weighed, and expressed as mass percentage of the initial quantity first placed in the sieve to the nearest 0.1%. The experiment was repeated for 90 μm and 212 μm sieves for both Portland cement and the pulverised copper slag samples. The sieves used for the experiment are shown in Figure 3.3.



Figure 3.3: Stack of sieves for fineness test



Figure 3.4: Blaine air permeability test setup

3.2.3 Blaine Air Permeability Test

The fineness of both slag and cement has a significant effect on the physical properties when used in concrete. Generally the finer the slag powder, the more rapidly the concrete will set, as there is an increase exposure of the surface area, consequently increasing the rate of micro reaction. The Blaine air permeability apparatus was used to determine the fineness of Portland cement and pulverized

copper slag in terms of the specific surface, expressed as total surface area in square centimetres per gram as per EN196-6.

The Blaine permeability apparatus is shown in Figure 3.4. The Blaine apparatus draws a defined volume of air through a prepared bed of compacted cement powder of defined porosity. The resistance to air flow is directly proportional to the fineness of the sample grains, as long as the same testing conditions are observed. The apparatus comprises of a stainless steel permeability cell 12.5 mm, 'U' tube manometer, perforated metal disc, plunger, rubber stopper and a tube about 30 cm long with rubber bulb. The results of the test performed for both cement and copper slag are presented in the Table 4.6.

3.2.4 Water Absorption and Specific Gravity Determination

The specific gravity and water absorption of the granulated copper slag and sand were determined in accordance with ASTM C128. For water absorption test, the fine aggregates were saturated for a period of 24 hours. After full saturation, the material was progressively dried and checked in a small cone.

Saturation was achieved when the weight of the material after it has slumped by a dime from the top of the cone. Repetitive drying of the aggregates was done until the appropriate slump was achieved. The water absorption was determined using the appropriate equation as per ASTM C128; the experiment was repeated for granulated copper slag.

For specific gravity, the weight of the bottle was measured dry on an electronic balance, afterwards filled to about one third with granulated copper slag, with water filled to the brim and reweighed. The same bottle containing the granulated copper slag was emptied then filled with distilled water, wiped clean and reweighed after all air bubbles have escaped through vacuum pumping. The procedure was repeated for sand, cement and the pulverised copper slag. The results were triplicated for each sample for accuracy and the average value was recorded.

3.3 Chemical Test Procedure for Pulverized Slag

3.3.1 Rietveld X-Ray Diffraction (XRD) Method

The Rietveld method was developed by Hugo M. Rietveld (1969) to refine neutron diffraction data. Later the method was adapted to X-ray diffraction data by Malmros and Thomas (1977) and by Young et al., (1977).

The underlying principle of this method is that, the intensities calculated from a model of the crystalline structure are fitted to the observed X-ray powder pattern by a least squares refinement. This is achieved by varying the parameters of the crystal structures and of the peak profiles to minimise the difference between observed and calculated powder patterns.

Because the whole powder pattern is taken into consideration, problems of peak overlap are minimised and accurate quantitative analyses can then be obtained. The results of the X-ray diffraction pattern analysis used to determine the mineralogical composition and the glass content of the copper slag is shown in Figure 4.1

3.3.2 X-Ray Fluorescence (XRF)

The elemental composition of the copper slag sample was obtained with the help of X-Ray fluorescence spectrometer to determine all the major oxides present in the sample. 4 g of oven-dried, finely ground copper slag sample and 1 g of micro crystalline methyl cellulose were mixed uniformly with isopropyl alcohol and kept for slow drying under a 200 W infrared lamp.

The dried sample was made into pellets by filling in an aluminium dish and was compressed under load with the help of a hydraulic jack. The compressed pellet was run in the XRF setup for computing the oxides composition of elements as percentage by weight of the slag sample. The copper slag sample was analysed in South Africa at Lafarge Chemical Laboratory (Pty) and Heidelberg Cement Technology Centre in Germany. The XRF results are tabulated in chapter four.

3.3.3 Total Threshold Limit Concentration (TTLC)

Total threshold limit concentration analysis determines the total concentration of each target analytes in a sample. Samples are analysed by EPA 7420 for lead and by EPA 6010 for other metals. The total trace metals constituent of the copper slag was analysed with the Inductively Coupled Plasma Emission Spectroscopy (ICP-AES) according to the EPA methods 200.7 and 200.8 at Heidelberg Cement Technology Centre GmbH Germany, the results is shown in Table 4.2

3.3.4 Loss on Ignition (LOI)

Loss on ignition consists of strongly heating or igniting a sample of the material at a specified temperature, allowing volatile substances to escape, until its mass ceases to change. The simple test typically consists of placing a small amount of the material in a pre-ignited crucible and determining its mass. Thereafter, the material is placed in a temperature-controlled furnace for a set time, cooling it in a controlled CO₂-free atmosphere and re-determining the mass as per SANS 50197-1. A small sample of the copper slag was oxidized with HNO₃ prior to ignition by heating in a furnace under controlled conditions for 15 minutes to a temperature of about 950 °C and the weight loss was measured in accordance with SANS 50197-1

3.4 Physical Test for Mortar Paste

3.4.1 Setting Time Determination

500 g of CEM I (52.5N) paste each was prepared with pulverized slag replacement at the required percentages i.e. 0, 2.5, 5, 10 and 15% at a laboratory with relative humidity of approximately 50% for about 4 minutes 10 seconds, for both mixing and moulding, afterwards immersed in distilled water at a temperature of 20 °C as per EN 196-3:2005.

The water requirements for standard consistency were determined for each percentage replacement prior to preparing the paste to determine the setting time. The

penetration depth of the plunger and the base-plate was within the required range of 4-8 mm as per EN 196-3:2005.

The initial and final setting time measurement was performed using the Manual Vicat apparatus and the penetration depth between the needle and the base-plate was within the distance range of 5-11 mm in accordance with EN 196-3:2005 under standard laboratory condition with relative humidity of approximately 50%.

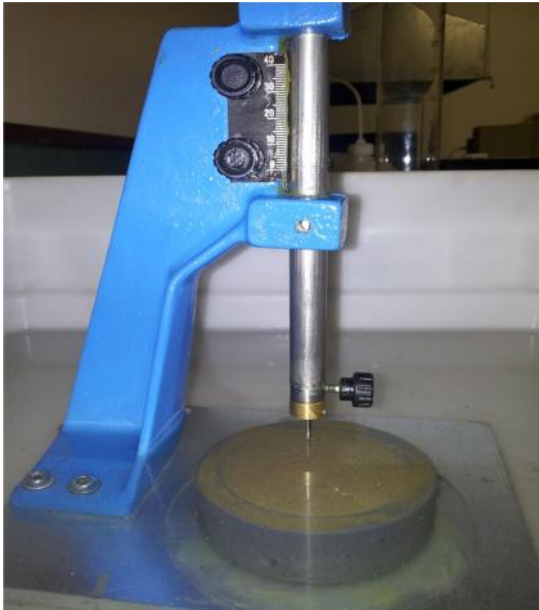


Figure 3.5: Initial setting time setup

Figure 3.6: Final setting time setup

3.4.2 Heat of Hydration

The heat of hydration for this experimental study was conducted using the induction isothermal calorimetric method. The procedure involved electronically mixing about 3 g of the cement combinations with about 2 ml of distilled water in a 20 ml disposable glass ampoule for about 1 minute to produce a mix of uniform consistency. The ampoule was placed in an induction calorimeter manufactured by Tam Air, connected to a computer and securely insulated to prevent any heat loss and maintained at a constant temperature of about 20 °C. A reference ampoule containing water to balance the heat capacity of the sample ampoule was used in order to reduce

the noise of the signal. The sample and reference ampoules were loaded at the same time to minimise the time to reach thermal equilibrium.

The heat generated by the paste sample, in the isothermal calorimeter is sent as electric signals by a sensitive thermopile to the computer for recording and calibration. The heat of hydration generated for 60 hours from the start of the test was progressively recorded to obtain the total heat generated. The length of the test was limited to 3 days as the rate of heat evolution becomes too low to measure beyond the time period. The test was performed at PPC (Ltd) laboratory in Johannesburg South Africa.

The heat evolution was investigated with different proportions of pulverised copper slag ranging from the control, 2.5, 5, 10 and 15% replacing Portland cement by weight.

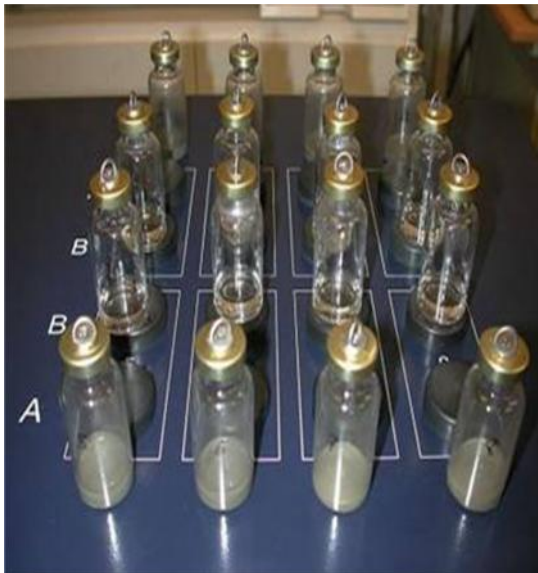


Figure 3.7: a) Induction calorimeter setup



Figure 3.7 b) Electronic syringe for mixing the cement paste

3.5 Mixing and Fresh Concrete Properties

3.5.1 Mixing of Concrete

A series of concrete mixes were cast in cubic moulds of nominal size 100 mm and prisms of cross section 100 mm × 100 mm and length 350 mm using the mix design shown in Table 3.1, Activation of pozzolanic reactions of the pulverized copper slag was done using 1.5% hydrated lime by weight of Portland cement based on a similar research by Arino and Mobasher (1999). The materials were weighed using a digital balance and mixed in a rotating pan mixer in accordance with SANS 5861-1.

The electronic pan mixer was thoroughly cleaned, dried and thereafter, wiped with a damp cloth. The mixer was loaded with approximately half the quantity of the coarse aggregates, then with the cement, thereafter, with the fine aggregate and with the rest of the coarse aggregate in such a way as to prevent loss of material as par SANS 5861-1.

Table 3.1: Concrete Mix Proportion

	0%	2.5%	5%	10%	15%
Copper slag replacement (%)	0%	2.5%	5%	10%	15%
Portland cement (kg/m ³)	352	343.2	334.4	316.8	299.2
Fine aggregate (kg/m ³)	758	758	758	758	758
Coarse aggregate (kg/m ³)	995	995	995	995	995
Pulverised copper slag (kg/m ³)	0.0	8.8	17.6	35.2	52.8
Hydrated lime Ca(OH) ₂ kg	5.3	5.3	5.3	5.3	5.3
Water (kg/m ³)	170	170	170	170	170
Water to binder ratio	0.5	0.5	0.5	0.5	0.5

The dry materials were mixed for not longer than 30 seconds and finally water was added slowly. The mixing was continued until all the concrete was uniform in appearance for a period not more than 3 minutes. After the mixing, the concrete was reworked with a trowel to ensure that all the fine material sticking to the drum was worked into the concrete mass. The mixing of concrete was done under standard laboratory condition as per SANS 5861-1, at the concrete and materials laboratory University of the Witwatersrand, Johannesburg South Africa.

3.5.2 Workability-Slump Test

The slump of the fresh concrete was determined to study the effect of copper slag on the workability of the concrete mixture in accordance with SANS 5862-1. This method was employed to explore the slump of fresh concrete cone under its own weight, using different mixes for control samples and for copper slag replacement of cement in the fresh concrete mix.

Prior to starting the slump test, the interior surface of the mould was cleaned and dampened. The mould was placed on a clean, smooth, horizontal, rigid levelled metal plate surface. While the mould was being filled, it was firmly held in place by standing on the foot pieces.

The mould was filled with freshly mixed concrete in three layers, each approximately one third of the height of the mould. Each layer was tamped with 25 strokes with a tamping rod by distributing the strokes uniformly over the cross-section of the layer. Each layer was tamped throughout its depth, to ensure that when the second and third layers were being tamped, the strokes penetrate into the underlying layer as per SANS 5862-1.



Figure 3.8: Determination of the slump of fresh concrete from the pan mixer

The concrete was demoulded by raising the mould vertically, slowly and carefully, in 5 to 10 seconds, in such a manner as to impart minimum lateral or tensional movement to the concrete. The entire process, from moulding and demoulding were carried out within 150 seconds. Immediately after demoulding as shown in Figure 3.8, the slump of the concrete was measured to the nearest 5 mm, by determining the difference in the height of the mould and the highest point of the specimen under test as shown in Figure 3.8. The results of the slump test were recorded and are presented in Table 4.9.

3.6 Curing of Concrete Specimen

After testing for slump, the fresh concrete mix were placed in two layers in the appropriate moulds, and compacted using the electronic vibrating table for not more than 30 seconds. Vibration was ceased when large air bubbles were no longer released and the surface of the concrete was relatively smooth and had a glazed appearance.

The specimens were covered with an impervious polyethylene sheet, cured under laboratory conditions of temperature $20\pm 2^{\circ}\text{C}$, relative humidity above 50% and demoulded after 24 hr. The specimens were carefully stored to prevent loss of moisture during transportation. During and after demoulding, the concrete samples were well protected against any form of shock or damage. A comparison of the temperature and relative humidity of all three curing methods used for up to 90 days and monitored by using a digital probe, are presented in Figure 4.7 and 4.8.

3.6.1 Air Curing of Concrete

The demoulded concrete cubes were air cured at the standard laboratory conditions. The laboratory records an average temperature of $24\pm 1^{\circ}\text{C}$ and $21\pm 1\%$ average relative humidity. Concrete cubes after demoulding were placed in stacks and ambient air was allowed to freely flow around the cubes.

The temperature and relative humidity were daily monitored until the required age of curing, for compressive strength determination and the results are thoroughly discussed in chapter four.



Figure 3.9: Stack of concrete cubes cured in ambient air for up to 90 days

3.6.2 Water Curing of Concrete

The series of concrete cubes of nominal size 100 mm and prisms of cross section 100 mm \times 100 mm and length 350 mm were demoulding after 24 hours curing in the standard laboratory conditions. The specimens were moist-cured in a water tank, at temperature of 20 ± 1 °C and tested at the required age of curing. The water curing encompasses the control of temperature since this affects the rate at which cement hydrates. The near constant water temperature was measured using a thermometer. The results for curing up to 90 days are shown in Table 4.10 and 4.11 respectively for both concrete cubes and prism specimens.

3.6.3 Solar Chamber Curing of Concrete

The solar chamber was made of ordinary rectangular plastic container of dimensions length 1300 mm, breadth 600 mm and height 700 mm; with a glass lid of average thickness 0.9 mm. The chamber was painted white in colour, to reflect the rays of the

sun and help keep the concrete specimens in a uniform temperature during extreme hot weather conditions.

Granite stones of average size 19 mm were placed at the bottom of the chamber to a depth of about 200 ± 20 mm and filled with ordinary tap water 100 mm underneath to keep a higher constant relative humidity inside the solar chamber. The chamber was tightly sealed after placing the demoulded cubes and a digital probe was attached to monitor the interior temperature and relative humidity.

The interior conditions of the chamber were not regulated, but however recorded an average temperature of $35\pm 1^\circ\text{C}$ and $90\pm 1\%$ relative humidity depending on the climatic conditions. Concrete specimens were quickly removed and tested at the required curing age to prevent excess loss of heat during the removal process.



Figure 3.10: Concrete cubes and beams immersed in water curing tanks



Figure 3.11 a) Concrete cubes cured inside the solar chamber



Figure 3.11 b) A temperature and humidity digital probe attached to monitor the internal conditions

3.7 Characteristics Strength Determination

3.7.1 Compressive Strength of Cubes

The bearing surfaces of the platens of the compression testing machine were wiped clean and the load was applied perpendicular to the cast faces of the concrete cubes specimens. The axis of the each specimen was aligned with the centre of thrust of the spherically seated platen and the platen adjusted gently by hand to achieve uniform contact prior to applying the load as par SANS 5863:2006.

To determine the unconfined compressive strength, ninety concrete cubes of size 100 mm × 100 mm × 100 mm were cast for each mixture. For all three curing method used for this experiment, the specimens were kept for 3, 7, 14, 21, 28, 60 and 90 days before the compressive strength test were conducted. The compressive strength of each specimen was calculated using the formula in equation 3.1 below.

$$F_c = \frac{P}{A} \quad (3.1)$$

Where

F_c is the compressive strength, in Megapascals;

P is the maximum load at failure, in Newtons;

A_c is the cross-sectional area of the specimen on which the compressive force acts, in square Millimetres.

An average of three samples were tested at constant loading rate of 1.0 kN/s at each required curing age in accordance with SANS 5863:2006 using the Tinius Olsen compressive machine at the concrete materials laboratory, Department of Civil and Environmental Engineering, University of the Witwatersrand, Johannesburg. The results of the average compressive strength of three specimens for each curing age are represented in Table 4.10

3.7.2 Flexural Strength of Beams

For flexural strength determination, concrete beam specimen of cross section length 300 mm, breadth 100 mm and width 100 mm were cured in water for 3, 7, 14, 21, 28, 60 and 90 days. The dimensions of the each beam were determined to the nearest mm and the mass of each specimen was determined before testing.

The rollers of the compression testing machine were wiped cleaned and the concrete beam specimen placed centrally on the supporting rollers, with orientation of the cast face perpendicular to the loading face. The axis of the specimen was aligned with the centre of thrust of the spherically seated top roller holder(s), while ensuring that the axes of both the top and the supporting rollers are normal to the longitudinal axis of the specimen in accordance with SANS 5864:2006.

Demoulded prism specimens were water cured and tested at the required curing age at a loading rate of 0.6 kN/s until failure. The failure load was recorded for computations using equation 3.2 listed below. For both the control samples and for each percentage replacement of Portland cement with copper slag, three beams were tested at the required curing age for flexural strength under four point bending conditions as shown in Figure 3.12, in accordance with SANS 5864:2006. The average modulus of rupture (flexural strength) was determined using the expression in equation 3.2 for the loading method used for this experiment.

$$F_{cr} = \frac{PL}{bd^3} \quad (3.2)$$

Where;

F_{cr} is the Flexural strength, in Megapascals;

P is the maximum load at failure, in Newtons;

L is the distance between the axes of the supporting rollers, in Millimetres;

b is the width of the specimen, in Millimetres;

d is the depth of the specimen, in Millimetres.

The results of the modulus of rupture of all mixtures showed similar trend to the compressive strength results as the replacement level of copper slag increased.



Figure 3.12(a): Flexural strength test performed on concrete prisms **Figure 3.12(b): Compressive strength test performed on concrete cubes**

3.8 Concrete Durability Test Procedure

3.8.1 Coring of Samples

Water-cooled diamond tipped core barrel, with a nominal internal diameter of 70 mm, attached to a suitable coring drill shown in Figure 3.13 was used for coring concrete discs from the cubes. The concrete cubes were clamped firmly unto a holding device and the core barrel was placed perpendicular to the centre of the face to be cored. For this experimental work, a total of 20 discs with an average diameter and thickness of 70 mm and 29 mm respectively, were cored and cut as per SANS 516-1 shown in Figure 3.14.

Immediately after cutting the concrete discs, the specimens were placed in the oven at 50 °C for 7 days. The disc specimens were thereafter transferred into a desiccator for cooling to about 21 °C and relative humidity of 18% maintained inside the desiccator

which lasted for about 3 hours. The concrete discs were measured with a vernier calliper at 4 different points equally spaced around the circumference to determine the diameter and the procedure repeated to determine the depth of the cored discs. Following the aforementioned procedure, three durability tests namely; oxygen permeability, water sorptivity and chloride conductivity were performed on the cored discs.



Figure 3.13: Coring drill for cutting concrete discs specimens

Figure 3.14: Cored discs specimens of average diameter 70 mm

3.8.2 Oxygen Permeability Test Procedure

The cored disc samples were placed in a compressible collar within a rigid sleeve, with the test face at the bottom and resting against the lip of the collar. The sample, collar and rigid sleeve were placed on the permeability cell so that it covers the hole in accordance with SANS 516-2. Afterwards, the cover plate was partially tightened with the top screw on to ensure that it was centred. The setup is now tightened adequately to ensure no leakage of gas as shown in Figure 3.15. The valve of the oxygen supply tank was open to between 110 kPa to allow oxygen to flow through the permeability cell for about 5 seconds. Prior to that, oxygen inlet and outlet valves of the permeability cell were both opened as per SANS 516-2. The oxygen outlet

valve of the permeability cell was tightly closed, to ensure that there are no leaks followed by an increase the pressure in the permeability cell to above 100 kPa. The time and pressure readings in the permeability cell were then recorded in 15 minutes time steps by the data logger connected to the apparatus for about 3 hours.



Figure 3.15(a): Oxygen permeability index measuring setup **Figure 3.15(b): A computer data logger**

3.8.3 Water Sorptivity Test Procedure

The vertical curved sides of the cored disc specimen were sealed with a packing tape extended to the extreme edges of the sides towards the test face and returned into the desiccator as shown in Figure 3.16, where the temperature was controlled to about 23 ± 2 °C and 60 ± 2 % relative humidity for about 2 hours.

The thickness and diameter of each disc specimen was measured with a vernier calliper at 4 points equally spaced around the perimeter of each disc and were recorded. 10 layers of paper towel were then placed on a tray and a solution of $\text{Ca}(\text{OH})_2$ poured unto the tray, the paper towel was saturated with water visible at the

top surface. All air bubbles were removed by smoothing the paper pad towards the edge with the final water level slightly above the bottom of the edge of the each disc specimen below a maximum of 2 mm up the side as per SANS 516-4.



Figure 3.16: Cored concrete discs samples stored in a desiccator



Figure 3.17: Cored concrete discs samples being tested for sorptivity

An additional piece of the towel paper was reserved for removing excess water from the specimen and was kept next to the tray. Within 30 minutes after removing the discs specimens from the desiccator, the dry mass of the each specimen was recorded and immediately placed with the test surface on the wet paper pad and the stopwatch was started.

The specimens were weighed at 3, 5, 7, 9, 20 and 25 minutes, after patting it once on the damp piece of the absorbent paper not longer than 15 seconds and replaced each time after weighing until the maximum time of 25 minutes as per SANS 516-4. The concrete discs specimens thereafter, were vacuum saturated in water to determine the effective porosity.

3.8.4 Chloride Conductivity Test

The chloride conductivity test was conducted to assess the quality of concrete as per SANS 516-3. 2.93 kg of NaCl was added to 10 litres of water to form a brine solution in a container. The solution was stirred until all the salt had dissolved and afterwards sealed and stored for one day at a temperature of 25 °C. The concrete disc specimens were arranged to maximise their exposed surface area by standing the individual specimens upon their curved edges, rather than the flat side as per SANS 516-3 shown in Figure 3.18.

The connecting points of the conduction cells were unscrewed and the lugging capillaries of the chloride cell connected to both chambers of the cell were filled with NaCl solution. With the flexible collar in the central ring portion of the cells, the concrete disc samples were placed within the collar with one face against the plastic lip of the rigid ring. The central portion of the cathode section of the cell was screwed ensuring that the solid plastic lip presses against and compresses the flexible collar.



Figure 3.18: Concrete discs samples immersed in NaCl Solution



Figure 3.19: Concrete disc being tested for chloride conductivity

Both parts sealing each sample were tightened to ensure that there were no signs of leakage. Both the ammeter and voltmeter were connected and the DC power supply adjusted until the voltage applied across the specimen was approximately 10V. The current and voltage readings were simultaneously recorded as shown in Figure 3.19. Testing was completed within 15 minutes of removing the specimen from the suspended NaCl solution. All other concrete discs awaiting testing were stored in the NaCl solution in accordance with SANS 516-4.

3.8.5 Sulphate Attack Test Procedure

In order to investigate the effects of sulphate attack, a total of 60 concrete cubes of nominal size of 100 mm were prepared. From them, 30 cubes were used for determining the compressive strength of concrete continuously immersed in water (normal condition), while 30 cubes were used for measuring the compressive strength of concretes immersed in sulphate solution (sulphate attack condition).



Figure 3.20: Concrete cubes immersed in 50g per litre of Na_2SO_4 solution

Concrete cubes were cured for 24 hours after demoulding under standard laboratory conditions of temperature 20 ± 2 °C and a relative humidity above 50% were immersed in water for days and afterwards transferred to the sulphate solution made of 50 g per litre of Na_2SO_4 (0.352 M or 5% Na_2SO_4) at 23 °C. Similar to research performed by Najimi *et al.*, (2011) on the durability of copper slag contained concrete exposed to sulphate attack.

The specimens were kept in sulphate solution for 7, 28 and 100 days as shown in Figure 3.20, before the compressive strength test were conducted. An average of two samples were tested at constant loading rate of 1.0 kN/s at each required curing age similar to the procedure described at section 3.7.1 to compare the strength lost due to sulphate attack and those of water cured.

Chapter Four

4.0 Results and Discussion

4.1 Mineralogy Composition of Copper Slag

The X-ray diffraction (XRD) study in Figure 4.1 shows that, the mineralogical composition of the copper slag used in the study is dominated by quartz-(SiO₂) and augite-Ca(Mg, Fe)Si₂O₆ compared to copper slags used in various research projects which contains fayalite, magnetite and quartz (Alp *et al.*, 2008; Arino and Mobasher, 1999).

The glass content of the copper slag represented in Table 4.1 is approximately 99.3%, similar to Ground Granulated Blast Furnace Slag (GGBS) glass content between 85 and 90% (Saddique and Khan, 2011).

The glassy nature of a slag is responsible for its cementitious properties, with a linear relation to the late compressive strength development of concrete (Smolczyk, 1980). However, slag with completely vitreous glass may lead to strength reduction (Frigione, 1986).

4.1.2 Chemical Analysis

The X-ray fluorescence chemical analyses results of the type 1 Portland cement, procured from PPC (Ltd) and copper slag is presented in Table 4.1. It can be seen from Table 4.1 that, the calcium oxide (CaO) contribute to nearly 63% of the chemical composition of the Portland cement, whereas copper slag has a very low lime content of approximately 12%.

This indicates that copper slag is not chemically a very reactive material to be used as a cementitious material since sufficient quantity of lime must be available in order to reach the required rate of hydration and to achieve the required early-age strength. On the other hand, copper slag has high concentrations of SiO₂ and Fe₂O₃ compared with Portland cement.

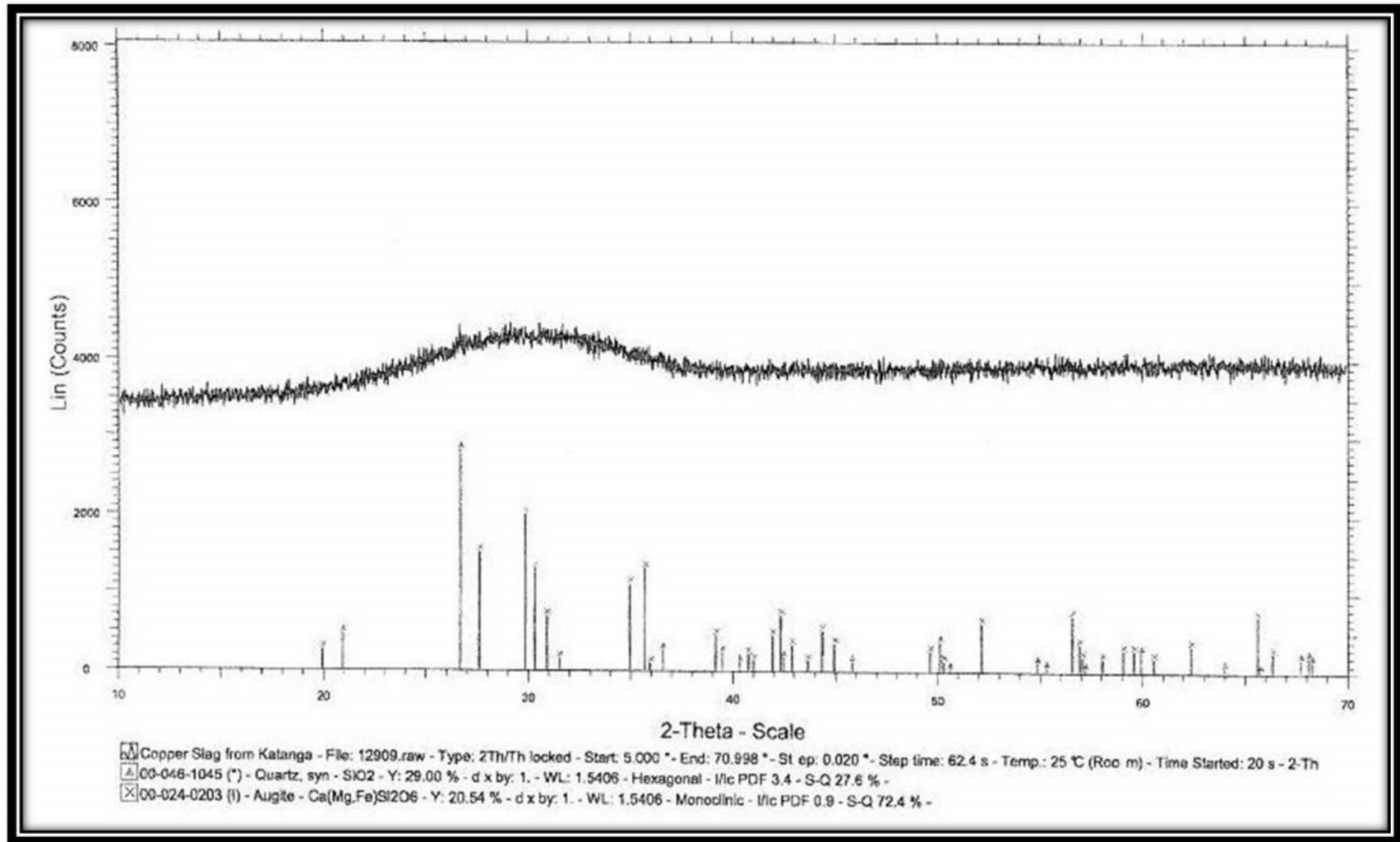


Figure 4.1: Mineralogy composition of copper slag

Table 4.1: Chemical Composition of Portland Cement and Copper Slag

Components	PC%	CS% (Lafarge ^a)	CS% (Heidelberg ^b)
SiO ₂	19.85	38.31	40.03
Al ₂ O ₃	4.78	7.28	7.24
Fe ₂ O ₃	2.38	25.91	24.40
CaO	63.06	12.31	12.53
MgO	2.32	6.41	6.62
K ₂ O	0.94	1.08	1.01
Na ₂ O	0.22	0.91	0.68
TiO ₂	0.25	0.61	0.64
Mn ₂ O ₃	0.05	0.14	0.11
P ₂ O ₅	0.26	0.20	0.19
SrO	0.3	0.02	-
ZnO	-	0.36	-
SO ₃	2.48	0.42	0.48
Loss on Ignition (LOI)	2.83	0.00	2.38
Glass content	-	-	99.3
SiO ₂ + Al ₂ O ₃ + Fe ₂ O ₃	27.01	71.5	71.7
(CaO + MgO)/SiO ₂	3.29	0.49	0.48
(CaO + 1.4 MgO + 0.56 Al ₂ O ₃)/SiO ₂	3.48	0.66	0.65

Laboratory where sample was tested; ^a - Lafarge Chemical Laboratory, Republic of South Africa, ^b - Heidelberg Cement Technology Centre GmbH, Germany

4.1.3 Pozzolanic Classification

In comparison with the chemical composition of natural pozzolans in accordance to ASTM C618-99, the summation of the three oxides (silica, alumina and iron oxide) in copper slag is nearly 72%, which exceeds the 70% percentile requirement for Class F fly ash and pozzolans. Therefore, the copper slag used is expected to have good potential to produce high quality pozzolans.

In comparison with ASTM C618-99 categorization of fly ash, Class F fly ashes are low in CaO and are normally produced from burning anthracite or bituminous coal. This class of fly ash exhibits pozzolanic property but rarely, if any, self-hardening property, with a maximum Loss on ignition (LOI) of 6.0%. Copper slag has an LOI

of 2.38% which falls below the maximum value of 6.0% as per ASTM C618-99, therefore can be categorized as a Class F fly ash.

4.1.4 Hydraulic Activity Index

In the assessment of hydraulic properties of slag as per SANS 55167-1:2011, the slag chemical composition should consist of at least two-thirds by mass of the sum of the calcium oxide (CaO), magnesium oxide (MgO) and silicon dioxide (SiO₂). The remainder shall be aluminium oxide (Al₂O₃), together with small amounts of other compounds. The most popular related formulae used to indicate the hydraulic value of a slag according to SANS 55167-1:2011 is shown in equation 4.1 below.

$$\text{Hydraulic value} = \frac{\text{CaO} + \text{MgO}}{\text{SiO}_2} \quad (4.1)$$

The result for copper slag is approximately 0.5, which is less than 1, the recommended requirement to be used as constituent for cement as per SANS 55167-1:2011.

A comprehensive assessment of the hydraulic properties of slag prescribed by Cheron and Lardinois (1968), have defined the hydraulic activity index of a slag represented in equation 4.2. The authors concluded that slag indices between 1.65 and 1.85 are considered normal for reactivity.

$$\text{Hydraulic activity index} = \frac{\text{CaO} + 0.5\text{Al}_2\text{O}_3 + 1.4\text{MgO}}{\text{SiO}_2 + \text{Al}_2\text{O}_3} \quad (4.2)$$

The XRF chemical oxides composition result for copper slag hydraulic activity index is approximately 0.65, which is significantly less than the required value for effective reactivity.

4.1.5 Results of Total Threshold Leaching Characteristics

The total trace metal constituent of the copper slag was analysed with Inductively Coupled Plasma Emission Spectroscopy (ICP-AES) in accordance with EPA methods 200.7 and 200.8 by Heidelberg Cement Technology Centre GmbH.

The value of 23,300 mg/kg for Zinc exceeds both the standard toxic leaching characteristics (STLC) (2,500 mg/kg) and total threshold leaching characteristics (TTLC) (5,000 mg/kg) limits.

The values for Chromium; Cobalt; Copper; and Lead respectively are 175; 3,200; 2,030; and 1,310 mg/kg as shown in Table 4.2, column 3. The results shows, Chromium; Cobalt; Copper; and Lead values are below the TTLC but above the STLC limits.

Further testing such as WET test or TCLP should be done for verification. If the copper slag sample concentration of Chromium, Cobalt, Copper and Lead is found to be equal to or greater than the STLC limit, then the slag is considered hazardous. However, if the outcome of the results shows less than STLC, then, copper slag could be classified as non-hazardous to the aforementioned trace elements as per EPA classification.

The values for Antimony, Arsenic, Barium, Beryllium, Cadmium, Mercury, Molybdenum, Nickel, Thallium, Selenium and Vanadium shown in Table 4.2 column 3, is below the both the STLC and TTLC limits.

Although the values for Chromium, Cobalt, Lead, Antimony, Arsenic, Barium, Cadmium, Mercury, Molybdenum, Nickel, Thallium, Selenium and Vanadium does not exceed the TTLC limits; nonetheless, the value of Zinc exceeds. On this basis alone, the copper slag can be classified as a hazardous waste as per EPA classification.

Table 4.2: TTLC Results of Trace Metals Found in Copper Slag

Substance	Range of STLC values for which further testing must be done (mg/kg)	Trace metals in Cu slag (mg/kg)	Comment	Hazardous/Non-Hazardous
Antimony	150	3.2	Low	Non-Hazardous
Arsenic*	50	4.42	Low	Non-Hazardous
Barium*	1000	337	Low	Non-Hazardous
Beryllium	7.5	3.39	Low	Non-Hazardous
Cadmium*	10	0.17	Low	Non-Hazardous
Chromium*	50	175	Exceeds STLC	Hazardous, further testing
Cobalt	800	3,200	Exceeds STLC	Hazardous, further testing
Copper	250	2,030	Exceeds STLC	Hazardous, further testing
Lead*	50	1,310	Exceeds STLC	Hazardous, further testing
Mercury*	2	0.01	Low	Non-Hazardous
Molybdenum	3,500	28	Low	Non-Hazardous
Nickel	200	2.3	Low	Non-Hazardous
Selenium*	10	4.4	Low	Non-Hazardous
Thallium	70	2	Low	Non-Hazardous
Vanadium	240	134	Low	Non-Hazardous
Zinc	2,500	23,300	Exceeds	Hazardous, further testing

* Toxic Characteristics Leaching Procedure (TCLP) metals

4.2 Results of Physical Properties of Granulated Copper Slag

4.2.1 Specific Gravity and Water Absorption

Tests to determine specific gravity and water absorption for granulated copper slag and sand were carried out in accordance with ASTM C128. Copper slag has a specific gravity of 3.12 which is higher than 2.65 for sand, which may result in the production of concrete with higher density when used as sand substitution.

Moreover, the measured water absorption for copper slag was 1.95%, slightly higher than the 0.15-0.55% documented in literature for copper slag by Shi *et al.*, (2008), this observation could be attributed to the prolonged exposure to weathering leading to increased porosity of the slag tailings.

The 1.95% measured water absorption for copper slag compared with 3.64% for sand suggests that copper slag would demand less water than that required by sand in the concrete mix. Therefore, it is expected that the free water content in concrete matrix will increase as the copper slag content increases which consequently will lead to increase in the workability of the concrete when used as fine aggregate replacement in concrete production.

Table 4.3: Physical Characteristics of Sand, Copper Slag and Coarse Aggregate

Test Type	Material		
	Sand	Copper Slag	Stone
Specific gravity	2.65	3.12	-
Fineness modulus	2.98	3.40	-
Water absorption (%)	3.64	1.95	-
Moisture content (%)	0.54	0.05	0.11
Bulk density(kg/m ³)	1550	1640	1650
Uniformity coefficient (C _u)	5.45	2.88	-
Coefficient of curvature (C _c)	0.80	1.02	-

4.2.2 Sieve Analysis

Figure 4.2 shows the sieve analysis test results conducted to determine the gradation of copper slag, fine aggregates (sand) and coarse aggregates (stone). The sand has

higher fines content than copper slag. The coefficients of curvature for sand and copper slag were 0.8 and 1.02 respectively, indicating that, the copper slag is better graded than the sand. The coefficients of uniformity values for sand and copper slag were 5.45 and 3.0 respectively; signifying that the copper slag could be classified as more uniformly graded than the sand. Both the sand and copper slag grading was within the limits as per ASTM C 33, and can be generally classified as satisfactory for the production of most concrete grades.

Table 4.4: Aggregates Gradation

Sieve Size	% Passing		Sieve size	% Passing
	Sand	Copper Slag		
4.75	96.88	99.90	-	-
2.36	81.19	96.56	-	-
1.18	63.23	75.63	-	-
0.6	38.49	25.09	26.5	100.00
0.3	17.36	8.90	19	79.90
0.15	4.77	4.39	13.2	16.65
0.075	0.85	2.14	9.5	2.49

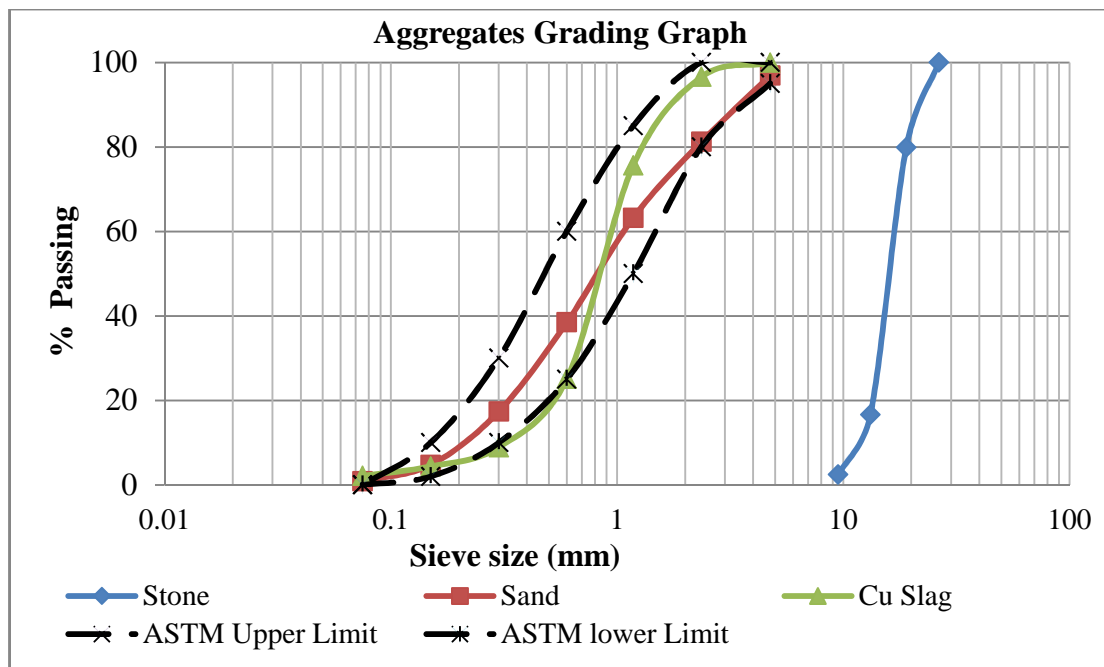


Figure 4.2: Sieve analysis of sand, copper slag and stone

4.3 Results of Physical Properties of Pulverised Copper Slag

4.3.1 Fineness Results of Copper Slag and Cement

The residue of the pulverised copper slag and cement passing through the sieves were removed, weighed and expressed as mass percentage of the quantity first placed into the sieve to the nearest 0.1%. Three sieves of sizes 45 μm , 90 μm and 212 μm were used. The results of the sieve analysis are presented below in Table 4.5.

Table 4.5: Fineness of Copper Slag and Cement

Materials	Sieve Sizes		
	45 μm	90 μm	212 μm
Copper slag	1.9	0.2	0.1
Cement	8.6	1.0	0.2

The results show that copper slag is slightly finer than Portland cement; which subsequently lead to an increase in the surface area for pozzolanic reactivity to enhance strength development. Joshi (1970) reported that, the average size of fly ash lies between 7-12 μm and the above results lies between the aforementioned ranges.

4.3.2 Blaine Air Permeability

The average Blaine air surface areas were 4000 m^2/kg and 3968 m^2/kg respectively for pulverised copper slag and cement. The results obtained above, represented below in Table 4.6, indicate that the copper slag used for this study is in the range of fineness as the Portland cement.

Table 4.6: Surface Area and Relative Density of Copper Slag and Cement

	Blaine Air Surface Area (m^2/kg)	Specific Gravity	Mass (g)
Copper slag	4000	3.13	3.05
Cement	3968	3.14	3.06

The increased surface area of the slag may lead to pronounced strength effects at early stages of hydration. This behaviour is typical of pozzolans and at later curing

ages other factors, such as influence of pore structure and diffusion controlled processes, become more significant. In general, the specific gravity varies with the iron content in the slag, from a low value of 2.8 to as high as 3.8 (Gorai *et al.*, 2002). The results of the specific gravity as represented in Table 4.6 shows that copper slag lies within the range and slightly less dense than Portland cement.

4.3.3 Setting Time

The setting time results are shown in Table 4.7. Figure 4.3 also highlights the delay in the setting time of the cement paste as the substitution level of pulverized copper slag increases. For all percentage replacement of Portland cement with copper slag, the range of setting time values conforms to the requirement as per SANS 50197-1:2000.

Table 4.7: Summary of the Initial and Final Setting Times Result

Mix Design (Replacement)	Initial Setting Time (min)	Final Setting Time (min)
Control	207	270
2.5%	333	402
5%	355	436
10%	385	480
15 %	412	512

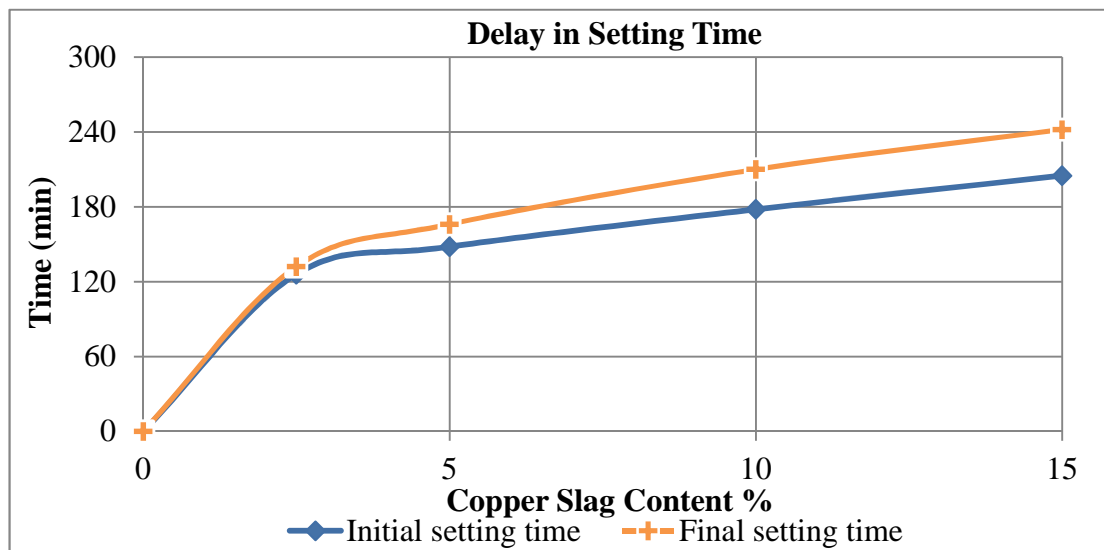


Figure 4.3: delay of initial and final setting time for cement paste

This observation could be due to delayed hydration induced by the heavy ions contained in the copper slag. This postulation is supported by Hashem *et al.*, (2011). According to the authors, the presence of Cu (II) ions retards cement hydration. Zain *et al.*, (2004) were also of the opinions that, the presence of Cu, Pb and Zn compounds in copper slag increases cement paste setting times.

4.3.4 Result of Heat of Hydration Test

4.3.4.1 Effect of Copper Slag on Heat of Hydration

A summary of the heat evolution pattern against time using the conduction calorimeter technique of the specimen is shown in Table 4.8. When water is added to the cement powder, an exothermic reaction occur generating heat to the immediate surroundings.

Table 4.8: Summary of the Heat Flow and Total Heat Dissipated

Specimen	First Hydration Phase		Second Hydration Phase		
	Time (min)	Qmax (mW/g)	Time (hr.)	Qmax (mW/g)	Total heat (J/g)
Control	10.0	5.542	15.75	1.175	37.79
2.5%	10.0	5.374	15.92	1.207	38.64
5%	10.0	4.968	15.90	1.114	35.62
10%	10.0	5.043	15.70	1.169	35.69
15%	10.0	4.882	15.80	1.124	34.85

The first peak heat rate (Qmax) occurs approximately at 10 minutes as shown in Table 4.8. With the addition of the copper slag, the shape of the curve is slightly altered and a lower peak was observed as shown in Figure 4.4. The drop in peak became more distinct with increasing copper slag content possibly due to the additional hydration of the copper slag. This hypothesis is supported by Ballim and Graham (2008) in a similar research on the hydration characteristics of GGBS.

Figure 4.5 shows an integrated graph of the total heat flow (mW/g) and total heat (J/g) up to 60 hours of hydration. The maximum heat evolution for all specimens

occurs within 15.70-15.90 hours as shown in Table 4.8 and then gradually tails off. This is similar to the rate of maximum hydration peak between 10 and 20 hours recorded in literature.

In a mix containing Portland cement only, most of the strength gain will occur about 28 days. Nonetheless, for copper slag concrete strength development may occur more slowly and continue for longer period.

For both rate of heat evolution and total heat dissipation shown in Figure 4.5, it was observed that the 2.5% cement replacement with copper slag was slightly higher than the control specimen, whereas in some cases their values overlapped each other. This aspect of the results is not conclusive and further investigation is required to confirm the outcome.

However for 5, 10 and 15% replacement with copper slag, the rate of heat evolution and the total heat gain decreased compared to the control. This result is particularly useful in the designing of mass concrete structures to control the temperature difference of the interior and external surface of the concrete.

Moreover, there was observed a delay in time to reach the second maximum hydration peak as the percentage replacement with the copper slag increased. These results demonstrated a similar trend to the initial and final setting time values determined in section 4.3.

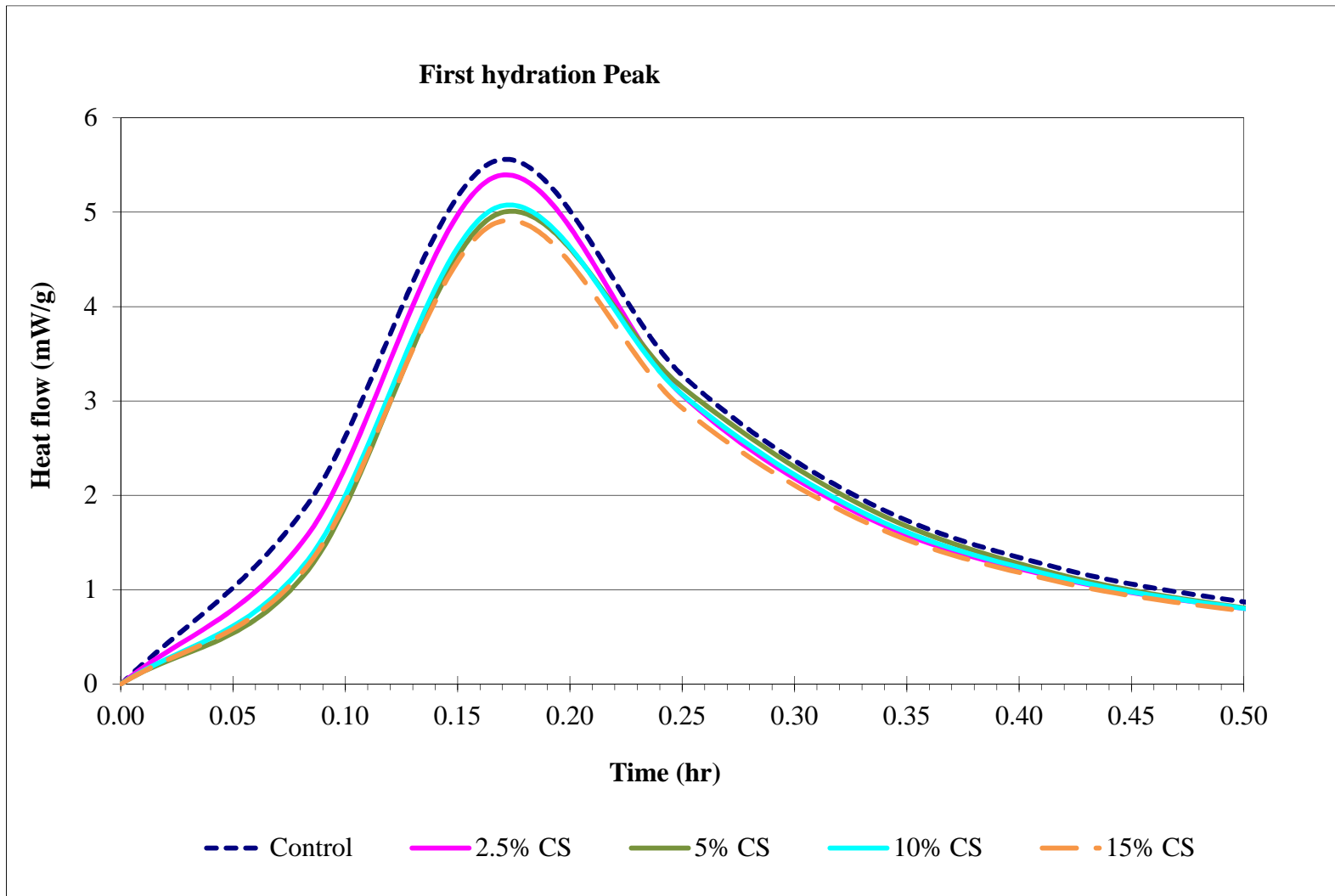


Figure 4.4: First hydration peak when adding water

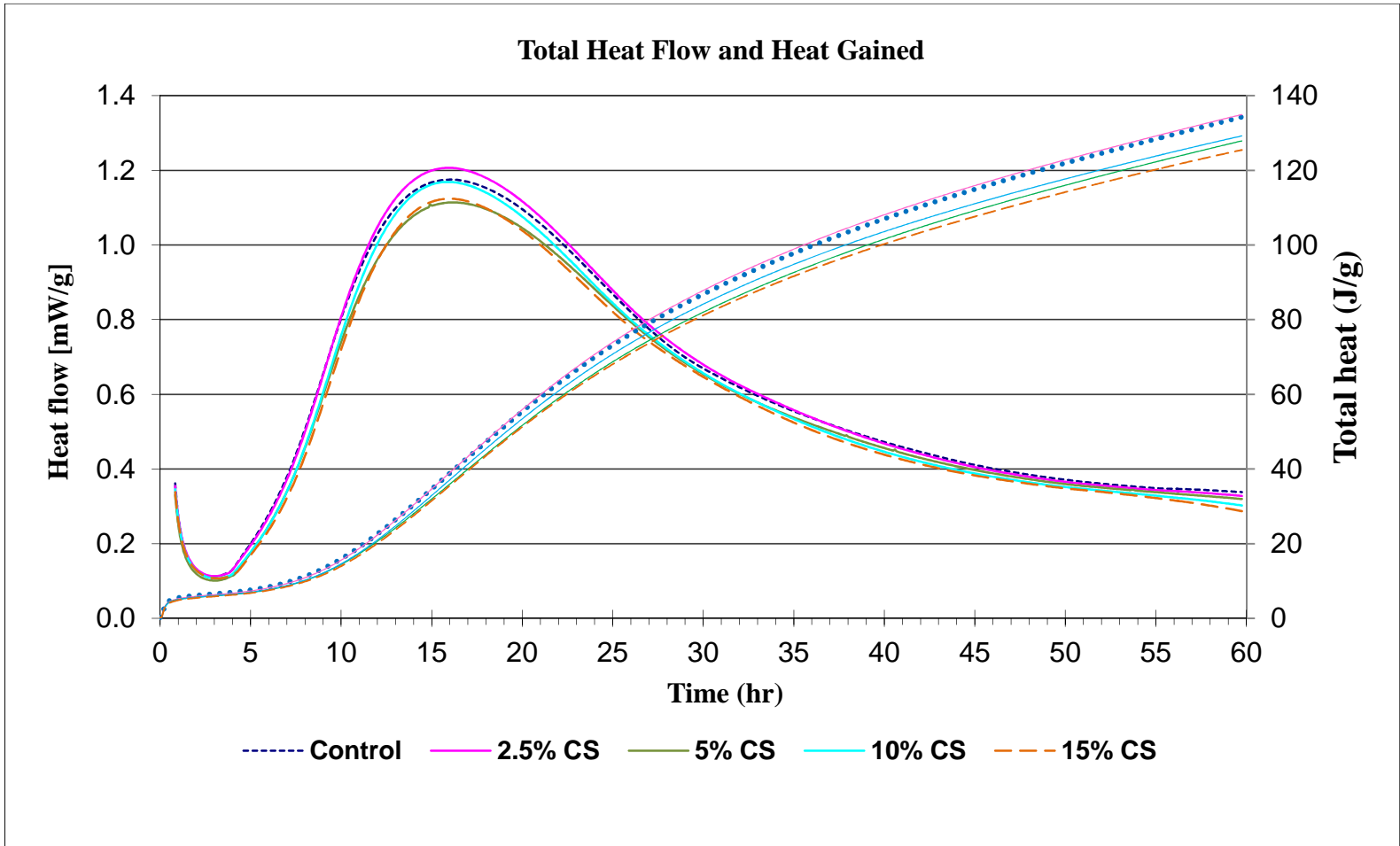


Figure 4.5: Total heat flow and total heat produced up to 60 hours of hydration

4.4 Results of Physical Properties for Copper Slag Concrete

4.4.1 Slump Test Results

Fresh concrete properties are presented in Table 4.9. From the slump results represented below, the copper slag does affect concrete workability; slumps of all concrete specimens made increased quite significantly as the proportion of the pulverized copper slag increases.

Table 4.9: Slump Properties of Fresh Concrete

Copper slag replacement	0%	2.5%	5%	10%	15%
Slump (mm)	90	100	125	130	160

Since copper slag is very similar to fly ash as a slightly less dense material compared to Portland cement, the improvement in workability was expected (Sri Ravindrarajah and Tam, 1989). This improvement would enable the reduction of water to cement ratio leading to a possible increase in the strength of concrete specimen for the same mix proportion.

4.4.2 Observed Bleeding of Concrete

Bleeding is a form of segregation where some of the water in the concrete tends to rise to the surface of the freshly placed material. This surface rise is due to the inability of the solid components of the concrete to hold all of the mixing water when they settle downwards. The bleeding of concrete was noticeably increasing with an increase in the substitution level of copper slag.

The excessive bleeding could be attributed to the glassy surface of copper slag (Ayano *et al.*, 2000). For all concrete mixes, the bleeding rate was found to decrease with elapsed time as the cement begins to harden.

4.5 Characteristic Strength Results of Copper Slag Concrete

4.5.1 Compressive Test Results

The measured compressive strength for concrete specimens up to 15% copper slag replacement with Portland cement by weight for all three curing methods, namely; water, solar and ambient air up to 90 days of curing is shown in Table 4.10. The values correspond to the mean strength of three replicate samples.

It was observed that, there was a significant decrease in the compressive strength as the copper slag content increases. The reduction trend was similar for all three curing methods namely; water, solar and ambient air up to 90 days of curing.

Moreover, for the water cured samples, the overall compressive strengths for 2.5, 5, 10 and 15% copper slag replacement at 90 days of curing were 93.8, 89.7, 88.8 and 86.5% respectively of the value for control specimen.

The overall decrease in the ultimate strength for copper slag concrete compared to control samples could be due to poor extent of hydration caused by the low hydraulic activity index of the copper slag. Alternatively, the decrease in the ultimate compressive strength for copper slag concrete samples could be attributed to the high glass content i.e. 99.3% of the copper slag.

As reported in a similar study, slag concrete with high glass content in excess of 95% significantly reduces in compressive strength (Demoulian *et al.*, 1980). Frigione (1986) acknowledged that a low percentage of crystallization between 3–5% in mass of slag is found to be beneficial to the compressive strength development of slag concrete.

For water cured samples as shown in Figure 4.6 (a) the computed percentage increase of the compressive strength between 28 to 90 days for the control sample were 5.6% compared to 7.9, 8.6, 9.0 and 9.5% respectively for 2.5, 5, 10 and 15% copper slag concrete. Thus, the strength gains in the copper slag concrete beyond 28 days were

higher than the control samples and the trend was similar for both solar and ambient air curing.

The increased in the compressive strength of copper slag concrete beyond 28 days of curing is attributed to the development in pozzolanic and hydraulic activity of copper slag. This hypothesis is supported by Arino-Moreno *et al.*, (1999). The authors concluded that significant increase in the compressive strength of hydrated lime activated copper slag concrete occurs up to 90 days of curing in water.

4.5.2 Effect of Different Curing Methods on Concrete Compressive Strength

4.5.2.1 Effect of Temperature and Humidity on Early Age Strength of Concrete

The measured compressive strength values for all three different curing methods for the copper slag concrete with a constant water-to-cement ratio are presented in Figure 4.6(a)-(e).

It is observed from Fig 4.6(a) i.e. for only the control cube samples, the water cured samples yielded a lower 3-day compressive strength of 22.0 MPa, followed by ambient air, 28.13 MPa and solar chamber curing, 28.90 MPa. This trend observed, was similar for all percentage replacement of copper slag with cement as shown in Figure 4.6(a)-(e).

It is believed that an increased in the curing temperature of average values 35°C and 25°C respectively for solar and ambient air environments, compared to water at 20°C as shown in Figure 4.7, increased the rate and extent of reaction through an increase in the heat of reaction; consequently increasing the early compressive strength development of the concrete cubes in both solar and ambient air curing methods compared to those cured in water.

Spears (1983) explained that cement hydration does not improve when cured at relative humidity below 80%. The solar chamber creates an average humidity of 90±1% compared to ambient air of 22±1% as shown in Figure 4.8. Henceforth the

overall strength development of specimen in the solar chamber performed better than those air cured.

4.5.4.2 Effect of Temperature and Humidity on Late Age Strength of Concrete

There was a significant reduction in the late strength development of all concrete specimen cured in both ambient air and solar chamber, compared to water cured specimen as shown in Fig 4.6(a)-(e). The late strength development up to 90 days of curing was high for water cured specimen followed by solar and ambient air.

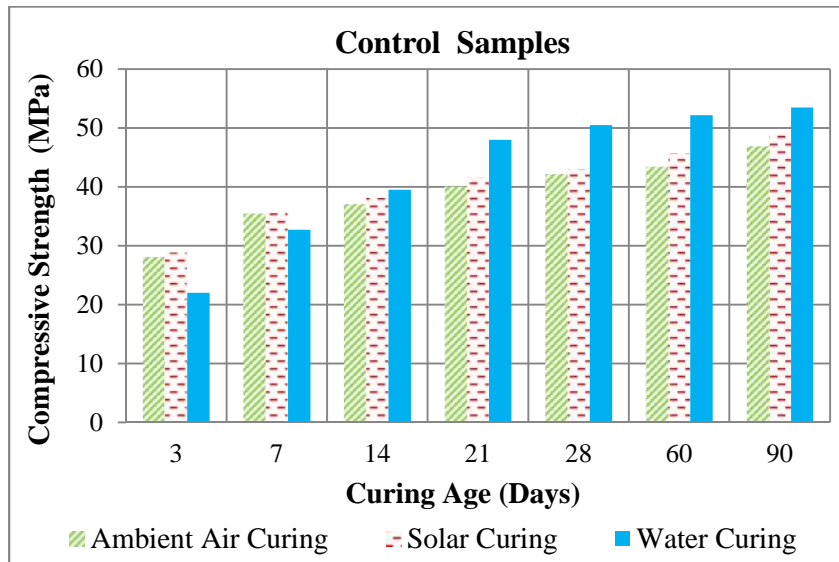
For the control samples up to 90 days of curing, the percentage increase in the compressive strength for water cured specimen, compared to the solar chamber and ambient air were respectively 8.5 and 12%. This trend was similar for all copper slag concrete from 2.5 to 15% replacement level. The higher late strength development for concrete samples cured in water could be attributed to water providing adequate moisture for improved quality and further hydration as compared to solar chamber and ambient air.

In a similar study conducted by Liu *et al.*, (2005) on the influence of steam curing on the compressive strength development of concrete containing supplementary cementing materials. The authors concluded that, at higher temperatures the rate of hydration of cement increases quickly leading to an increase in the formation of gel around individual cement particles. Faster hydration and diffusion rate of hydration product occurs, however the dissolving rate is slow. Hence, the gel layer becomes thick and dense gradually. This cause the penetration of water into the gel layer to be countered and the hydration of the remaining un-hydrated cement particles becomes retarded; causing lesser increment in the later compressive strength.

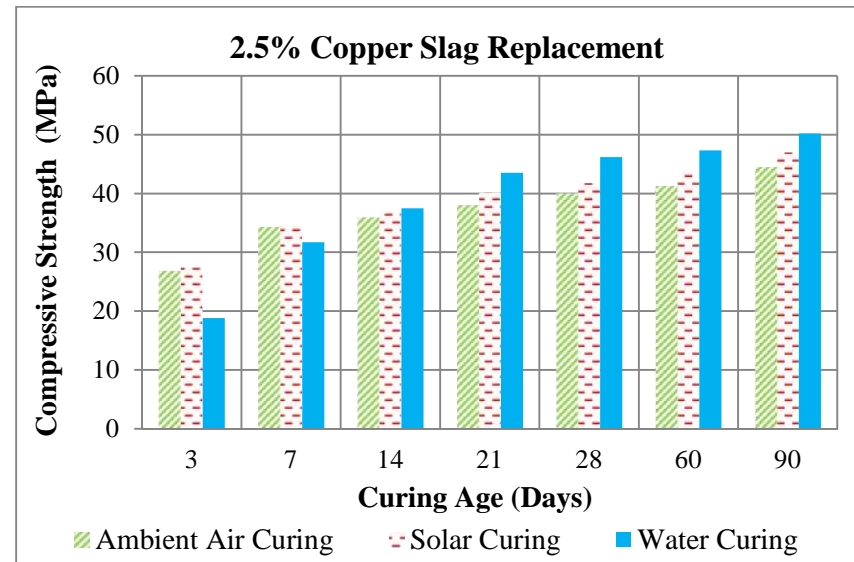
A similar research conducted by Soroka (1994) showed that at 28 days, compressive strength of cube specimens continuously wet cured were 40% higher than those cured in ambient air and attributed the higher compressive strength of the wet cured cubes specimens to the improved gel/space ratio in concrete.

Table 4.10: Compressive Strength Results of Copper Slag Concrete

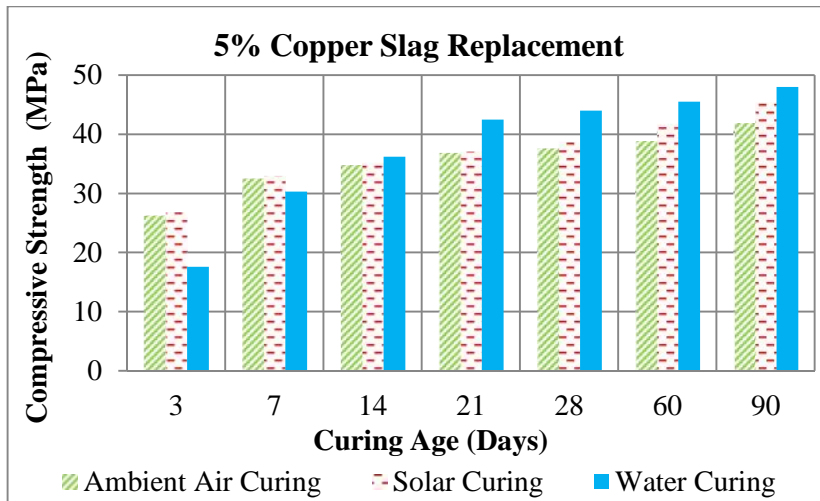
Curing Days	Copper Slag Replacement (%)														
	0%			2.5%			5%			10%			15%		
	Air	Solar	Water	Air	Solar	Water	Air	Solar	Water	Air	Solar	Water	Air	Solar	Water
3	28.13	28.90	22.00	26.90	27.53	18.80	26.23	26.87	17.60	24.37	24.70	16.90	22.30	22.67	16.50
7	35.57	35.70	32.70	34.37	34.77	31.70	32.53	32.93	30.30	30.73	30.93	28.30	28.37	28.59	27.40
14	37.10	38.23	39.50	36.03	37.20	37.50	34.80	35.23	36.20	33.43	33.87	34.50	32.50	32.53	33.30
21	40.10	41.70	48.00	38.10	40.20	43.50	36.87	37.09	42.50	34.33	35.20	40.40	33.03	34.00	38.29
28	42.22	43.12	50.50	40.08	41.83	46.20	37.60	38.75	44.00	35.35	36.25	43.20	34.35	35.53	42.30
60	43.48	45.75	52.20	41.33	44.03	47.30	38.85	41.80	45.50	36.68	39.72	44.50	35.38	38.25	44.10
90	46.98	48.95	53.50	44.57	47.04	50.20	41.91	45.39	48.00	40.08	43.01	47.50	38.60	41.15	46.30



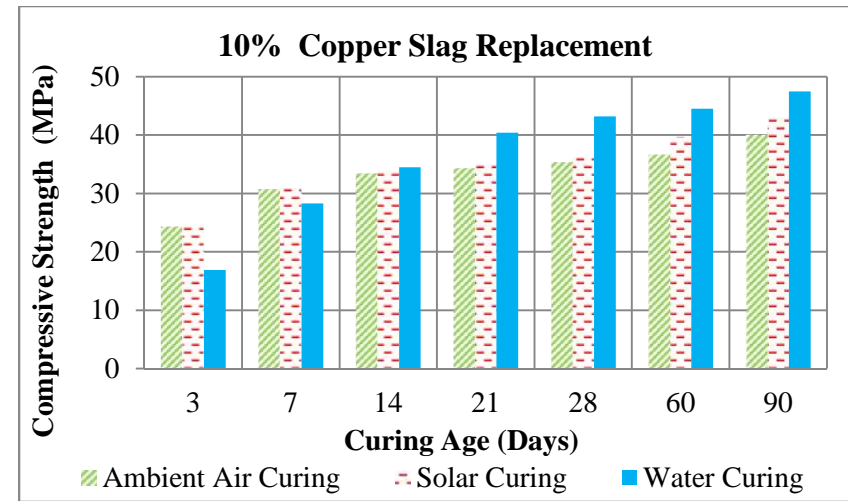
(a)



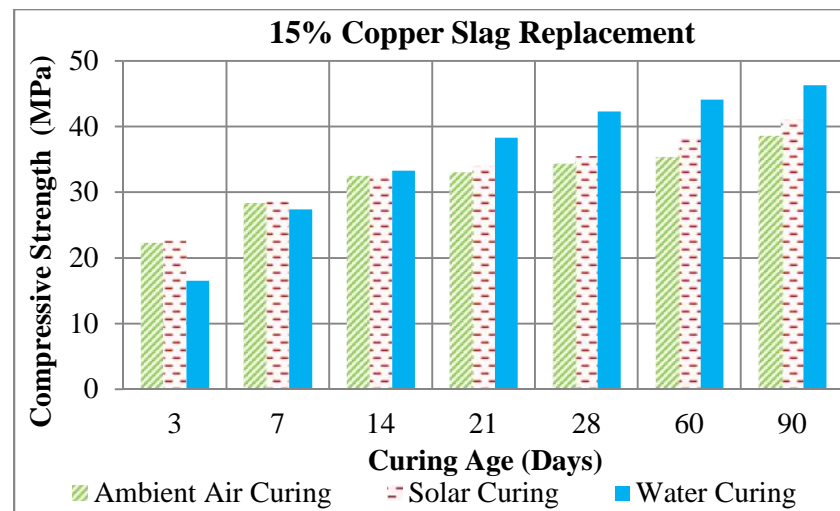
(b)



(c)



(d)



(e)

Figure 4.6 Effect of curing type on the compressive strength of concrete at (a) 0% (b) 2.5% (c) 5% (d) 10% and (e) 15% copper slag replacement

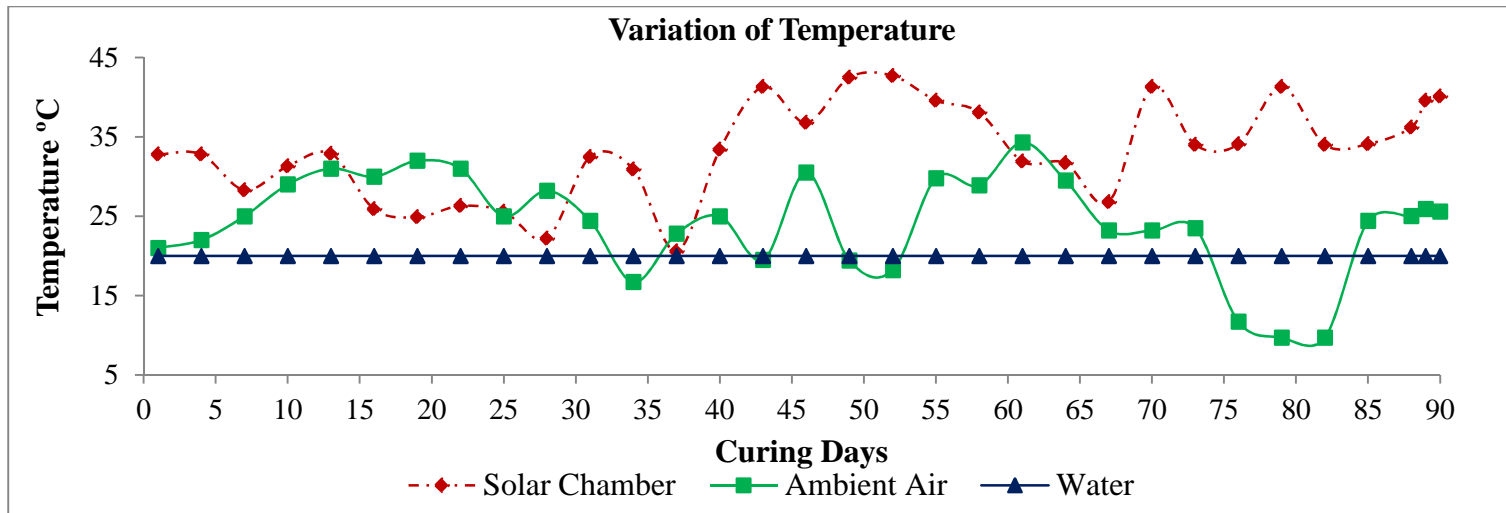


Figure 4.7: Variation of temperature for all curing methods up to 90 days of curing

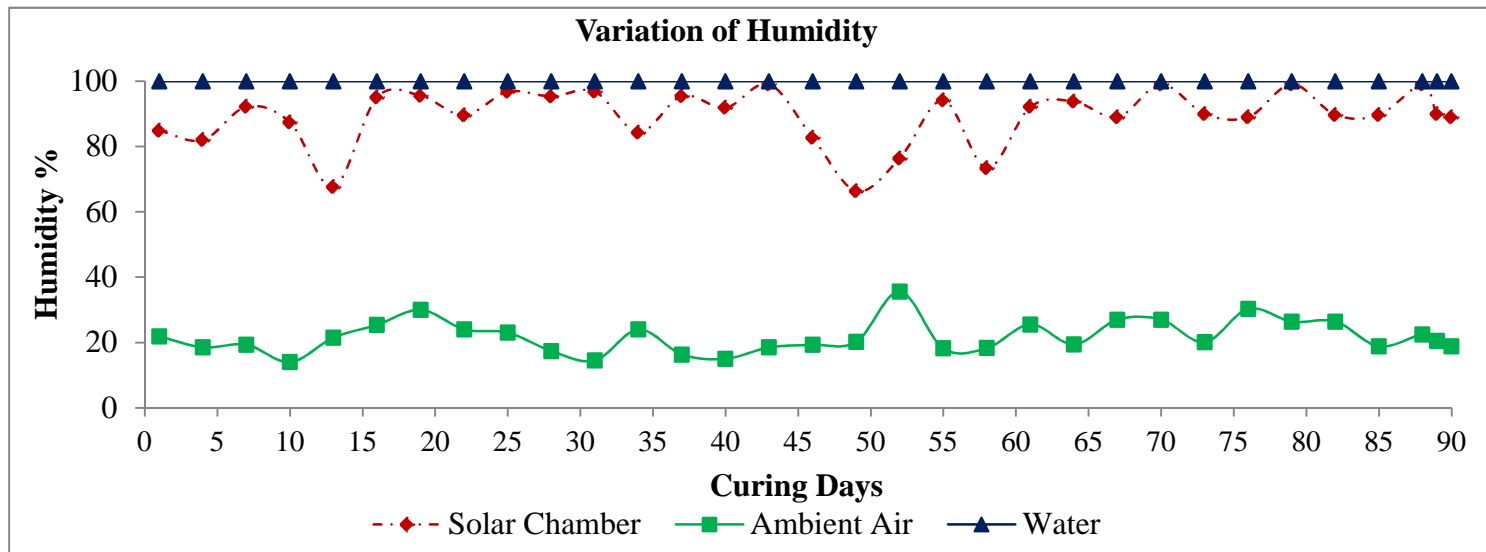


Figure 4.8: Variation of relative humidity for all curing methods up to 90 days of curing

The solar chamber creates a condition of high temperature in the surrounding concrete specimens, henceforth during the early stage of the concrete hardening process results in the formation of larger pores, which consequently increases the cumulative pore volume in the concrete interior microstructure, resulting in a negative effect on the late mechanical strength formation at later stage.

This hypothesis is supported by a similar study on the effect of curing temperature on the development of hard structure of metakaolin based geopolymer (Rovnanik, 2010). The author demonstrated that, higher curing temperatures and longer curing time increases the early age of the compressive and flexural strengths of concrete as opposed to the late mechanical strength.

The variation of relative humidity for all curing method up to 90 days is also shown in Figure 4.8. The results demonstrated in Figure 4.6(a)-(e) signify that, a higher relative humidity leads to higher later compressive strength development for water cured samples followed by solar chamber and ambient air, presumably because moisture necessary for hydration process is supplied at a higher relative humidity, consequently leading to a higher late strength for all concrete specimens.

For compressive strength development of concrete samples in relation to vapour pressure, the degree of hydration of cement is dependent on the vapour pressure within the concrete pore space (Powers, 1947). Powers (1947) explained that, the degree of hydration is negligible at vapour pressure below 30% of the saturation pressure and reduces when the vapour pressure is below 80% of the saturation pressure.

This postulation explains the importance of saturating concrete specimen by continuously wetting with water to saturate the pores, thereby promoting cement hydration. Furthermore, the quality of hydrates decreases with high curing temperature at later stages such as the case in steam curing.

4.6 Flexural Strength Test Results

The flexural strength results are shown in Table 4.11. The flexural strength generally shows a decreasing strength profile as more copper slag is added to replace cement, analogous to the trends of the compressive strength.

Table 4.11: Flexural Strength Results of Prisms Up to 90 Days of Water Curing

Curing Days	Percentage Replacement (%)				
	0	2.5	5	10	15
3	3.36	3.10	2.86	2.65	2.46
7	4.36	4.08	3.78	3.56	3.28
14	4.62	4.37	4.00	3.68	3.60
21	5.05	4.58	4.32	4.08	3.98
28	5.41	4.88	4.64	4.45	4.30
60	5.94	5.66	5.48	5.01	4.92
90	6.25	6.10	5.86	5.59	5.40

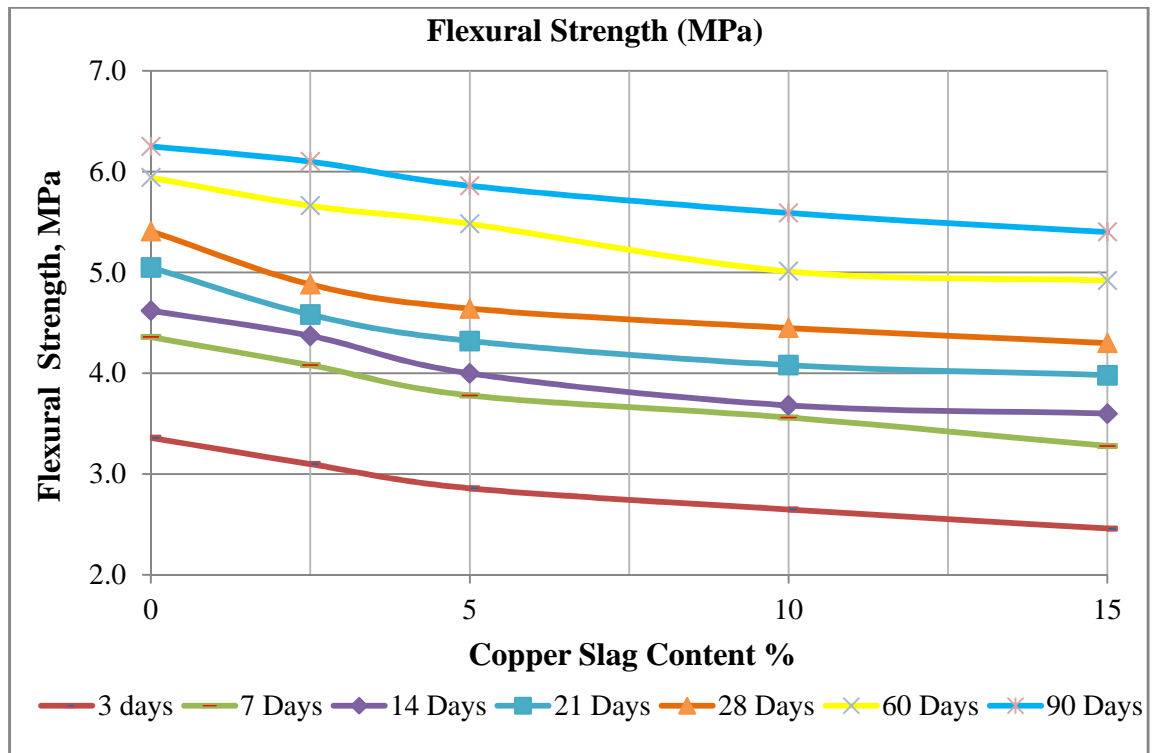


Figure 4.9: Flexural strength of pulverized copper slag concrete up to 90 days of water curing

The decline of the flexural strength as shown in Figure 4.9 is similarly attributed to poor extent of hydration caused by the low hydraulic activity index value of copper slag, similar to the trend of the compressive strength. The effect became severe as the percentage of copper slag content increased resulting in drastic drop of flexural strength. Moreover, the average computed values for the flexural strength were within 10-17% of the value of the compressive strength.

4.7 Durability Test Results

4.7.1 Results for Oxygen Permeability and Water Sorptivity Test

Table 4.12 below shows the results of oxygen permeability index (OPI) and water sorptivity below, the results of the water sorptivity trends are more consistent than the results of the oxygen permeability. This is probably due to the fact that bleed voids and other macro-defects have a smaller effect on the rate of water absorption than on air permeability. Detailed experimental results for both oxygen permeability index and water sorptivity tests are showed in the appendix, Table B2-B6 and Table B7-B11 respectively.

Table 4.12: Test Results of Oxygen Permeability Index and Water Sorptivity

Mix Design	Durability Indexes	
	Coefficient of Oxygen Permeability (mm/s)	Water Sorptivity Test (mm/hr ^{0.5})
Control	10.0	11.5
2.5% Replacement	10.0	11.0
5% Replacement	10.1	10.7
10% Replacement	10.1	10.5
15% Replacement	10.2	10.2

From the coefficient of oxygen permeability results shown in Figure 4.10, it was observed that the copper slag can be effectively used in concrete to reduce the pore size of the concrete matrix. As shown in Figure 4.11, the sorptivity of the concrete sample decreases significantly as the percentage of copper slag content increases.

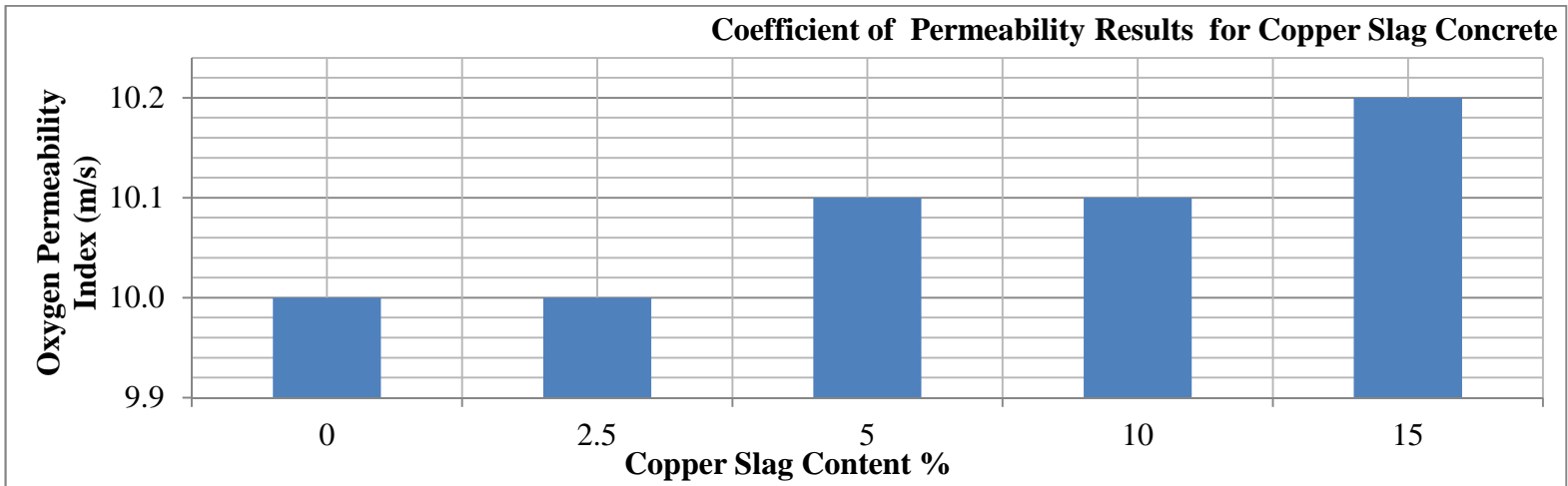


Figure 4.10: Coefficient of oxygen permeability test results

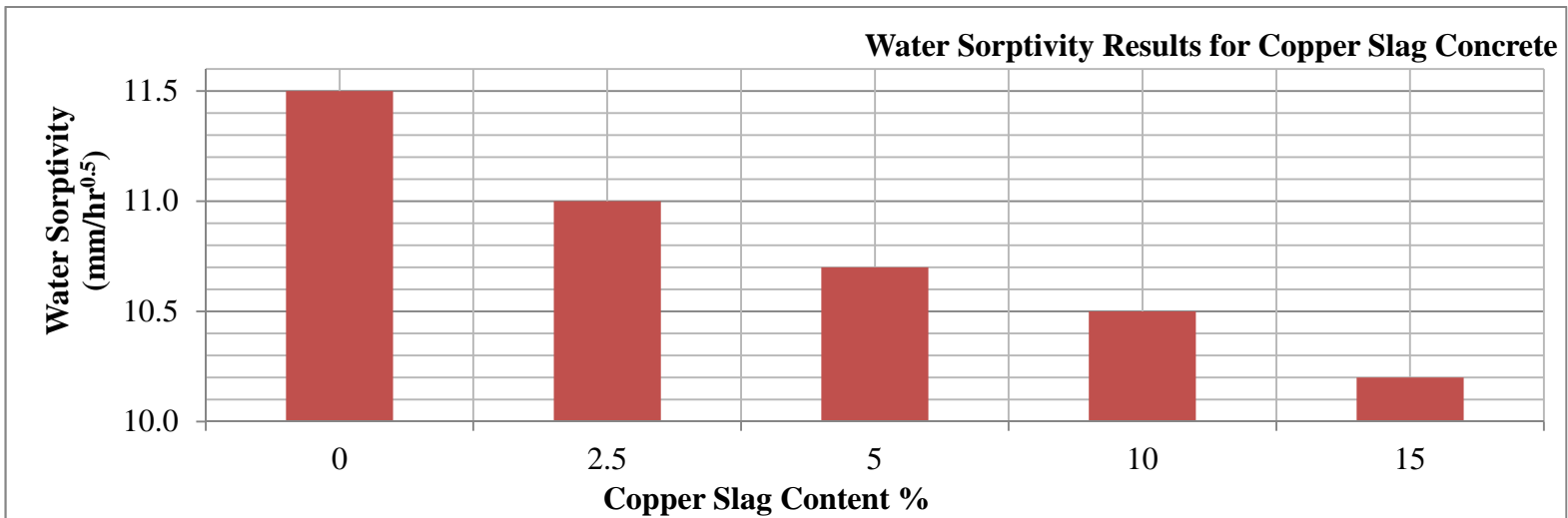


Figure 4.11: Water sorptivity test results

The reduction of sorptivity in concrete due to the addition of copper slag suggests improvement in the durability properties, which could lead to reduced ingress of chlorides, sulphates, carbon-dioxide, moisture and other deleterious ions responsible for concrete deterioration.

For all percentage replacement of cement with copper slag, the concrete samples generally performed better than the control sample; this is probably due to the pore refining effect of copper slag on Portland cement concrete because of its finer particle size and pozzolanic effect. Higher copper slag percentage replacement produced denser structure and prevents concrete from water penetration. Moreover, the copper slag reacts with water in the highly alkaline environment of the concrete pore matrix and then with calcium hydroxide to form cement hydration product through pozzolanic reaction which forms extra *C-S-H* gel in the concrete paste and slows down the strength development at early age.

This conjecture is supported by a similar research by Daube and Bakker (1986) on the addition of ground granulated blast furnace slag (GGBS) in concrete. The authors indicated that, the addition of GGBS modifies the products and the pore structure in hardened cementitious material.

4.7.2 Results for Chloride Conductivity Test

Table 4.13 below shows the average results of chloride conductivity test performed on two concrete discs per each percentage replacement. Detailed chloride conductivity test results are presented in the appendix, Table B12-B16.

Table 4.13: The Results of Chloride Conductivity Test

Mix design	Chloride Conductivity (mS/cm)
Control	2.42
2.5% Replacement	2.02
5% Replacement	1.82
10% Replacement	1.49
15% Replacement	1.30

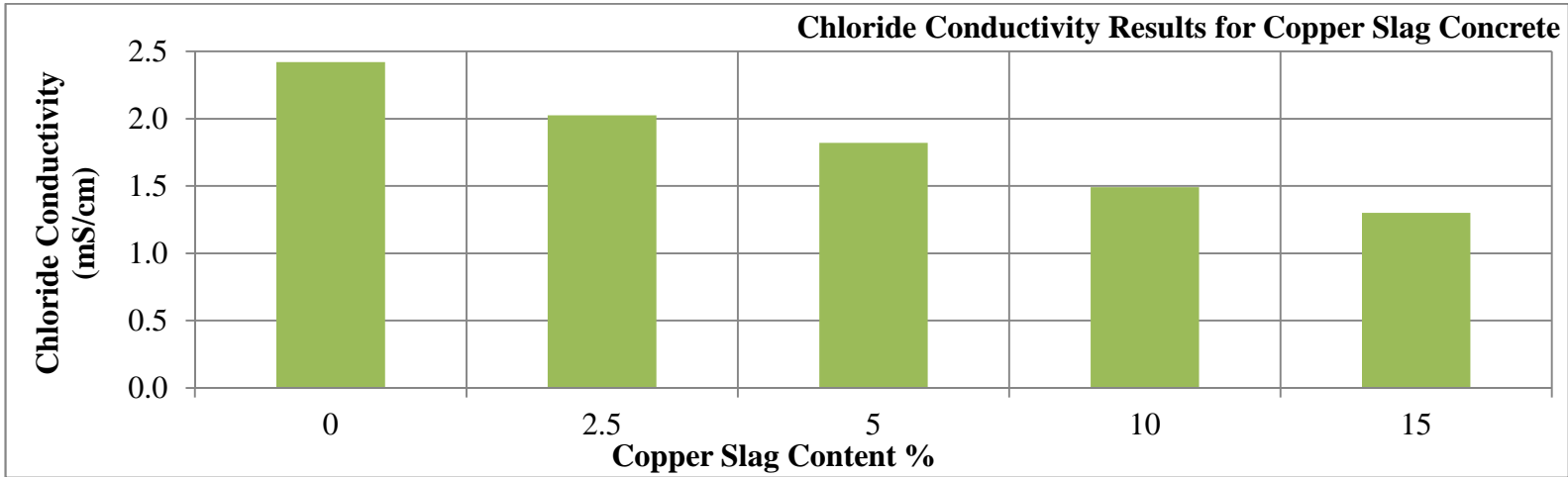


Figure 4.12: Chloride conductivity test results

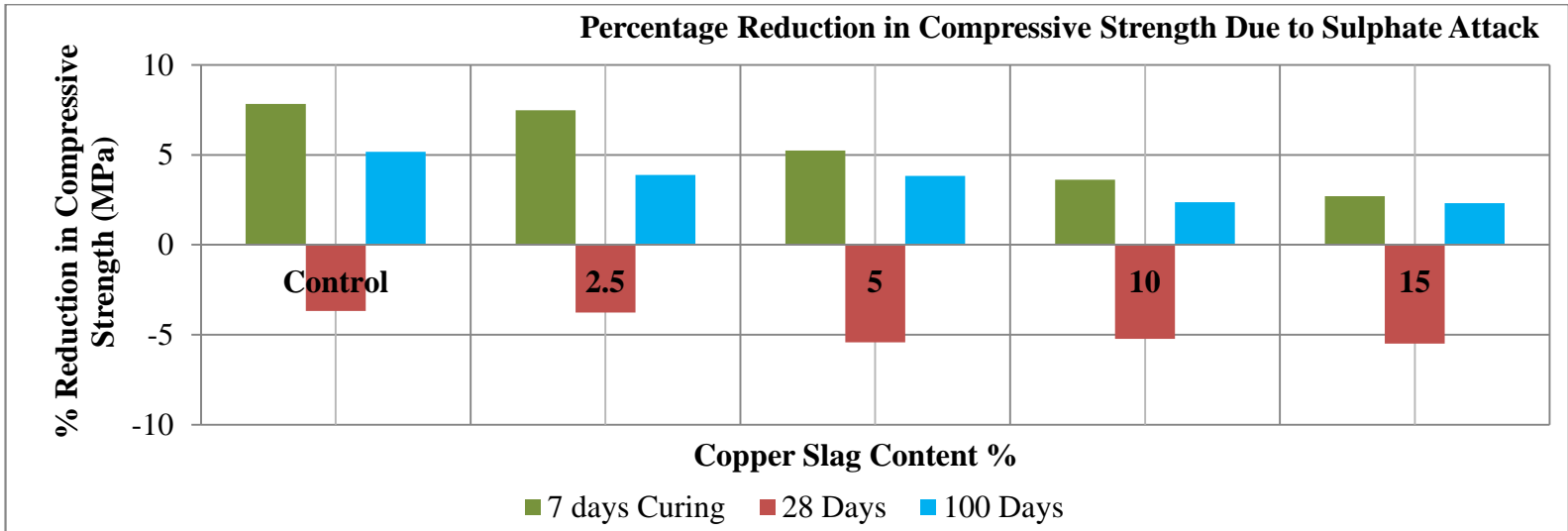


Figure 4.13: Compressive strength reduction results for sulphate attack test

As observed in Figure 4.12, the chloride conductivity of the concrete sample decreases with percentage increase of copper slag content, which could lead to reduced ingress of chlorides, and other deleterious ions responsible for concrete deterioration.

The improved chloride resistance may also be the result of refinement of the pore structure, such as occurs with silica fume concretes, or may be due to increased chloride binding by aluminate phases contained in the slag (Alexander *et al.*, 2003).

4.7.3 Results for Sulphate Immersion Test

The results of the compressive strength of samples cubes subjected sulphate attack are shown in Table 4.14. Figure 4.13 shows the change in compressive strength for concrete samples cured in water compared to those cured in 5% Na₂SO₄ at 23±2°C.

Table 4.14: Summary of Compressive Strength Test Results for Sulphate Attack

Days of Immersion	CS Content (%)	Compressive Strength (MPa)			
		Water Immersion	Sulphate Immersion	Change	Reduction (%)
7 Days	Control	42.10	38.80	3.30	7.84
	2.5	39.45	36.50	2.95	7.48
	5	37.25	35.30	1.95	5.23
	10	35.90	34.60	1.30	3.62
	15	33.20	32.30	0.90	2.71
28 Days	Control	51.60	53.50	-1.90	-3.68
	2.5	46.50	48.25	-1.75	-3.76
	5	45.15	47.60	-2.45	-5.43
	10	40.20	42.30	-2.10	-5.22
	15	38.20	40.30	-2.10	-5.50
100 Days	Control	58.63	55.60	3.03	5.17
	2.5	56.77	54.57	2.20	3.88
	5	55.60	53.47	2.13	3.83
	10	51.97	50.73	1.24	2.39
	15	50.50	49.33	1.17	2.32

As observed in Figure 4.13, for 7 and 100 days of immersion in Na_2SO_4 , the Portland cement showed little effect in resisting sulphate attack compared to the copper slag cubes. The decline in the compressive strength significantly reduced as the content of copper slag increases.

However, at 28 days of immersion, the sulphate immersed concrete showed an improved compressive strength development, compared to the water cured samples. The observation in the improved strength could be attributed to continuous hydration and filling up of pores by compounds formed due to the reactions between sulphate and cement hydration products.

Similar observations were reported by Brown (1981), the strength decline occurring in earlier age of concrete specimen, could be attributed to the leaching and conversion of cement hydrates such as $\text{Ca}(\text{OH})_2$ into gypsum.

Najimi *et al.*, (2011) concluded that, the compressive strength of concrete specimens cured in sulphate condition experienced a decreasing trend as compared to those cured in normal condition. After 21 days of suspension in sulphate solution, the amount of compressive strength decrease were 10.8, 8, 10.8, and 14.8% for control, 5, 10 and 15% respectively, whereas after 120 days, these values reached 28, 21.7, 25.9 and 23.5%.

Chapter Five

5.0 Conclusions and Recommendations

5.1 Summary

In this study, the effect of using copper slag in improving the strength and durability of concrete properties was thoroughly investigated. Pulverised copper slag was added to cement paste and concrete samples in varying proportions ranging from 2.5, 5, 10 and 15% replacing Portland cement compared to control samples.

Prior to pulverizing into powder, the granulated copper slag was assessed for its physical characteristics such as, grading, water absorption and relative density as a comparison to conventional fine aggregates (sand) used in concrete production. Chemical oxides and mineralogical composition of the copper slag were investigated using X-ray fluorescence and X-ray diffraction pattern respectively.

Total threshold leaching characteristics of the copper slag was also performed using the Inductive Coupled Plasma-Atomic Emission Spectroscopy (ICP-AES) to evaluate the limit of hazardous trace metals. For cement paste, initial and final setting time was performed using the manual Vicat apparatus and the total heat of hydration conducted using the isothermal induction calorimeter.

Characteristic strength development test performed were, compressive strength using three curing methods namely, water, solar chamber and ambient air. For flexural strength, concrete beams were only water cured up to 90 days. For concrete durability assessment, test performed included oxygen permeability, water sorptivity, chloride conductivity and sodium sulphate attack.

Detailed experimental results for all test performed are presented in the appendix.

5.2 Conclusion

Based on the experimental outcome, observations and trends determined from the results of the above experimentations, the following conclusions were made:

- i. The results of the X-ray diffraction (XRD) pattern signifies quartz-(SiO₂) and augite-Ca(Mg, Fe)Si₂O₆ as the major mineralogical composition of the copper slag, slightly different for those found in literature, which contains mainly fayalite, magnetite and quartz.
- ii. The glass content of the copper slag was approximately 99.3%, comparable to Ground Granulated Blast Furnace Slag (GGBS), with glass content between 85 and 90%. The high glassy content of the copper slag could be credited to the reduction of the overall compressive strength of the concrete.
- iii. In comparison with the chemical composition as per ASTM C618-99 natural pozzolans, the summation of the three oxides, namely, silica, alumina and iron oxides in the copper slag was approximately 72%, which exceeds the 70% percentile requirement for Class F pozzolans. Therefore, copper slag is expected to have good potential to produce high quality pozzolans.
- iv. In assessment of the hydraulic properties of slag, The XRF chemical oxides composition result for copper slag was approximately 0.5, which is less than 1, the recommended requirement to be used as constituent for cement as per SANS 55167-1:2011.
- v. The total trace metal constituent of the copper slag analysis was performed using the Inductive Coupled Plasma-Atomic Emission Spectroscopy (ICP-AES) in accordance with EPA methods 200.7 and 200.8. The results demonstrated that, copper slag is classified as a hazardous waste due to Zinc

exceeding the threshold limit in accordance with EPA classification of hazardous waste. However, the values for Chromium, Cobalt, Copper and Lead were below the total threshold leaching characteristics (TTLC) limit.

- vi. In assessment of granulated copper slag as replacement for fine aggregates in concrete production, the specific gravity test performed shows that, copper slag had a specific gravity of 3.12 significantly higher than 2.65 for sand. The higher specific absorption may result in the production of concrete with higher density when used as sand substitution. Moreover, the measured water absorption for copper slag was 1.95%, compared with 3.64% for sand suggesting that, copper slag would demand less water than required by sand for the same workability.
- vii. Sieve analyses were conducted to compare the fineness of granulated copper slag when used as concrete fine aggregates replacement. The aggregates grading curves show that, both copper slag and sand met the specification requirements in accordance to BS 882. However, the granite sand had higher fines content than the copper slag. Furthermore, the coefficients of curvature for both the sand and granulated copper slag were 0.8 and 1.02 respectively, signifying copper slag to be more uniformly graded than the sand. The coefficients of uniformity values for the sand and copper slags were 5.45 and 3.0 respectively; signifying that the copper slag could be classified as more uniformly graded than the sand. Both the sand and the granulated copper slag grading were shown to be within the limits as per ASTM C33.
- viii. The screen residue of the pulverised copper slag and cement passing through three sieves of sizes 45, 90 and 212 μm results show that, the powdered copper slag was slightly finer than Portland cement; which subsequently lead to an increase in the surface area for pozzolanic reactivity to enhance strength development.

- ix. The average Blaine air surface areas were 4000 m²/kg and 3968 m²/kg respectively for pulverised copper slag and Portland cement. The results confirmed copper slag used was about the same fineness as Portland cement.
- x. There was observed a delay in the setting time of the cement paste as the substitution level of pulverized copper slag increase. This observation could be due to delayed pozzolanic action induced by the heavy ions contained in the copper slag.
- xi. The first peak of heat flow occurred exactly at 10 minutes at 5.54 for the control sample and 5.37, 4.99, 5.04, 4.88mW/g respectively for 2.5, 5, 10 and 15% respectively. The values signified a drop in hydration peak as the copper slag content increases.
- xii. For both the rate of heat evolution and total heat dissipation, it was observed that the 2.5% cement replacement with copper slag was slightly higher than the control specimen, whereas in some cases their values overlapped each other. However, for 5, 10 and 15% replacement level with copper slag, the rate of heat evolution and the total heat evolved decreased as compared to the control cement paste. The decrease in the total amount of heat evolution is particularly useful in the designing of mass concrete structures to control the temperature difference of both internal and external surface.
- xiii. The fresh concrete properties test results, show that, copper slag affects concrete workability; slumps of all concrete specimen increased as the proportion of the pulverized copper slag increases. It is therefore possible to reduce water to cement ratio for the same mix proportion to subsequent strength increase.

- xiv. For compressive strength results, there was observed a significant decrease as the copper slag content increases. The reduction trend was similar for all the three curing methods, namely, water, solar and ambient air up to 90 days of curing. The overall decrease in the ultimate strength for copper slag concrete compared to control samples could be due to the low hydraulic activity index of the copper slag.
- xv. For the water cured samples, the compressive strength reduction was more pronounced at early curing ages. The early strength reduction of the copper slag concrete could be due to the slower rate of hydration, which is a typical characteristic of metallurgical slag influence on concrete. However, beyond 28 to 90 days, the rate of strength gain of copper slag concrete was higher than for control samples. The increase in the compressive strength of the copper slag concrete beyond 28 days of curing was attributed to the late pozzolanic and hydraulic activities.
- xvi. The measured compressive strength values all three different curing methods both for copper slag concrete with a constant water-to-cement ratio were presented. The water curing samples yielded a lower 3-day compressive strength followed by ambient air, and solar chamber curing. The trend observed was similar for all percentage replacement of copper slag. It is believed an increase in the curing temperature of average values 35°C and 25°C respectively for solar and ambient air curing environment compared to water at 20°C increased the rate and extent of reaction through an increase in the heat of reaction; consequently increasing the early compressive strength development of the concrete cubes in both solar and ambient air curing methods compared to those cured in water.
- xvii. For compressive strength development beyond 28 up to 90 days, there was a significant reduction in the late compressive strength development of all concrete cube specimens cured in both ambient air and solar chamber,

compared to water cured specimens. The late strength development was high for water cured specimens followed by solar and ambient air. The higher late strength development for concrete samples cured in water was attributed to water providing adequate moisture for further hydration as compared to solar chamber and ambient air.

Nonetheless, at higher temperatures the rate of hydration of cement increases quickly leading to an increase in the formation of gel around individual cement particles. Faster hydration and diffusion rate of hydration product occurs, however the dissolving rate is slow. As a result, the gel layer becomes thick and dense gradually causing the penetration of water into the gel layer to be countered. The hydration of the remaining un-hydrated cement particles becomes retarded; causing lesser increment in the later compressive strength.

- xviii. The flexural strength of the concrete sample generally showed a decreasing profile as more copper slag was added to replace cement up to 90 days of water curing, with a similar trend to the compressive strength profile. Moreover, the average computed values for the flexural strength were within 10-17% of the value of the compressive strength.
- xix. The chloride conductivity and water sorptivity of the concrete sample decreases as the percentage of copper slag content increases. The reduction of the water sorptivity and chloride conductivity suggests an improvement in the durability performance of the slag samples compared to control, which could lead to reduce ingress of chlorides, sulphates, carbon-dioxide, moisture and other deleterious ions responsible for concrete deterioration.
- xx. The results of the coefficient of oxygen permeability trends were irregular compared to those of chloride conductivity and water sorptivity. The observed trend could probably be due to the fact that bleed voids and other macro-defects have a smaller effect on the rate of water absorption than on air

permeability. However, the oxygen permeability results indicate that, the copper slag could be effectively used in concrete to reduce the pore size of the concrete matrix.

- xxi. For 7 and 100 days of immersion in 5% Na_2SO_4 , the Portland cement showed little effect in resisting sulphate attack compared to copper slag cubes. The decline in the compressive strength significantly reduced as the content of copper slag increased. However, at 28 days of immersion, the sulphate immersed concrete showed an improved compressive strength development, compared to the water cured samples.

This report is based on the study of the performances of concrete with partial replacement of Portland cement with pulverised copper slag up to 15%. For all percentage replacement of cement with copper slag resulted in a drop in both the compressive and flexural strength. However, the concrete disc samples generally performed better in all the three durability tests, namely oxygen permeability, water sorptivity and chloride conductivity. Additionally, for immersion in 0.325M Na_2SO_4 , the decline in the compressive strength significantly reduced as the content of copper slag increased.

A clear observation from this study is that, pulverised copper slag can be used reliably up to 15% to replace ordinary Portland cement to improve concrete durability properties.

5.3 Recommendations

While much information regarding the compressive strength performance on three different curing methods used; leaching characteristics, rate of heat evolution, initial and final setting times of copper slag concrete were also explored.

Nonetheless, a number of concerns could not be addressed due to limited time constraints. The following recommendations are therefore suggested for future work:

- The possibility of using granulated copper slag as fine and coarse aggregates replacement in concrete should be explored for compressive and flexural strength development.
- Further investigation is needed on the potential use for corrosion of reinforcement in concrete, since the copper slag has potential to resist corrosion.
- Carbonation tests should be performed to further assess its durability properties.
- There is need to study the behaviour of copper slag additive in the presence of other pozzolans such as fly ash and ground granulated blast furnace slag (GGBS).
- Long term curing period beyond 1 year should be thoroughly studied to assess later characteristics strength development.
- In addition to the cement alkali metals, the copper slag also consists of minor compounds such as K_2O and Na_2O ; which can react with some concrete aggregates causing alkali silica reaction. The copper slag concrete should therefore be tested for alkali silica reaction for durability performances.

References

- Addis, B. (2001). *Cementitious Materials and Strength of Hardened Concrete*. Fulton's Concrete Technology, Edited by Brian Addis and Gill Owens, 8th edition, Cement and Concrete Institute Midrand, South Africa. ISBN 0-9584085-5-6, pp. 7-11, 85-92.
- Addis, B. J. (1994). *Portland Cement and Cement Extenders*, Fulton's Concrete Technology, Edited by Addis, B. J, 7th edition, Cement and Concrete Institute Midrand, South Africa. ISBN 0-620-18227-X, pp. 2-7.
- Alamri, A., M. (1988). *Influence of Curing on the Properties of Concrete and Mortars in Hot Climates*, PhD thesis, Leeds University, U.K. 1988.
- Al-Ani, S., H. Mokdad, A. K, Al-Zaiwary (1998). *The Effect of Curing Period and Curing Delay on Concrete in Hot Weather*. Mater Struct 1988; 21:205–12.
- Al-Dulaijan A. U, Maslehuddin M, Al-Zahrani M. M, Sharif A. M, Shameem M, Ibrahim M. (2003). *Sulphate Resistance of Plain and Blended Cements Exposed to Varying Concentrations of Sodium Sulphate*. Cem Concr Compos. 25:429–37.
- Alexander, M. G. (2004). *Durability Indexes and Their Use in Concrete Engineering*. International RILEM Symposium on Concrete Science and Engineering: A Tribute to Arnon Bentur. Print-ISBN: 2-912143-46-2, e-ISBN: 2912143586, Publisher: RILEM Publications SARL, pp. 9-22.
- Alexander, M. G., Ballim, Y., Mackechnie, J. R. (1999). *Concrete Durability Index Testing Manual*, Research Monograph no. 4, Departments of Civil Engineering, University of Cape Town and University of the Witwatersrand.
- Alexander, M. G., Ballim, Y., Mackechnie, J. R. (1999). *Guide to The Use of Durability Indexes for Achieving Durability in Concrete Structures*. Research Monograph no. 2, Departments of Civil Engineering, University of Cape Town and University of the Witwatersrand.
- Alexander, M. G., Ballim, Y., Stanish, K. (2008). *A Framework for Use of Durability Indexes in Performance Based Design and Specifications for Reinforced Concrete Structures*. Materials and Structures, Vol. 41, pp. 921–936.
- Alexander, M. G., Jaufeerally, H. Mackechnie, J. R. (2003). *Structural And Durability*

Properties of Concrete made with Corex Slag. University of Cape Town, Research Monograph No.6

- Alexander, M. G., Mackechnie, J. R., and Ballim, Y. (2001). *Guide To The Use Of Durability Indexes For Achieving Durability in Concrete Structures*, Research monograph no 2, published by the Department of Civil Engineering, University of Cape Town in collaboration of University of the Witwatersrand, pp. 5-25
- Al-Jabri K. S., Taha, R. A, Al-Hashmi, A., and Al-Harthy, A. S, (2006). *Effect of Copper Slag and Cement by-Pass Dust Addition on Mechanical Properties of Concrete*, Construction Building Material. 20 (5) 322-331
- Al-Jabri, K. S., Hisada, M., Al-Saidy, A. H., Al-Oraimi, S. K., (2009). *Copper Slag as Sand Replacement for High Performance Concrete*. Journal of Cement and cement composite (31) 483-488
- Alnuaimi, A. S., (2009). *Use of Copper Slag as Replacement to Fine Aggregate in RC Slender Columns*. The Fourth International Conference on Computational methods and experiments in material characterization, MC'09, New Forest, UK.
- Alpha, I., et al., (2008). *Utilization of Flootation Wastes of Copper Slag as Raw Material in Cement Production*. Journal of Hazardous Materials.159,390-395
- Alter, H. (2005). *The Composition and Environmental Hazard of Copper Slags in the Context of the Basel Convention*. Resour Conserv Recycl 43(4):353–360
- Arino-Moreno, A., and Mobasher B. (1999). *Effect of Ground Copper Slag on Strength and Toughness of Cementitious Mixes*. American Concrete Institute Material Journal 96(1):68 -73.
- ASTM C 989: Standard Specification for Ground Granulated Blast-furnace Slag for Use in Concrete and Mortars. Annual Book of ASTM Standards, American Society for Testing and Materials, West Conshohocken (1999)
- ASTM C128: Standard Test Methods for Density, Relative Density, and Absorption of Fine Aggregates
- ASTM C33-03. Standard Specification for Concrete Aggregates. West Conshohocken, PA: ASTM International; 2007.
- ASTM C618-99. Standard Specifications for Coal Fly Ash and Raw or Calcined Natural

Pozzolan for Use as a Mineral Admixture in Concrete. West Conshohocken (PA): ASTM International; 1999.

- Ayano T., Sakata, K. (2000). *Durability of Concrete with Copper Slag Fine Aggregate*. The 5th CANMET/ACI international conference on durability of concrete, pp. 141–158
- Bai, J., Wild, S., Sabir, B.B. (2002). *Sorptivity and Strength of Air-Cured PC-PFA-MK Concrete and the Influence of Binder Composition on Carbonation Depth*, Cement and Concrete Research, vol. 32, pp. 1813-1821.
- Ballim, Y. and Graham, P., C. (2003). *A Maturity approach To the Rate of Heat Evolution in Concrete*. Magazine of Concrete Research, 55, No. 3, June 249-256
- Baronia, G. and Binda, L. (1994). *Study of the Pozzolanicity of some Bricks and Clays*. In Proceedings of the 10th International. Building Materials Conference, Calgary, UK; pp. 1189-1197.
- Bingol, A., and Tohumcu, I. (2013). *Effects of Different Curing Regimes on the Compressive Strength Properties of Self-Compacting Concrete Incorporating Fly Ash and Silica Fume*. Department of Civil Engineering, Atatürk University, Erzurum, Turkey. Materials and Design 51 (2013) 12–18.
- Bogue, R. H. (1947). *The Chemistry of Portland Cement*. Reinhold Publishing, New York, USA. pp. 148-160.
- Bricka, R. M., Holmes, T. T., and Cullinane, M. J. (1992). *A Comparative Evaluation of Two Extraction Procedures: The TCLP and the EP*. Technical Report EL-92-33. U.S. Army Engineer Waterways Experiment Station, Vicksburg, Mississippi
- Brindha, D., and Nagan, S. (2010). *Utilization of Copper Slag as a Partial Replacement of Fine Aggregate in Concrete*. International Journal of Earth Sciences and Engineering. ISSN 0974-5904, Vol. 03, No. 04, pp. 579-585
- Brown, P., W. (1981). *An Evaluation of the Sulphate Resistance of Cements in a Controlled Environment*. Cement and Concrete Research, vol. 11 (5/6), pp. 719-727
- BS 812. British Standard Institution (1985). Testing Aggregates-Part 103: Methods for determination of particle size distribution, Section 103.1 Sieve tests. London,
- BS EN 197-1:2000 Cement Composition, Specification and Conformity Criteria for Common Cement

- BS EN 932-1:1997. Tests for General Properties of Aggregates, Methods for Sampling
- Caliskan, S. and Behnood, A. (2004). *Recycling Copper Slag as Coarse Aggregate: Hardened Properties of Concrete*. Proceedings of the 7th International conference on concrete technology in developing countries. pp. 91-8
- Chen, W. (2006). *The hydration of slag cement, Theory, Modelling and Application*. Ph.D. thesis, University of Twente, The Netherlands.
- Cheron, M., and Lardinois, C. (1968). Proceedings of the 5th International Congress on the Chemistry of Cement, Tokyo, Vol. IV, pp. 277–285.
- Chew, S. H. and Bhariti S. K. (2009). *Use of Recycled Copper Slag in Cement Treated Singapore Marine Clay*. Proceedings of International Symposium on Geo-environmental Engineering. ISGE 2009, Hangzhou, China
- Copper Development Association (CDA) (2012). <http://www.copper.co.za/copper-ore>. Accessed 7 March 2012.
- Courard, L., Darimont, A., Schouterden, M., Ferauche, F., Willem, X., Degeimbre, R. (2003). *Durability of mortars modified with metakaolin*, Cement and Concrete Research, vol. 33, pp. 1473-1479.
- Curing of concrete, 2006, Accessed 20th October, 2013<<http://www.concrete.net.au/publications/pdf/Curing06.pdf>>
- Das, B. M, Tarquin, A. J, and Jones, A. D. (1993). *Geotechnical Properties of Copper Slag*. Transportation Research Record. Washington, DC: Transportation Research Board, 1993.
- Daube, J., and Bakker, R. (1986). *Portland Blast-Furnace Slag Cement. A Review Blended Cement*, ASTM-STP 897 pp. 5–14
- Day, R. L. and Shi, C. (1994). *Influence of the Fineness of Pozzolan on the Strength of lime Natural Pozzolan Cement Paste*. Cement and Concrete Research Journal, Vol. 24, Issue 8, PP. 485-491.
- Demoulian, E., Gourdin, P., Hawthorn, F., and Vernet, C. (1980). Proceedings of the 7th International Congress on the Chemistry of Cement, Paris, vol. 2, no. III, pp. 89-94.
- Emery, J. J. (1986). *Manitoba Slags, Deposits, Characterization, Modifications, Potential Utilization*. Toronto, Ontario: JEGEL Report, Geotechnical Engineering Limited.

- EN 196-3: 2005 European Standard, Methods of Testing Setting Time of Mortar Paste
- EN 196-6: 2005 European Standard, Methods of Testing Fineness of Cement
- Environmental Protection Agency (EPA (2005). *Solid Waste and Energy Response* (5305W). Introduction to Hazardous Waste Identifications.40 CFR Parts 261.
- Feasby, D. G. (1975). *Mineral Wastes as Railroad Ballast*. Canada Centre for Mineral and Energy Technology, National Mineral Research Program, Mineral Sciences Laboratories Report MRP/MSL (OP), Ottawa, Canada: pp. 75-6.
- Forrester, J. A. (1970). *A Conduction Calorimeter for the Study of Cement hydration*. Cement Tech. vol. I, no 3, pp. 95
- Frigione, G. (1986). *Manufacture and Characteristics of Portland Blast-Furnace Slag Cements*, in G. Frohnsdorff (ed.), *Blended Cements*, ASTM STP 897, ASTM, Philadelphia, Pennsylvania, U.S., pp. 15–28.
- Global Business Report (2012). <http://www.gbreports.com/industry>. Accessed June 2012.
- Gonnerman, H., F and Shuman, E., C. (1928). *Flexure and Tension Tests of Plain Concrete*. Major Series 171, 209 and 210. Report of the director of research. Portland cement association, pp. 149 &163
- Gorai, B., Jana, R. K., and Premchand, (2002). *Characteristics and Utilization of Copper Slag*. Resources Conservation and Recycling. 39; 299–313.
- Grafe, H. and Grube, H. (1984). *The Influence of Curing on the Gas Permeability of Concrete with Different Compositions*. Proc, RILEM seminar on the durability of concrete structures under normal outdoor exposure. Hannover University; pp. 80–7.
- Grimalt, J. O., Ferrer M., and Macpherson, E., (1999). *Science Total Environment*, 242, 3-11.
- Güneyisi, E., Gesoglu, M., Özturan, T. (2004): *Properties of Rubberized Concretes Containing Silica Fume*. Cem. Concr. Res. 34(12), 2309–2317
- Hanifi B., Orhan A. (2006). *Sulphate Resistance of Plain and Blended Cement*, Cement and Concrete Research, vol. 28, pp. 39-46.
- Haque, M., N. (1990). *Some Concretes Need 7 Days Initial Curing*. Concr Int; 12(2):42–6.
- Hardjito, D. and Rangan, B. V., (2005). *Development and Properties of Low Calcium Fly*

Ash Based Geopolymer Concrete. Research Report GCI, Faculty of Engineering, Curtin University of Technology, Perth Australia.

- Hashem, F. S., Amin, M. S., and Hekal, E. E., (2011). *Construction Building Materials* 25 (8) 3278-3282
- Ho, D. W. S. (2003). *Durability of Concrete*. In W. F. Chen & J. Y. R. Liew (Eds.), the *Civil Engineering Handbook* (2nd ed.). Boca Raton, London, New York, Washington D.C.: CRC Press.
- Hughes, M. L. and Haliburton, T. A. (1973). *Use of Zinc Smelter Waste as Highway Construction Material*. Highway Research record. 430;16-25
- Hui-sheng, S., Bi-wan, X., and Xiao-Chen Z. (2009). Influence of Mineral Admixtures on Compressive Strength, Gas Permeability and Carbonation of High Performance Concrete. *Construction Building Material*. 23(5), 1980–1985 (2009)
- Hwang, C. L and Laiw, J. C (1989). Properties of Concrete Using Copper as a Substitute for Fine Aggregates. Proceedings of the 3rd international conference on fly ash, silica fume, slag and natural pozzolans in concrete.SP-114-82 pp.1677-95
- IS: 1905-1987. *Code of Practice for Structural use of Unreinforced Masonry*. Bureau of Indian Standards, New Delhi.
- Javed, I. B. and Kenneth, J. R. (1985). *Use of Thermal Analysis in the Hydration Studies of a Type I, Portland Cement Produced From Mineral Tailings*. *Thermo chimica Acta*, Vol 91, pp. 95-105.
- Joshi, R., C. (1970): *Experimental Production of Synthetic Fly ash from Kaolinite*. MS Thesis, Iowa State University.
- Khan, S.M. and Ayers, M.E (1995). *Minimum length of curing of silica fume concrete*. *J. Mater. Civil Eng.* 7(3): 134-139.
- Khandazi, M. and Behnood, A. (2007). *Mechanical Properties of High Strength Concrete Incorporating Copper Smelter Slag*. *Cement and Concrete Composite* (under review)
- Kitobo, W. and Ilunga, N. (2012). *Use of Katanga Copper Slag in Concrete*. Department of Industrial Chemistry, University of Lubumbashi, Democratic Republic of Congo.
- Kiyak, B., Ozer A., Altundogan, S. H, Erden M., and Tumen F. (1999). *Reduction in Aqueous Solution by Using Copper Smelter Slag*. *Waste Manage.* 19:333-8.

- Komar, A. G. (1973). *Building Material and Components*. Moscow S.I; MIR Publishers. pp. 16-28
- Kumar, P. Paulo, J. M. and Monteiro (1993). *Concrete Microstructure, Properties and Materials*, McGraw-hall, 3rd edition, ISBN 0-07-146289-9, pp. 15, 21-54.
- Lafarge, 2013. *Types of Aggregates and Applications*. Accessed 30th October, 2013. <www.lafarge.ua>
- Lea, F. M. (1970). *The Chemistry of Cement Concrete 3rd Edition*; London, Edward Aranold Ltd, PP. 23-45, 358-396.
- Lind, L. (2002). *Recycling and Waste Treatment in Mineral Metal Processing: Technical and Economic Aspects*, In: Conference proceedings. Pp. 392-299, Luleå, Sweden
- Liu Baoju, Xie Youjun and Li Jian (2005). *Influence of Steam Curing on the Compressive Strength of Concrete Containing Supplementary Cementing Materials*. *Cement and Concrete Research* 35: 994–998
- Long, A. E., Henderson, G. D., & Montgomery, F. R. (2001). *Why Assess the Properties of near Surface Concrete*. *Construction and Building Materials*, 15(2-3), 65 79
- Lungu, J. (2008). *Socio-economic Change and Natural Resource Exploitation: A Case Study of the Zambian Copper Mining Industry*. *Development. Southern Africa*, 25 (5) 543-560.
- Malmros, G., and Thomas, J., D. (1977). *Least Squares Structure Refinement Based on Powder Film Intensity Data*, *J. Appl. Cryst.* 10, 107-111
- Mantel, D., G. (1991). *The Manufacture, Properties and Applications of Portland Cements, Cements Additives and Blended Cements*. PPC ISBN 0-620-16338-7
- Marghussian, V. K, and Maghsoodipor A. (1999). *Fabrication of Unglazed Floor Tiles Containing Iranian Copper Slags*. *Ceramics International*. 25:167-22.
- Marku, J., and Vaso K., (2010). *Optimisation of Copper Slag Waste Content in Blended Cement Production*. *Scientific Paper Zastita Materials*(51)
- Mehta, P. K. (2002). *Sulphate Attack on Concrete – A Critical Review*. *Material Sciences of Concrete III*, Ed. J. Skalny, The American Ceramic Society, Westerville, OH, 1992, pp. 105-130
- Micro Analytical Laboratories (2013). accessed 30th October, 2013

<<http://www.labmicro.com/chemistry/ICP/waste.htm>>.

- Mihailova, I., et al., (2011). *Catalytic Activity in Oxidation Reactions of Copper furnace Slag and Converter Slag*. Journal of the University of Chemical Technology and metallurgy, 46,2, 2011, 143-150
- Mihailova, I., Ivanov, G., and Mehandjiev, D. (2011). *Catalytic Activity in Oxidation Reactions of Copper Furnace Slag and Converter Slag*. Journal of the University of Chemical Technology and Metallurgy, 46, 2, 2011, 143-150
- Mobasher, B., Devaguptapu, R. and Arino, A. M. (1996). *Effect of Copper Slag on the Hydration of Blended Cementitious Mixtures*. In: Chong K, editor. Proceedings of the ASCE Materials Engineering Conference, Materials for the New Millennium; pp. 1677-86
- Moura, W., Goncalves, J. P. and Lima, M. B., (2007). Journal of Materials Science, 42 (7) 2226-2230.
- Moura, W., Masuero, A., Molin, D., and Vilela, A., (1999). *Concrete Performance with Admixtures of Electrical Steel Slag and Copper Slag Concerning Mechanical Properties*. Am Concrete Inst. 1999; 186:81-100.
- Mutombo, M. A., and Ilunga, N. (2011). *Development of Mining Waste in Katanga*. Case Study of Slag from the Pyro-Metallurgical Copper as Cementitious Material. University of Lubumbashi.
- Nabil, M., A. (2006). *Durability of metakaolin concrete to sulphate attack*. Cement and Concrete Research, vol. 36, pp. 1727-1734.
- Najimi, M., and Pourkhorshidi, A., R. (2011). *Properties of Concrete Containing Copper Slag*. Magazine of Concrete Research Vol 63, Issue 8.
- Najimi, M., Sobhani J., and Pourkhorshidi, A., R. (2011). *Durability of Copper Slag Contained Concrete Exposed To Sulphate Attack*. Construction and Building Materials 25 2011: 1895-1905
- Neville, A., M. (1981). *Properties of Concrete 3rd Edition*. Pitman Publishing Ltd, London, 318p
- Omar, S., B. (2002). *Attack on Plain and Blended Cements Exposed to Aggressive Sulphate Environments*, Cement and Concrete Research, vol. 24, pp. 305-316.

- Oner, A., Akyuz S. (2007). *An experimental Study on Optimum Usage of GGBS for the Compressive Strength of Concrete*. Cement Concrete Composite. 29(6), 505–514 (2007)
- Onuaguluchi, O. and Ozgur, E. (2012). *Copper Tailings as a Potential Additive in Concrete Consistency, Strength and Toxic Metal Immobilization Properties*. Indian Journal of engineering And Materials Sciences Vol. 19, April 2012, pp. 79-86.
- Osborne, G. J. (1999). *Durability of Portland Blast Furnace Slag Cement Concrete*, Cement and Concrete Composites, vol. 21, pp. 11-21.
- Powers, T. C. (1947). *A Discussion of Cement Hydration in Relation to the Curing of Concrete*. Proceedings of Highway Research Board. Vol. 27, pp. 177-88
- Price, H. W. (1951). *Factors Influencing Concrete Strength*. Journal of American Concrete Institute. Vol. 47, pp. 417-32
- Ramezani-pour, A. A. and Malhotra V., M. (1995). *Effect of curing on the Compressive Strength, Resistance to Chloride Ion Penetration and Porosity of Concretes Incorporating Slag, Fly ash, or Silica fume*. Cement Concrete Comp 1995; 17:125–33.
- Rietveld, H. M. (1969). *A Profile Refinement Method for Nuclear and Magnetic Structures*, J. Appl. Cryst. 2, 65-71
- Rodriguez-Camacho, R. E. and Uribe-Afif, R. (2002). *Important of Using the Natural Pozzolans on Concrete Durability*, Cement and Concrete Research, vol. 32, pp. 1851-1858.
- Rovnanik, P. (2010). *Effect of Curing Temperature on the Development of Hard Structure of Metakaolin-Based Geopolymer*. Construction and Building Materials, 24 pp. 1176-1183.
- Roy, W., Griffin, D. and Schuller, R. (1984). *Illinois Basin Coal Fly Ashes 1 and 2*, Environmental Science and Technology, v.18, n. 10:734 (1984)
- SABS 829: 1994. Sieve Analysis, Fines Content and Dust Content of Aggregates
- Salah, U., A. (2007). *Sulphate Resistance of Plain and Blended Cements Exposed to Magnesium Sulphate Solutions*, Construction and Building Materials, vol. 21, pp. 1792–1802.
- Sanchez de Rojas, M. I., Rivera, J., Frias, M., Esteban, J. M, and Olaya, M. (2004). *Leaching Characteristics of Blended Mortars Containing Copper Slag*. In: Proceedings

of the sixth CAN- MET/ACI International Conference on Durability of Concrete, SP-221-56; 2004. pp. 925–40.

- Sanchez de Rojas, M. I., Rivera, J., Frias, M. and Marin, F. (2008). *Review – Use of Recycled Copper Slag for Blended Cements*. Journal of Chemical Technology and Biotechnology 83(3): 209–217.
- SANS 50197-1 South African National Standard for Cement Part 1: Composition, Specifications and Conformity Criteria for Common Cements
- SANS 516-1:2012 South African National Standard for Concrete Durability Index Testing Part 1: Preparation of Samples of Test Specimen Department of Civil Engineering, University of the Cape Town publication
- SANS 516-2:2011 South African National Standard for Concrete Durability Index Testing Part 2: Oxygen permeability test. Department of Civil Engineering, University of the Cape Town publication
- SANS 516-3:2011 South African National Standard for Concrete Durability Index Testing Part 3: Chloride Conductivity
- SANS 516-4:2011 South African National Standard for Concrete Durability Index Testing Part 4: Water Sorptivity
- SANS 55167-1:2011. Ground Granulated Blast Furnace Slag for Use in Concrete, Mortar and Grout Part 1: Definitions, Specifications and Conformity Criteria
- SANS 5861-1:2006 South African National Standard Concrete tests -Mixing of Fresh Concrete
- SANS 5862-1:2011 South African National Standard Concrete tests -Slump test
- SANS 5863:2006 Concrete Tests-Compressive strength of hardened concrete
- SANS 5864:2006 Concrete Tests-Flexural strength of hardened concrete
- Senhadji, Y., Mouli, M., Khelafi, H. and Benosman, A.S. (2005). *Comportment Des Mortiers Des Ciments De l'Ouest Algérien En Environnements Acides*. 3rd Colloque Internationale de Rhéologie “CIR 05”, Bejaia, Algeria, 12-1
- Sha, W., Neill E. A. O. and Guo, Z. (1999). *Differential Scanning Calorimetry Study of Ordinary Portland cement*. Cement and Concrete Research, vol. 29, pp. 1487-1489.
- Shanxi Provincial Construction Standard Association (SPCSA) (1999). *Technical*

Specifications for the Replacement of Sand with Copper Slag in Concrete and Masonry Mortar. DBJ04-99

- Siddique, R. & Khan, M. I. (2011). *Supplementary Cementing Materials*, DOI: 10.1007/978-3-642-17866-54, Springer-Verlag Berlin Heidelberg 2011
- Sideris, K. K., Savva, A. E. and Papayianni, J. (2006). *Sulphate Resistance and Carbonation of Plain and Blended Cements*. Cement and Concrete Composites, Vol. 28, pp. 47-56.
- Skalny, J., Marchand, J. and Odler, I. (2002). *Sulphate Attack on Concrete*. Spon Press, New York, 2002.
- Smolczyk, H. G. (1980). *Slag Structure and Identification of Slags*, Proc. 7th ICCG, Vol. I, Paris, France, pp. III 1–III 3.
- Soroka, I. and Stern, N., (1979). *Effect of Calcareous Fillers on Sulphate Resistance of Portland Cement*. The Bulletin of the American Ceramic Society, 55, 594-599
- Soroka, I., Baum, H. (1994). *Influence of Specimens Size on Effect of Curing Regime on Concrete Compressive Strength*. Journal of Materials in Civil Engineering. ASCE. 6(1), pp15-22 1979
- Spears R., E. (1983). *The 80 Percent Solution to Inadequate Curing Problems*. Concrete International. Vol. 5, pp. 15-18.
- Spence, R. J. S. (1980). *Small-Scale Productions of Cementitious Materials*. ITDG. Retrieved: June 21, 2005 from: www.villageearth.org. pp.1-39
- Sri Ravindrarajah R., and Tam, C. T. (1989). *Properties of Concrete Containing Low-Calcium Fly Ash Under Hot And Humid Climate*. ACI Special Publication SP-114- 139-156
- Sudarvizhi, M., and Ilangovan R. (2011). *Performance of Copper slag and ferrous slag as partial replacement of sand in Concrete*. International Journal of Civil and Structural Engineering
- Sustainable Development-Environmental, European Commission, www.ec.europa.eu. accessed February 2012
- Tarun, R. N., Shiw, S., S. and Mohammad, M., H. (1994). *Permeability of Concrete Containing Large Amounts of Fly Ash*, Cement and Concrete Research, vol. 24, pp. 913-

922.

- Tasong, W. A., Wild, S., and Tilley, R. J. D. (1999). *Mechanism by which Ground Granulated Blast Furnace Slag Prevents Sulphate Attack of Lime Stabilized Kaolinite*. Cement Concrete Research. 29(7), 975–982
- Taylor, W. H. (1991). *Concrete Technology and Practice*, 4th Edition, New York: McGraw Hill, PP. 33-35, 47-57.
- Tixier R., Arino-Moreno, A. and Mobasher, B. (1996). *Properties of Cementitious Mixture Modified by Copper Slag*. Symposium: HH, Structure Property Relationships in Hardened cement paste and composites. Tucson, Arizona, USA: Minerals Research and Recovery
- Togerö, Å. (2004). *Leaching of Hazardous substances from Concrete Constituents and Painted Wood Panels*. Ph.D. thesis, ISBN 91-7291-527-7, Chalmers University of Technology, Gothenburg, Sweden
- Torres, S. M., Sharp, J. H., Swamy, R. N., Lynsdale, C. J. and Huntley, S. A. (2003). *Long Term Durability of Portland-Limestone Cement Mortars Exposed to Magnesium Sulphate Attack*. Cement and Concrete Composites, 25, 8947-8954
- Torri, K., Taniguchi, K. and Kawamura, M. (1995). *Sulphate Resistance of High Ash Content Concrete*, Cement and Concrete Research, vol. 25, pp. 759-768.
- Tossavainen, M., (2005). *Leaching Results in the Assessment of slag and Rock Materials as Construction Materials*. Ph.D. Thesis, ISSN:1402-1544, Luleå University of Technology, Department of Chemical and Geosciences, Division of Mineral processing
- Tsivilisa, S., Tsantilas, J., Kakali, G., Chaniotakis, E., Sakellariou, A. (2003). *The Permeability of Portland Limestone Cement Concrete*. Cement and Concrete Research, vol. 33, pp. 1465-1471.
- Wei, W., Weide, Z., and Guowei, M. (2010). *Optimum Content of Copper Slag as a Fine Aggregate in High Strength Concrete*. Materials and Design 31 (2010) 2878–2883 Contents
- Yang, H., et al., (2010). *Copper Slag with High MgO as Pozzolanic Material*. Journal of Wuhan University of Technology, vol 32 no. 17
- Young, R. A., Mackie, D. B., & Von-Dreele, R., B. (1977). *Application of The Patter*

Fitting Structure Refinement Method to X-Ray Powder Diffractometer Pattern, J. Appl. Cryst., 10, 262-269

- Yucel, O., Sahin, F. C., Sirin, B., and Addemir, O. (1999). *A Reduction Study of Copper Slag in a DC Arc Furnace*. *Scand J Metal* 1999; 28:93-9.
- Zai, M. F., Islam, M. N., Radin, S., and Yap, S. G. (2004). *Cement-based Solidification for the Safe Disposal of Blasted Copper Slag*. *Cement and Concrete Composites* 26 (7):845–851.

Appendix

Appendix A: Detailed Strength Results

Table A1: Compressive Strength Results

3 DAYS CURING									
CONTROL (5-10-2012)		2.5% CU SLAG (08-11-12)		5% Cu (09-11-2012)		10% CU SLAG(10-11-12)		15% CU SLAG(11-11-12)	
<i>WEIGHT(g)</i>	<i>FORCE(KN)</i>	<i>WEIGHT(g)</i>	<i>FORCE(KN)</i>	<i>WEIGHT(g)</i>	<i>FORCE(KN)</i>	<i>WEIGHT(g)</i>	<i>FORCE(KN)</i>	<i>WEIGHT(g)</i>	<i>FORCE(KN)</i>
2404.73	231	2350.16	190	2409.67	179	2392.1	161	2465.35	171
2465.4	211	2426.34	194	2385.15	180	2334.24	166	2430.68	171
2481.72	219	2378.05	180	2375.74	170	2427.03	167	2439.4	167
2450.62	220.33	2384.85	188.00	2390.19	176.33	2384.46	164.67	2445.14	169.67
7 DAYS CURING									
CONTROL(09-10-2012)		2.5% CU SLAG(12-11-12)		5% Cu (13-11-2012)		10% CU SLAG(14-11-12)		15% CU SLAG(15-11-12)	
<i>WEIGHT(g)</i>	<i>FORCE(KN)</i>	<i>WEIGHT(g)</i>	<i>FORCE(N)</i>	<i>WEIGHT(g)</i>	<i>FORCE(KN)</i>	<i>WEIGHT(g)</i>	<i>FORCE(KN)</i>	<i>WEIGHT(g)</i>	<i>FORCE(KN)</i>
2324.68	328	2360.36	265	2429.8	301	2426.94	230	2396.77	240
2501.76	319	2439.4	273	2312.33	314	2362.52	251	2441.7	235
2432.02	333	2415.52	261	2397.77	294	2373.26	249	2323.2	227
2419.49	326.67	2405.09	266.33	2379.97	303.00	2387.57	243.33	2387.22	234.00
14 DAYS CURING									
CONTROL(16-10-2012)		2.5% CU SLAG(19-11-12)		5% Cu (20-11-2012)		10% CU SLAG(21-11-12)		15% CU SLAG (22-11-12)	
<i>WEIGHT(g)</i>	<i>FORCE(KN)</i>	<i>WEIGHT(g)</i>	<i>FORCE(KN)</i>	<i>WEIGHT(g)</i>	<i>FORCE(KN)</i>	<i>WEIGHT(g)</i>	<i>FORCE(KN)</i>	<i>WEIGHT(g)</i>	<i>FORCE(KN)</i>
2390.89	388	2396.09	336	2425.25	370	2474.95	324	2362.15	306
2370.76	374	2437.12	330	2399.62	362	2428.73	336	2364.14	312

2386.85	364	2425.22	327	2436.61	383	2415.6	376	2402.09	321
2382.83	375.33	2419.48	331.00	2420.49	371.67	2439.76	345.33	2376.13	313.00
21 DAYS CURING									
CONTROL(23-10-2012)		2.5% CU SLAG (26-11-12)		5% Cu (27-11-2012)		10% CU SLAG (28-11-12)		15% CU SLAG (29-11-12)	
<i>WEIGHT(g)</i>	<i>FORCE(KN)</i>	<i>WEIGHT(g)</i>	<i>FORCE(KN)</i>	<i>WEIGHT(g)</i>	<i>FORCE(KN)</i>	<i>WEIGHT(g)</i>	<i>FORCE(KN)</i>	<i>WEIGHT(g)</i>	<i>FORCE(KN)</i>
2461.33	475	2366.65	396	2437.56	434	2414.17	404	2535.01	357
2464.05	485	2435.47	388	2418.54	421	2415.21	403	2454.68	360
2357.06	480	2394.67	382	2514.81	449	2432.01	405	2449.25	369
2427.48	480.00	2398.93	388.67	2456.97	434.67	2420.46	404.00	2479.65	362.00
28 DAYS CURING									
CONTROL(30-10-2012)		0.25% CU SLAG (03-12-12)		5% Cu (04-12-2012)		10% CU SLAG (05-12-12)		15% CU SLAG (06-12-12)	
<i>WEIGHT(g)</i>	<i>FORCE(KN)</i>	<i>WEIGHT(g)</i>	<i>FORCE(KN)</i>	<i>WEIGHT(g)</i>	<i>FORCE(KN)</i>	<i>WEIGHT(g)</i>	<i>FORCE(KN)</i>	<i>WEIGHT(g)</i>	<i>FORCE(KN)</i>
2418.2	515	2426.3	395	2433.82	438	2362.77	426	2360.48	412
2502.29	493	2430.56	393	2542.44	439	2506.36	430	2462.94	420
2439.64	508	2352.9	394	2337.09	443	2417.54	439	2452.07	436
2453.38	505.33	2403.25	394.00	2437.78	440.00	2428.89	431.67	2425.16	422.67
60 DAYS CURING									
CONTROL (04-12-2012)		2.5% CU SLAG(04-01-12)		5% Cu (05-01-2013)		10% CU SLAG (06-01-13)		15% CU SLAG (07-01-13)	
<i>WEIGH(g)T</i>	<i>FORCE(KN)</i>	<i>WEIGHT(g)</i>	<i>FORCE(KN)</i>	<i>WEIGHT(g)</i>	<i>FORCE(KN)</i>	<i>WEIGHT(g)</i>	<i>FORCE(KN)</i>	<i>WEIGHT(g)</i>	<i>FORCE(KN)</i>
2496.05	520	2476.2	425	2435.7	450	2365.9	440	2360.48	444
2329.05	520	2399	430	2372.1	455	2469.1	445	2462.94	442
2470.45	528	2489.1	422	2323.7	460	2476.4	450	2452.07	438
2431.85	522.67	2454.77	425.67	2377.17	455.00	2437.13	445.00	2425.16	441.33

90 DAYS CURING									
CONTROL (31-12-2012)		2.5% CU SLAG(04-02-13)		5% CU (05-02-2013)		10% CU SLAG (06-02-13)		15% CU SLAG (07-02-13)	
<i>WEIGHT(g)</i>	<i>FORCE(KN)</i>	<i>WEIGHT(g)</i>	<i>FORCE(kN)</i>	<i>WEIGHT(g)</i>	<i>FORCE(KN)</i>	<i>WEIGHT(g)</i>	<i>FORCE(KN)</i>	<i>WEIGHT(g)</i>	<i>FORCE(KN)</i>
2358.3	528	2440.9	460	2341	480	2365.9	490	2445.2	442
2404.3	538	2335.4	490	2441.3	480	2469.1	480	2464.1	476
2385.5	538	2395.1	470	2424.5	475	2476.4	456	2489.7	472
2382.70	534.67	2390.47	473.33	2402.27	478.33	2437.13	475.33	2466.33	463.33

Table A2: Flexural Test Results

3 DAYS CURING									
CONTROL (16-01-2013)		2.5% CU SLAG (06-12-12)		5% Cu (09-12-2012)		10% CU SLAG(10-12-12)		15% CU SLAG(11-12-12)	
<i>WEIGHT (kg)</i>	<i>FORCE (KN)</i>	<i>WEIGHT (kg)</i>	<i>FORCE (KN)</i>	<i>WEIGHT (kg)</i>	<i>FORCE (KN)</i>	<i>WEIGHT (kg)</i>	<i>FORCE (KN)</i>	<i>WEIGHT (kg)</i>	<i>FORCE (KN)</i>
9.5	11.4	8.24	10.2	9.2	9.6	9436.1	8.5	8751.4	8.2
9.4	11	8.36	10.4	8.32	9.4	8760.2	8.8	9292.9	8.2
8.5	11.2	8.34	10.4	8.64	9.6	8426.1	9.2	8473.6	8.2
9.13	11.20	8.31	10.33	8.72	9.53	8874.13	8.83	8839.30	8.20
7 DAYS CURING									
CONTROL(21-01-2013)		2.5% CU SLAG(13-12-12)		5% Cu (16-12-2012)		10% CU SLAG(17-12-12)		15% CU SLAG(18-12-12)	
<i>WEIGHT (kg)</i>	<i>FORCE (KN)</i>	<i>WEIGHT (kg)</i>	<i>FORCE (KN)</i>	<i>WEIGHT (kg)</i>	<i>FORCE (KN)</i>	<i>WEIGHT (kg)</i>	<i>FORCE (KN)</i>	<i>WEIGHT (kg)</i>	<i>FORCE (KN)</i>
8.02	14.7	8.27	13.8	8.43	12.4	8.45	12	8.53	11
8.68	14.3	8.39	13.4	8.46	12.8	83.49	11.8	8.45	11
8.7	14.6	8.45	13.6		12.6	8.98	11.8	9.04	10.8
8.47	14.53	8.37	13.60	8.45	12.60	33.64	11.87	8.67	10.93

14 DAYS CURING									
CONTROL(28-01-2013)		2.5% CU SLAG(20-12-12)		5% Cu (23-11-2012)		10% CU SLAG(24-12-12)		15% CU SLAG (25-12-12)	
<i>WEIGHT</i> (kg)	<i>FORCE</i> (KN)	<i>WEIGHT</i> (kg)	<i>FORCE</i> (KN)	<i>WEIGHT</i> (kg)	<i>WEIGHT</i> (kg)	<i>WEIGHT</i> (kg)	<i>FORCE</i> (KN)	<i>WEIGHT</i> (kg)	<i>WEIGHT</i> (kg)
8.7	15.4	9.2	14.6	8.9	13.2	9	12.4	8.8	12
9.16	15.6	8.88	14.4	9.4	13.4	9.6	12.2	9	11.8
9.52	15.2	9.04	14.7	9.04	13.4	8.98	12.2	9.4	12.2
9.13	15.40	9.04	14.57	9.11	13.33	9.19	12.27	9.40	12.00
21 DAYS CURING									
CONTROL(04-02-2013)		2.5% CU SLAG(27-12-12)		5% Cu (20-11-2012)		10% CU SLAG(21-11-12)		15% CU SLAG (22-11-12)	
<i>WEIGHT</i> (kg)	<i>FORCE</i> (KN)	<i>WEIGHT</i> (kg)	<i>FORCE</i> (KN)	<i>WEIGHT</i> (kg)	<i>FORCE</i> (KN)	<i>WEIGHT</i> (kg)	<i>FORCE</i> (KN)	<i>WEIGHT</i> (kg)	<i>FORCE</i> (KN)
8.46	16.7	8.56	15.2	8.23	14.4	8.66	13.6	8.88	13.2
8.32	16.8	8.02	15.2	8.32	14.2	8.92	13.8	8.9	13.6
8.62	17	8.67	15.4	8.74	14.6	8.2	13.4	8.82	13
8.47	16.83	8.42	15.27	8.43	14.40	8.59	13.60	8.87	13.27
28 DAYS CURING									
CONTROL(11-02-2012)		2.5% CU SLAG(03-01-13)		5% Cu (06-01-2013)		10% CU SLAG(07-01-13)		15% CU SLAG (08-01-2013)	
<i>WEIGH</i> <i>T(g)</i>	<i>FORCE</i> (KN)	<i>WEIGHT</i> (kg)	<i>FORCE</i> (KN)	<i>WEIGHT</i> (kg)	<i>FORCE</i> (KN)	<i>WEIGHT</i> (kg)	<i>FORCE</i> (KN)	<i>WEIGHT</i> (kg)	<i>FORCE</i> (KN)
8.46	18.2	8.46	16.4	8.46	15.6	8.46	14.8	8.46	14.2
8.32	17.9	8.32	16.2	8.32	15.4	8.32	14.9	8.32	14.4
8.62	18	8.62	16.2	8.62	15.4	8.62	14.8	8.62	14.4
8.47	18.03	8.47	16.27	8.47	15.47	8.47	14.83	8.47	14.33
60 DAYS CURING									
CONTROL(15-03-2013)		2.5% CU SLAG(03-02-13)		5% Cu (06-02-2013)		10% CU SLAG(07-02-2013)		15% CU SLAG (08-02-2013)	
<i>WEIGHT</i> (kg)	<i>FORCE</i> (KN)	<i>WEIGHT</i> (kg)	<i>FORCE</i> (KN)	<i>WEIGHT</i> (kg)	<i>FORCE</i> (KN)	<i>WEIGHT</i> (kg)	<i>FORCE</i> (KN)	<i>WEIGHT</i> (kg)	<i>FORCE</i> (KN)
8.68	19.8	9.26	18.8	8.46	18.2	9.54	16.4	8.78	16.2

8.36	19.9	8.36	18.8	9	18.6	8.58	16.8	9.28	16.4
9	19.7	8.8	19		18	9.32	16.9	8.76	16.6
8.68	19.80	8.81	18.87	8.73	18.27	9.15	16.70	8.94	16.40
90 DAYS CURING									
CONTROL(16-04-2013)		2.5% CU SLAG(05-03-13)		5% Cu (08-03-2013)		10% CU SLAG(09-03-13)		15% CU SLAG (10-03-2013)	
<i>WEIGHT</i> (kg)	<i>FORCE</i> (KN)	<i>WEIGHT</i> (kg)	<i>FORCE</i> (KN)	<i>WEIGHT</i> (kg)	<i>FORCE</i> (KN)	<i>WEIGHT</i> (kg)	<i>FORCE</i> (KN)	<i>WEIGHT</i> (kg)	<i>FORCE</i> (KN)
8.54	20.9	9.34	20.4	8.46	19.6	8.72	18.5	8.46	18.2
8.44	21.6	8.5	20.4	8.4	19.2	8.72	18.6	8.4	17.8
8.27	20	8.46	20.2	8.36	19.8	8.48	18.8	8.62	18
8.42	20.83	8.77	20.33	8.41	19.53	8.64	18.63	8.49	18.00

Appendix B: Detailed Durability Results

Table B1: Sample of the Cored Concrete Disc Dimensions

Sample 1		Sample 2		Sample 3		Sample 4	
Mean diameter (mm)	68.06	Mean diameter (mm)	68.37	Mean diameter (mm)	68.15	Mean diameter (mm)	68.19
Diameter 1 (mm)	67.33	Diameter 1 (mm)	68.68	Diameter 1 (mm)	67.99	Diameter 1 (mm)	68.27
Diameter 2 (mm)	68.33	Diameter 2 (mm)	68.28	Diameter 2 (mm)	68.28	Diameter 2 (mm)	67.94
Diameter 3 (mm)	68.28	Diameter 3 (mm)	68.38	Diameter 3 (mm)	68.17	Diameter 3 (mm)	68.21
Diameter 4 (mm)	68.30	Diameter 4 (mm)	68.15	Diameter 4 (mm)	68.15	Diameter 4 (mm)	68.32
Mean thickness (mm)	33.56	Mean thickness (mm)	31.94	Mean thickness (mm)	31.37	Mean thickness (mm)	30.20
Thickness 1 (mm)	33.27	Thickness 1 (mm)	31.73	Thickness 1 (mm)	31.00	Thickness 1 (mm)	29.99
Thickness 2 (mm)	33.63	Thickness 2 (mm)	32.11	Thickness 2 (mm)	31.45	Thickness 2 (mm)	30.26
Thickness 3 (mm)	33.60	Thickness 3 (mm)	32.20	Thickness 3 (mm)	31.00	Thickness 3 (mm)	30.33
Thickness 4 (mm)	33.72	Thickness 4 (mm)	31.70	Thickness 4 (mm)	32.04	Thickness 4 (mm)	30.23

Sample 5		Sample 6		Sample 7		Sample 8	
Mean diameter (mm)	68.22	Mean diameter (mm)	68.13	Mean diameter (mm)	68.12	Mean diameter (mm)	68.17
Diameter 1 (mm)	67.79	Diameter 1 (mm)	67.44	Diameter 1 (mm)	68.20	Diameter 1 (mm)	68.10
Diameter 2 (mm)	68.45	Diameter 2 (mm)	68.27	Diameter 2 (mm)	68.01	Diameter 2 (mm)	68.29
Diameter 3 (mm)	68.29	Diameter 3 (mm)	68.37	Diameter 3 (mm)	68.10	Diameter 3 (mm)	68.02
Diameter 4 (mm)	68.34	Diameter 4 (mm)	68.44	Diameter 4 (mm)	68.15	Diameter 4 (mm)	68.28
Mean thickness (mm)	29.23	Mean thickness (mm)	33.95	Mean thickness (mm)	29.58	Mean thickness (mm)	31.55
Thickness 1 (mm)	28.97	Thickness 1 (mm)	33.92	Thickness 1 (mm)	29.95	Thickness 1 (mm)	31.34
Thickness 2 (mm)	28.71	Thickness 2 (mm)	33.91	Thickness 2 (mm)	29.41	Thickness 2 (mm)	31.33
Thickness 3 (mm)	29.60	Thickness 3 (mm)	33.88	Thickness 3 (mm)	29.46	Thickness 3 (mm)	31.75
Thickness 4 (mm)	29.64	Thickness 4 (mm)	34.09	Thickness 4 (mm)	29.51	Thickness 4 (mm)	31.77

Oxygen Permeability Index (OPI)

Table B2: Oxygen Permeability Index Results for Control

Sample ID:	Control			Operator:	Daniel		
Date:	10/12/2013						
Average k (m/s):	1.1E-10	COV: 24.5%					
OPI:	10.0						
	33A	33B		36A		36B	
Diameter (mm)	68.12	Diameter (mm)	68.19	Diameter (mm)	68.22	Diameter (mm)	68.19
Thickness (mm)	29.58	Thickness (mm)	33.37	Thickness (mm)	29.23	Thickness (mm)	30.20
k (m/s)	1.21486E-10	k (m/s)	1.3856E-10	k (m/s)	1.139E-10	k (m/s)	7.386E-11
r ²	0.9995	r ²	0.9996	r ²	1.0000	r ²	0.9999
Time (hh.min)	Pressure (kPa)	Time (hh.min)	Pressure (kPa)	Time (hh.min)	Pressure (kPa)	Time (hh.min)	Pressure (kPa)
12.48	104.67	12.48	103.69	15.31	100.07	15.31	95.07
13.03	102.50	13.03	101.54	15.46	98.06	15.46	93.84
13.18	100.18	13.18	99.18	16.01	96.04	16.01	92.65
13.33	98.01	13.33	97.09	16.16	94.06	16.16	91.46
13.48	95.95	13.48	94.91	16.31	92.17	16.31	90.32
14.03	93.88	14.03	92.89	16.46	90.29	16.46	89.11
14.18	91.94	14.18	90.99	17.01	88.48	17.01	88.00
14.33	90.06	14.33	89.03	17.16	86.68	17.16	86.90
14.48	88.19	14.48	87.13	17.31	84.96	17.31	85.80

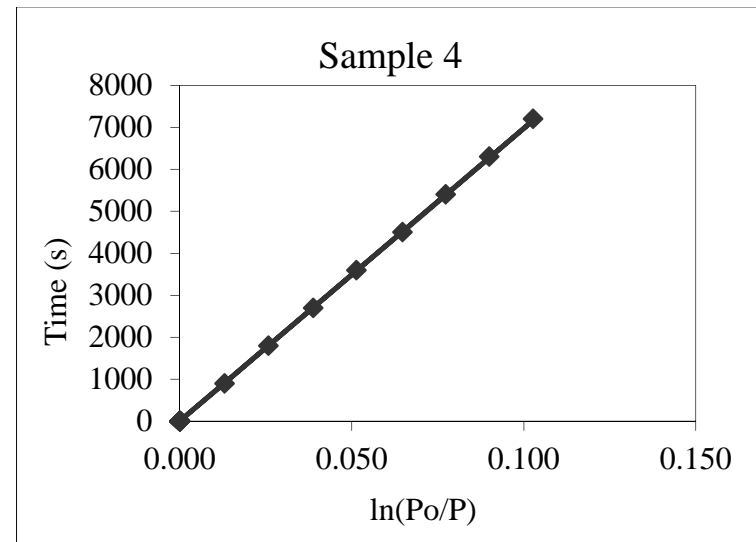
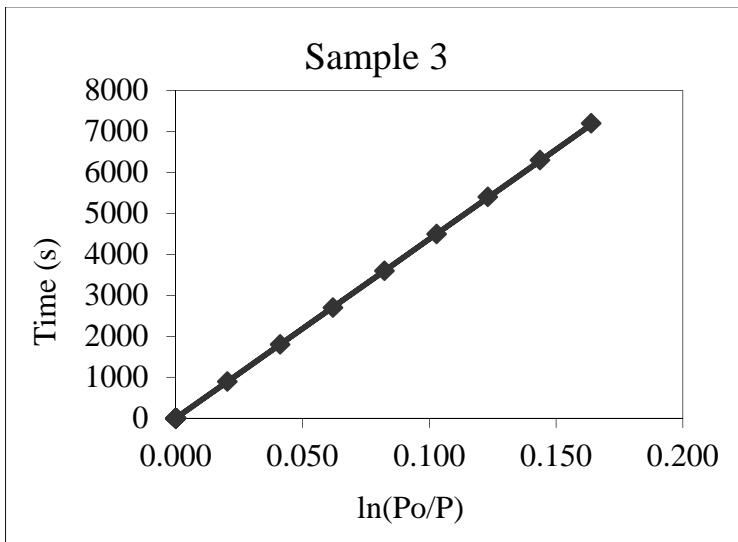
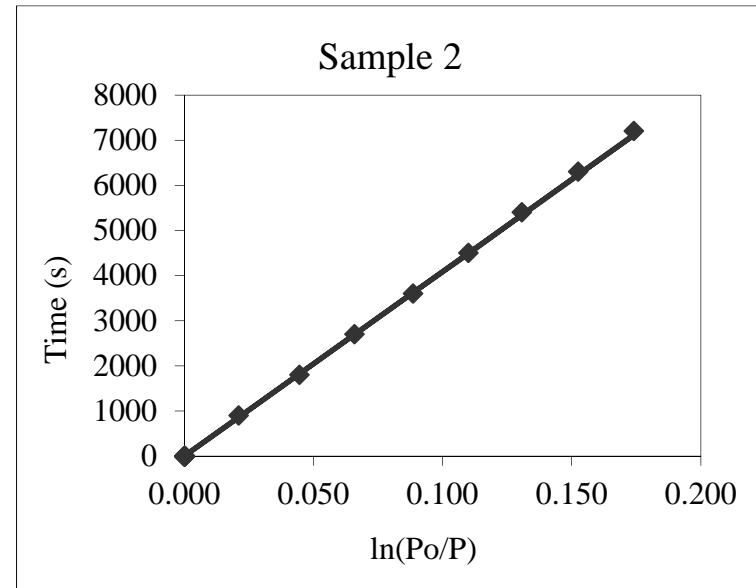
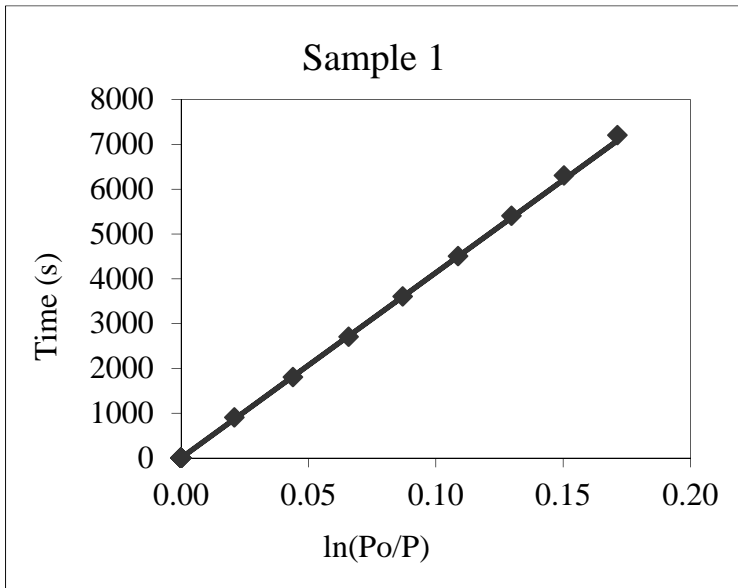


Table B3: Oxygen Permeability Index Results for 2.5% Replacement

Sample ID:	2.5% Replacement			Operator:	Daniel		
Date:	10/12/2013						
Average k (m/s):	1.1E-10	COV: 15.6%					
OPI:	10.0						
	33A	33B		36A		36B	
Diameter (mm)	68.25	Diameter (mm)	68.27	Diameter (mm)	68.32	Diameter (mm)	68.48
Thickness (mm)	30.23	Thickness (mm)	27.39	Thickness (mm)	25.05	Thickness (mm)	34.53
k (m/s)	1.00126E-10	k (m/s)	8.9244E-11	k (m/s)	1.281E-10	k (m/s)	1.136E-10
r ²	0.9998	r ²	0.9999	r ²	0.9992	r ²	0.9998
Time (hh.min)	Pressure (kPa)	Time (hh.min)	Pressure (kPa)	Time (hh.min)	Pressure (kPa)	Time (hh.min)	Pressure (kPa)
12.48	101.86	12.48	102.81	15.31	103.06	15.31	101.86
13.03	100.08	13.03	101.07	15.46	100.21	15.46	100.08
13.18	98.34	13.18	99.31	16.01	97.51	16.01	98.34
13.33	96.62	13.33	97.69	16.16	94.87	16.16	96.62
13.48	94.95	13.48	95.93	16.31	92.36	16.31	94.95
14.03	93.30	14.03	94.34	16.46	89.97	16.46	93.30
14.18	91.74	14.18	92.74	17.01	87.60	17.01	91.74
14.33	90.16	14.33	91.11	17.16	85.40	17.16	90.16
14.48	88.63	14.48	89.66	17.31	83.20	17.31	88.63

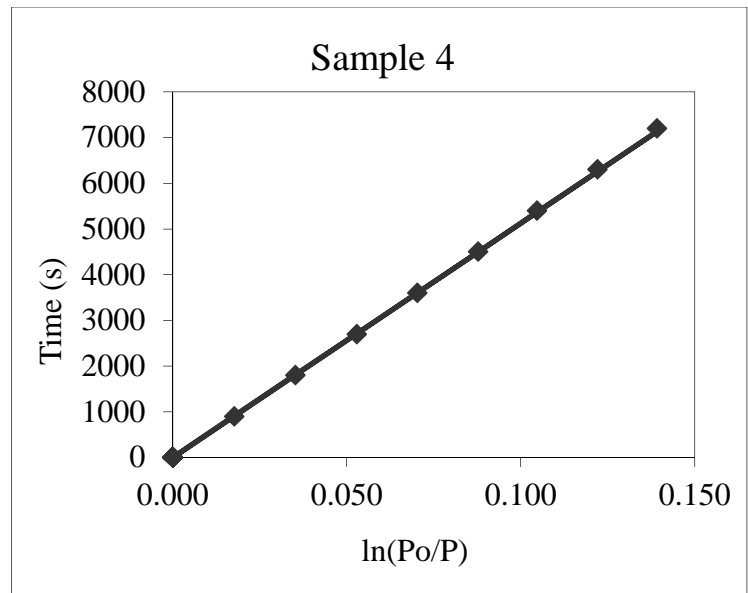
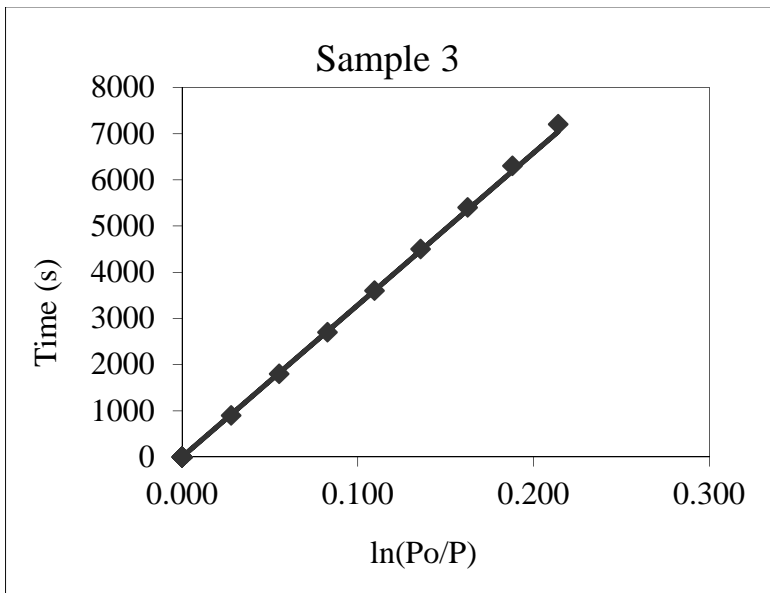
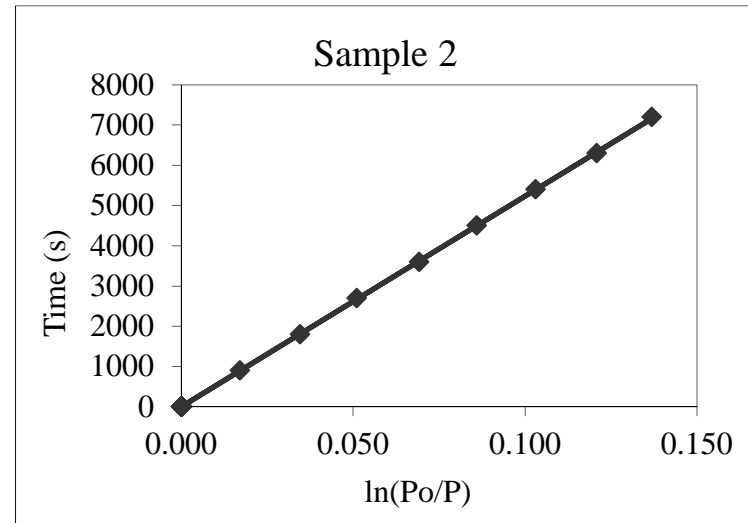
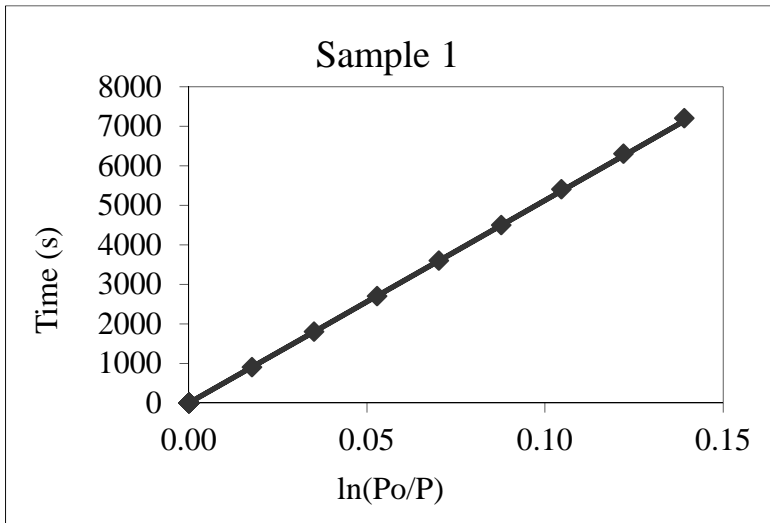


Table B4: Oxygen Permeability Index Results for 5% Replacement

Sample ID:	5% Replacement			Operator:	Daniel		
Date:	11/12/2013						
Average k (m/s):	7.6E-11	COV: 37.7%					
OPI:	10.1						
	33A	33B		36A		36B	
Diameter (mm)	68.32	Diameter (mm)	68.59	Diameter (mm)	68.52	Diameter (mm)	67.52
Thickness (mm)	30.27	Thickness (mm)	30.78	Thickness (mm)	27.05	Thickness (mm)	30.23
k (m/s)	4.4162E-11	k (m/s)	6.0314E-11	k (m/s)	1.067E-10	k (m/s)	9.136E-11
r ²	0.9983	r ²	0.9996	r ²	0.9995	r ²	0.9991
Time (hh.min)	Pressure (kPa)	Time (hh.min)	Pressure (kPa)	Time (hh.min)	Pressure (kPa)	Time (hh.min)	Pressure (kPa)
12.48	100.69	12.48	105.63	15.31	105.37	15.31	101.15
13.03	100.05	13.03	104.50	15.46	103.11	15.46	99.47
13.18	99.26	13.18	103.39	16.01	100.91	16.01	97.97
13.33	98.42	13.33	102.33	16.16	98.87	16.16	96.57
13.48	97.65	13.48	101.24	16.31	96.79	16.31	94.92
14.03	96.91	14.03	100.28	16.46	94.87	16.46	93.52
14.18	96.15	14.18	99.25	17.01	92.94	17.01	92.02
14.33	95.41	14.33	98.22	17.16	91.02	17.16	90.77
14.48	94.60	14.48	97.18	17.31	89.19	17.31	89.40

Table B5: Oxygen Permeability Index Results for 10% Replacement

Sample ID:	10% Replacement			Operator:	Daniel		
Date:	12/12/2013						
Average k (m/s):	8.1E-11	COV: 40.8%					
OPI:	10.1						
	33A	33B		36A		36B	
Diameter (mm)	68.51	Diameter (mm)	68.25	Diameter (mm)	67.52	Diameter (mm)	67.52
Thickness (mm)	29.82	Thickness (mm)	31.71	Thickness (mm)	30.51	Thickness (mm)	30.23
k (m/s)	5.10365E-11	k (m/s)	8.0931E-11	k (m/s)	1.269E-10	k (m/s)	6.472E-11
r ²	0.9982	r ²	0.9992	r ²	0.9999	r ²	0.9996
Time (hh.min)	Pressure (kPa)	Time (hh.min)	Pressure (kPa)	Time (hh.min)	Pressure (kPa)	Time (hh.min)	Pressure (kPa)
12.48	97.91	12.48	101.65	15.31	105.13	15.31	102.21
13.03	96.92	13.03	100.17	15.46	102.89	15.46	101.07
13.18	96.04	13.18	98.86	16.01	100.64	16.01	99.97
13.33	95.24	13.33	97.56	16.16	98.55	16.16	98.79
13.48	94.33	13.48	96.27	16.31	96.45	16.31	97.80
14.03	93.56	14.03	95.02	16.46	94.41	16.46	96.68
14.18	92.72	14.18	93.75	17.01	92.49	17.01	95.64
14.33	91.93	14.33	92.58	17.16	90.53	17.16	94.64
14.48	91.10	14.48	91.33	17.31	88.54	17.31	93.60

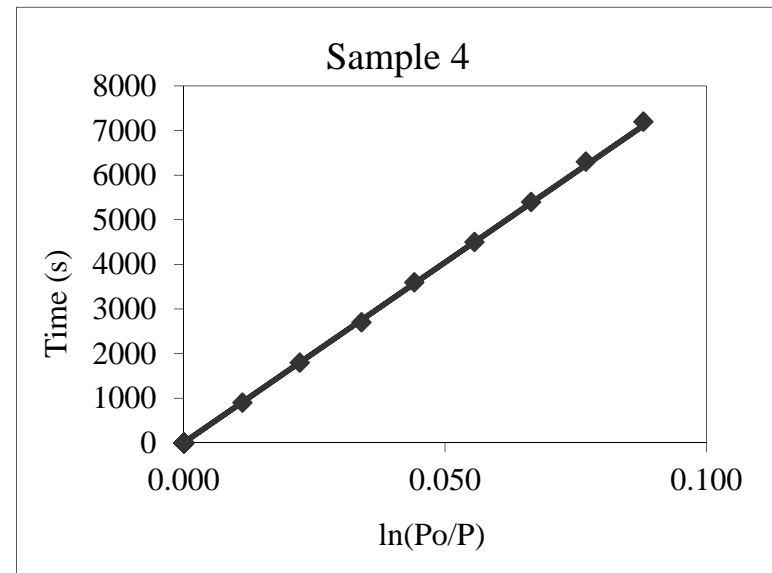
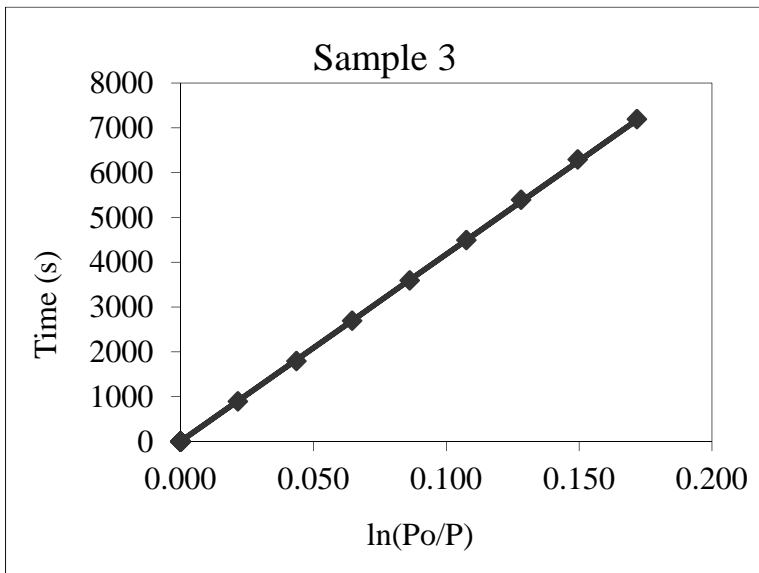
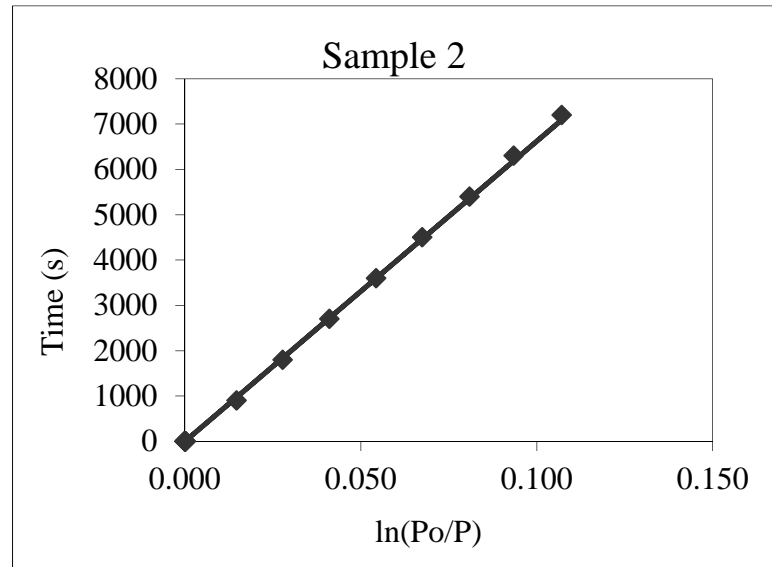
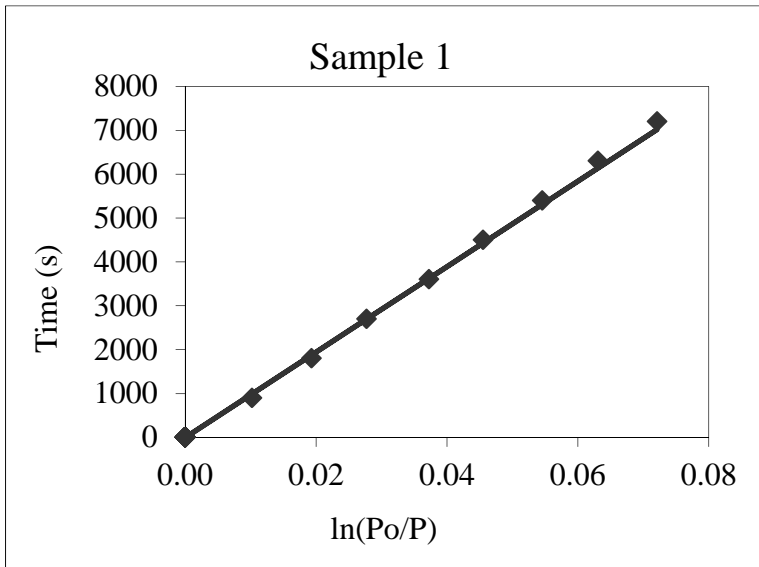
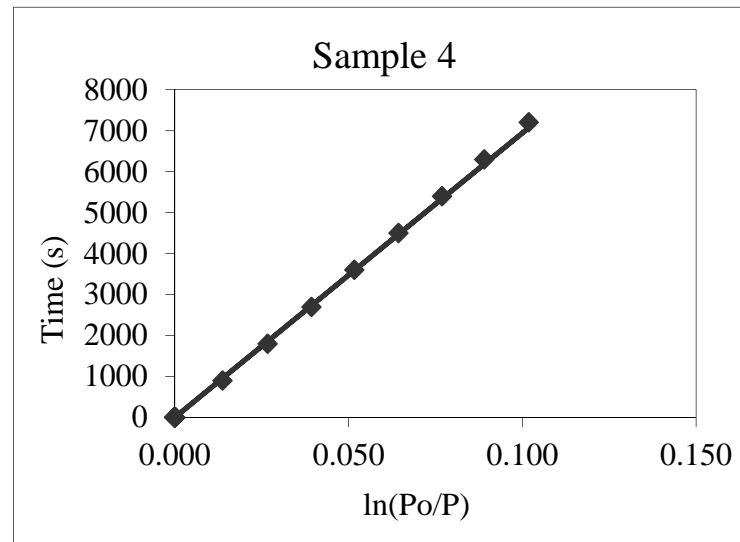
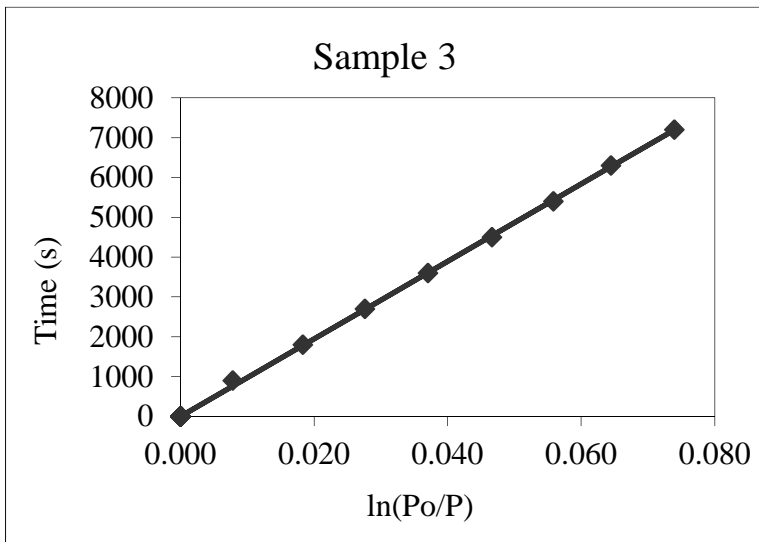
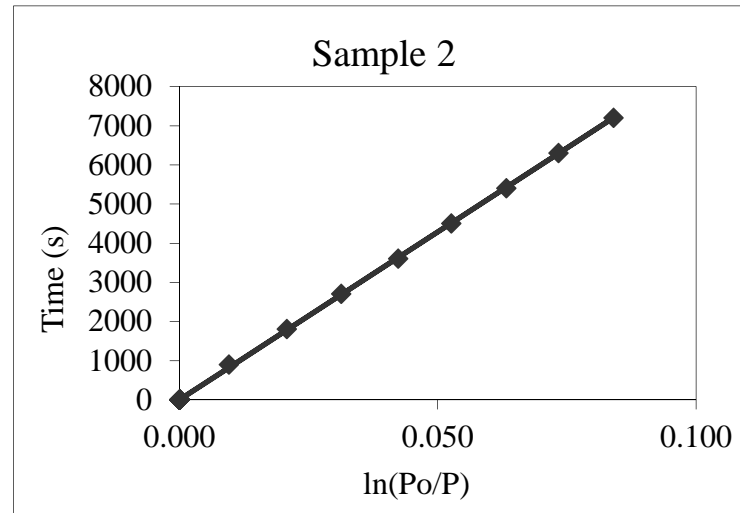
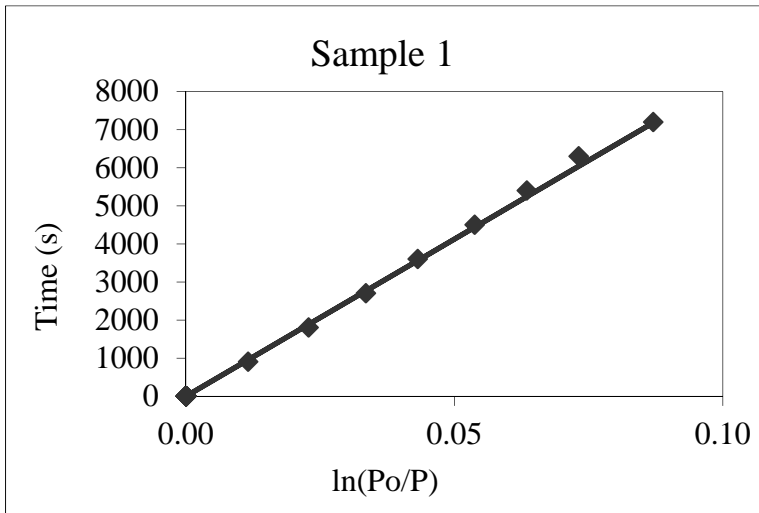


Table B6: Oxygen Permeability Index Results for 15% Replacement

Sample ID:	15 % Replacement			Operator: Daniel			
Date:	13/12/2013						
Average k (m/s):	6.4E-11	COV: 13.1%					
OPI:	10.2						
	33A	33B		36A		36B	
Diameter (mm)	68.17	Diameter (mm)	68.25	Diameter (mm)	67.52	Diameter (mm)	67.52
Thickness (mm)	30.61	Thickness (mm)	31.71	Thickness (mm)	30.51	Thickness (mm)	30.23
k (m/s)	6.24995E-11	k (m/s)	6.319E-11	k (m/s)	5.47E-11	k (m/s)	7.504E-11
r ²	0.9976	r ²	0.9998	r ²	0.9995	r ²	0.9991
Time (hh.min)	Pressure (kPa)	Time (hh.min)	Pressure (kPa)	Time (hh.min)	Pressure (kPa)	Time (hh.min)	Pressure (kPa)
12.48	104.21	12.48	108.13	15.31	102.99	15.31	101.04
13.03	103.01	13.03	107.09	15.46	102.18	15.46	99.67
13.18	101.85	13.18	105.90	16.01	101.12	16.01	98.38
13.33	100.78	13.33	104.80	16.16	100.18	16.16	97.15
13.48	99.81	13.48	103.65	16.31	99.24	16.31	95.96
14.03	98.75	14.03	102.58	16.46	98.30	16.46	94.75
14.18	97.80	14.18	101.50	17.01	97.40	17.01	93.57
14.33	96.86	14.33	100.48	17.16	96.56	17.16	92.44
14.48	95.52	14.48	99.42	17.31	95.65	17.31	91.26



Water Sorptivity Test

Table B7: Water Sorptivity Test for Control

Sample ID:	Control			
Date:	09/10/2013			
Av. Sorptivity:	11.5	COV:	7.6	
Av. Porosity:	13.9	COV:	4.7	
	1A	1B	2A	2B
Diameter (mm)	68.06	68.37	68.19	68.19
Thickness (mm)	33.56	31.94	31.37	30.20
Time (min)	Mass (g)	Mass (g)	Mass (g)	Mass (g)
0	263.44	238.95	227.47	279.91
3	265.16	240.70	228.92	281.53
5	265.58	241.13	229.27	281.89
7	265.93	241.46	229.54	282.16
9	266.22	241.75	229.78	282.41
12	266.60	242.14	230.11	282.73
16	267.03	242.58	230.46	283.10
20	267.42	242.95	230.77	283.42
25	267.84	243.39	231.10	283.79
Saturated Mass (g)	281.48	255.19	242.92	294.58
R ² (Must be >0.98)	0.9999	0.9999	0.9999	0.9999
Range	3-25 min	3-25 min	3-25 min	3-25 min
Sorptivity (mm/hr ^{0.5})	11.8	12.5	10.5	11.0
Porosity (%)	14.8	13.8	13.5	13.3

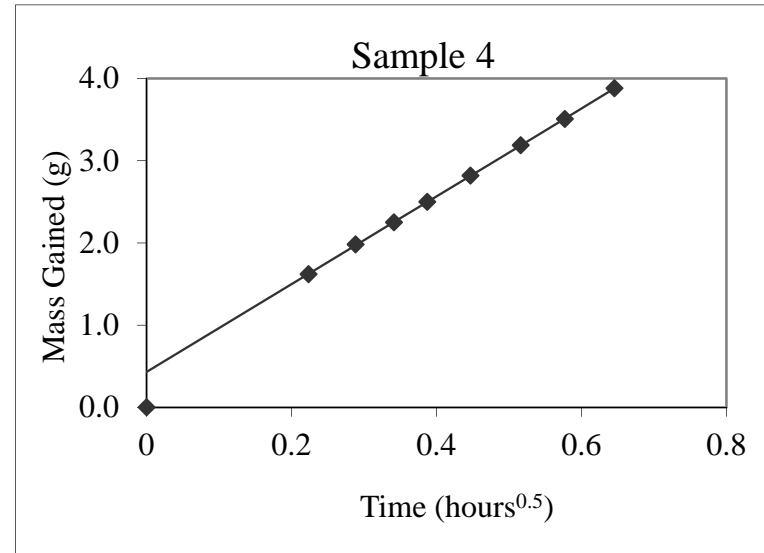
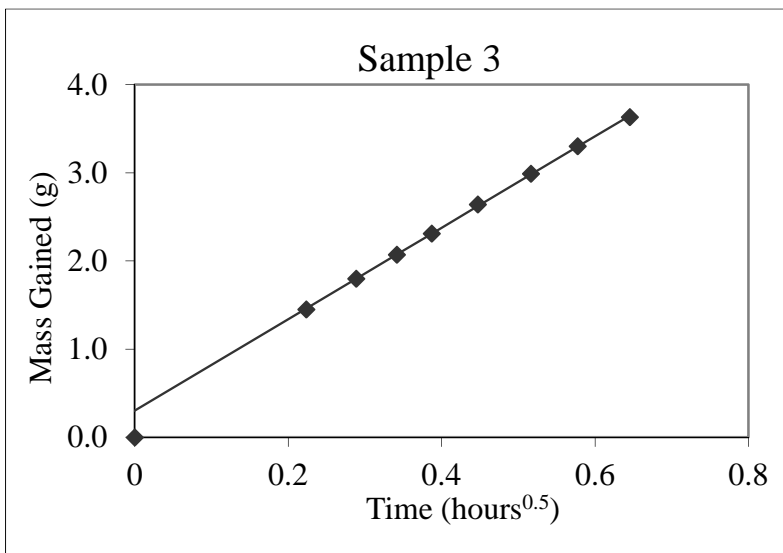
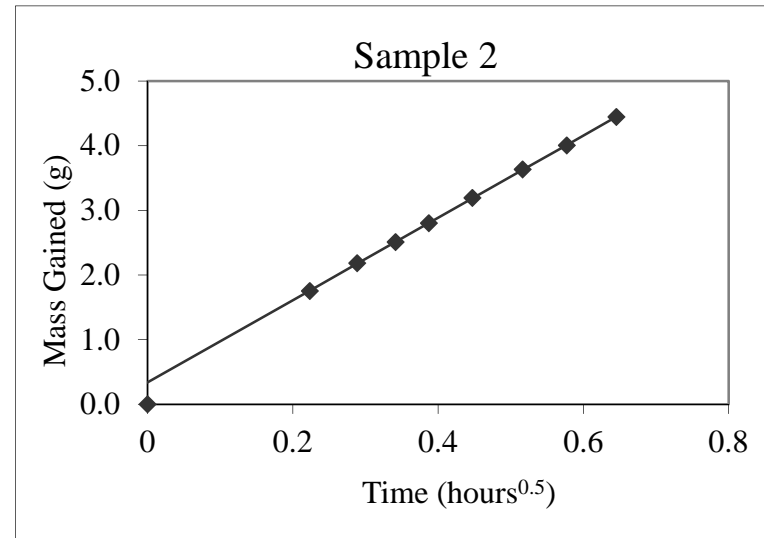
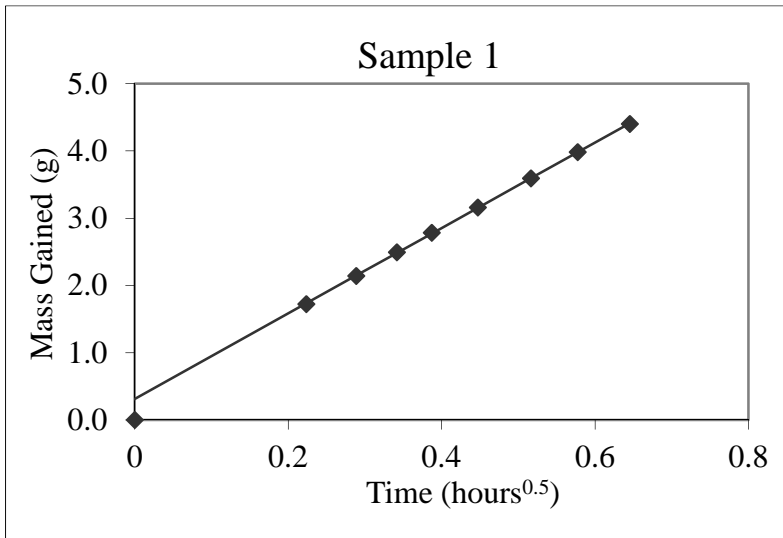


Table B8: Water Sorptivity Test for 2.5% Replacement

Sample ID:	2.5% Replacement			
Date:	09/10/2013			
Av. Sorptivity:	11.0	COV:	6.9	
Av. Porosity:	12.0	COV:	9.0	
	1A	1B	2A	2B
Diameter (mm)	68.25	68.22	68.27	68.32
Thickness (mm)	31.55	30.64	27.39	25.05
Time (min)	Mass (g)	Mass (g)	Mass (g)	Mass (g)
0	250.17	250.57	222.71	203.57
3	251.85	252.01	224.28	205.06
5	252.28	252.33	224.61	205.33
7	252.63	252.59	224.88	205.62
9	252.90	252.77	225.08	205.81
12	253.23	253.03	225.35	206.10
16	253.66	253.34	225.66	206.42
20	253.97	253.58	225.94	206.67
25	254.35	253.84	226.23	206.97
Saturated Mass (g)	265.64	262.72	235.01	214.26
R ² (Must be >0.98)	0.9985	0.9985	0.9984	0.9984
Range	3-25 min	3-25 min	3-25 min	3-25 min
Sorptivity (mm/hr ^{0.5})	12.0	10.9	10.2	10.7
Porosity (%)	13.4	10.8	12.3	11.6

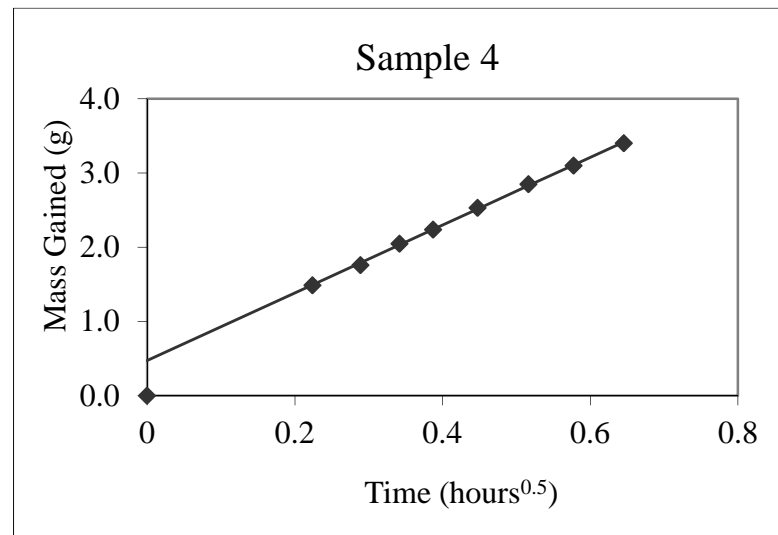
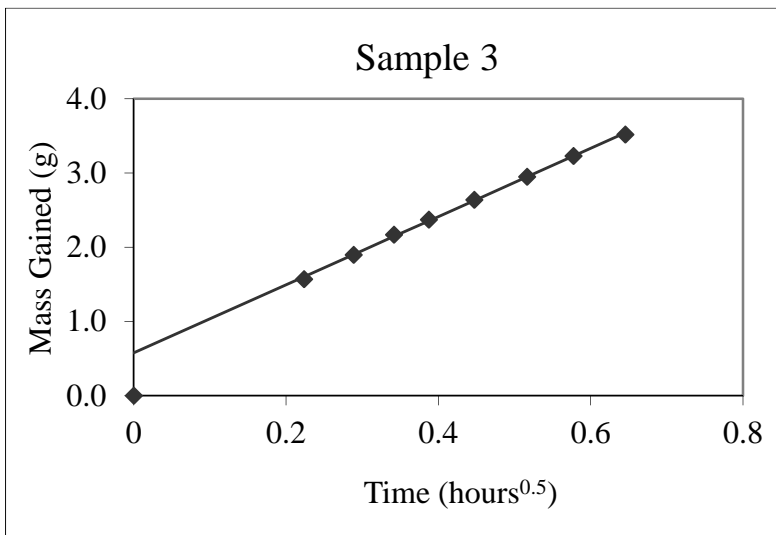
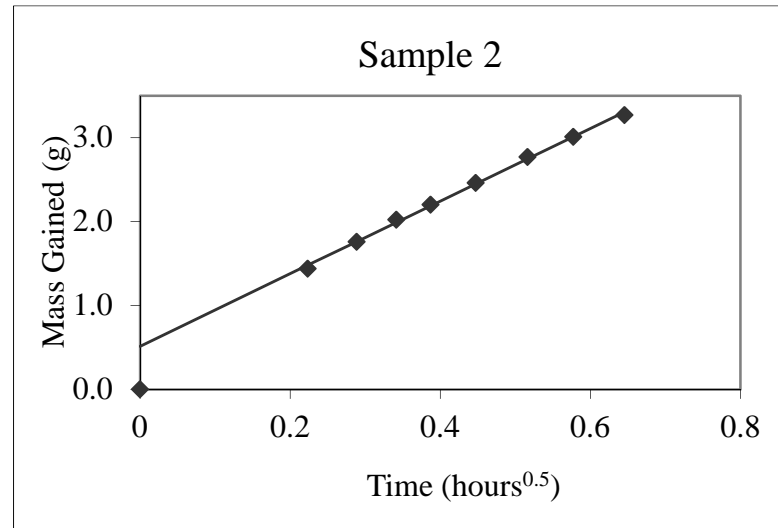
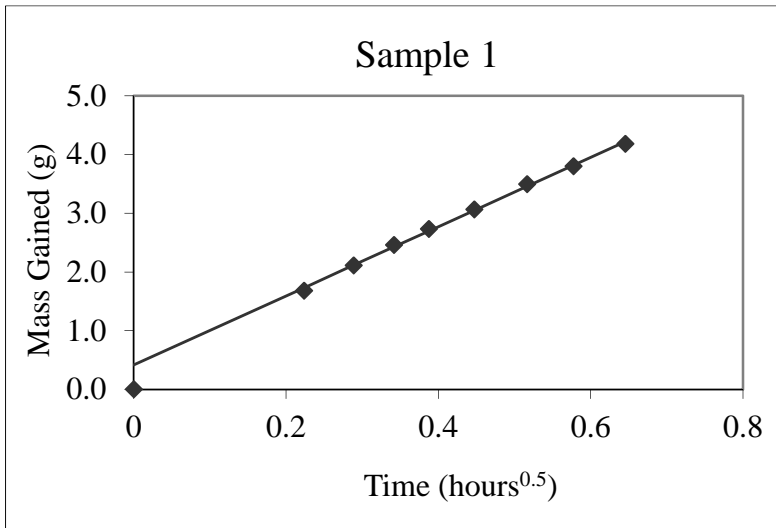


Table B9: Water Sorptivity Test for 5% Replacement

Sample ID:	5% Replacement			
Date:	09/10/2013			
Av. Sorptivity:	10.7	COV:	8.3	
Av. Porosity:	12.3	COV:	5.9	
	1A	1B	2A	2B
Diameter (mm)	68.49	68.32	68.59	68.52
Thickness (mm)	30.31	27.18	30.78	27.05
Time (min)	Mass (g)	Mass (g)	Mass (g)	Mass (g)
0	248.27	219.72	254.01	219.40
3	250.08	221.23	255.41	221.18
5	250.42	221.54	255.67	221.48
7	250.74	221.85	255.91	221.77
9	251.00	222.09	256.10	221.98
12	251.33	222.38	256.36	222.27
16	251.71	222.72	256.62	222.61
20	252.03	223.02	256.87	222.87
25	252.38	223.34	257.15	223.17
Saturated Mass (g)	262.42	232.80	267.17	231.21
R ² (Must be >0.98)	0.9996	0.9996	0.9993	0.9993
Range	3-25 min	3-25 min	3-25 min	3-25 min
Sorptivity (mm/hr ^{0.5})	11.8	10.4	9.7	10.9
Porosity (%)	12.7	13.1	11.6	11.8

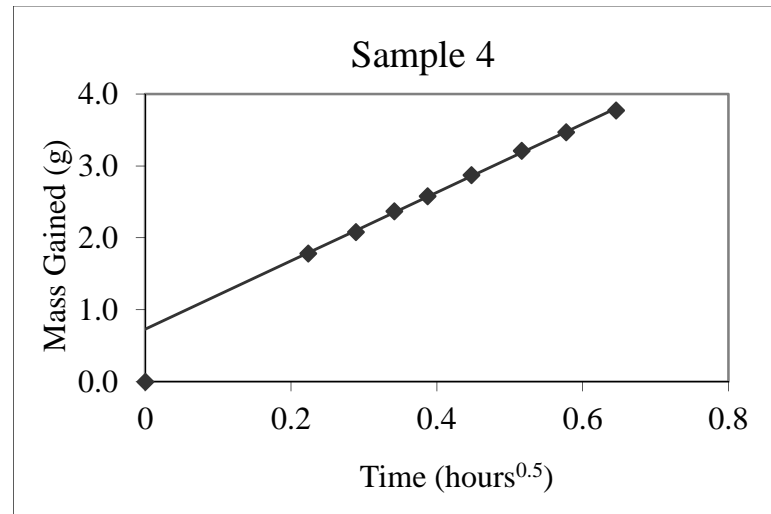
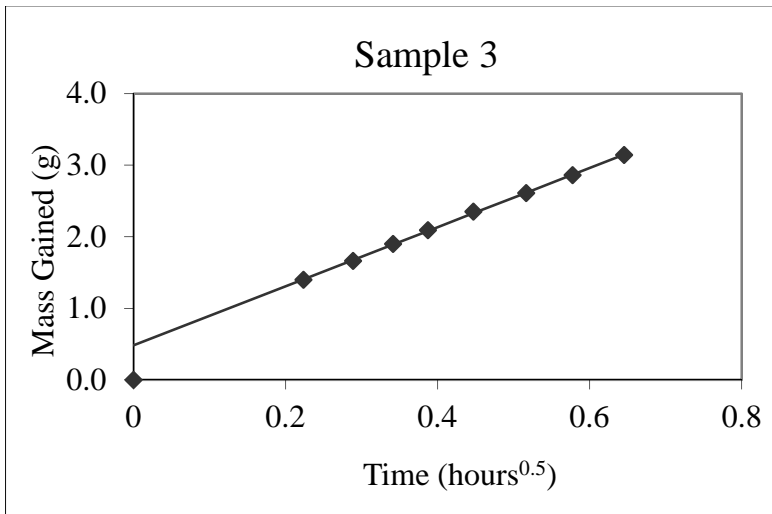
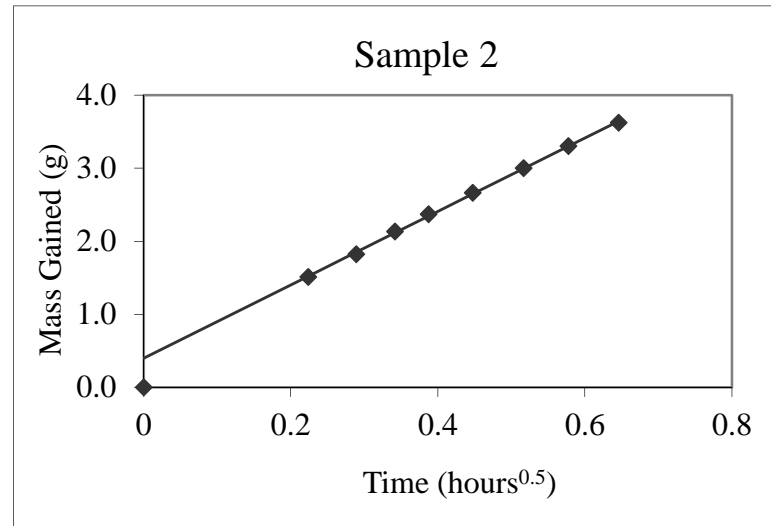
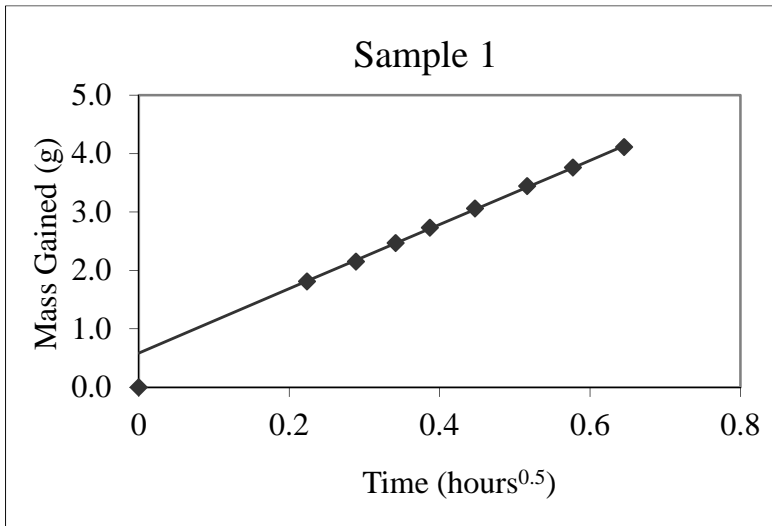


Table B10: Water Sorptivity Test for 10% Replacement

Sample ID:	10% Replacement			
Date:	10/11/2013			
Av. Sorptivity:	10.5	COV:	15.3	
Av. Porosity:	9.9	COV:	5.7	
	1A	1B	2A	2B
Diameter (mm)	68.08	68.10	68.08	68.10
Thickness (mm)	29.86	29.54	29.86	29.54
Time (min)	Mass (g)	Mass (g)	Mass (g)	Mass (g)
0	265.40	263.10	272.70	249.60
3	266.60	264.90	274.10	250.70
5	266.80	265.20	274.30	250.90
7	266.90	265.30	274.60	251.10
9	267.20	265.50	274.80	251.30
12	267.30	265.80	275.10	251.50
16	267.50	266.00	275.30	251.80
20	267.70	266.20	275.60	252.00
25	268.00	266.50	275.90	252.20
Saturated Mass (g)	276.3	274.50	282.9	259.80
R ² (Must be >0.98)	0.9896	0.9896	0.9954	0.9954
Range	3-25 min	3-25 min	3-25 min	3-25 min
Sorptivity (mm/hr ^{0.5})	8.9	9.7	12.6	10.6
Porosity (%)	10.0	10.6	9.4	9.5

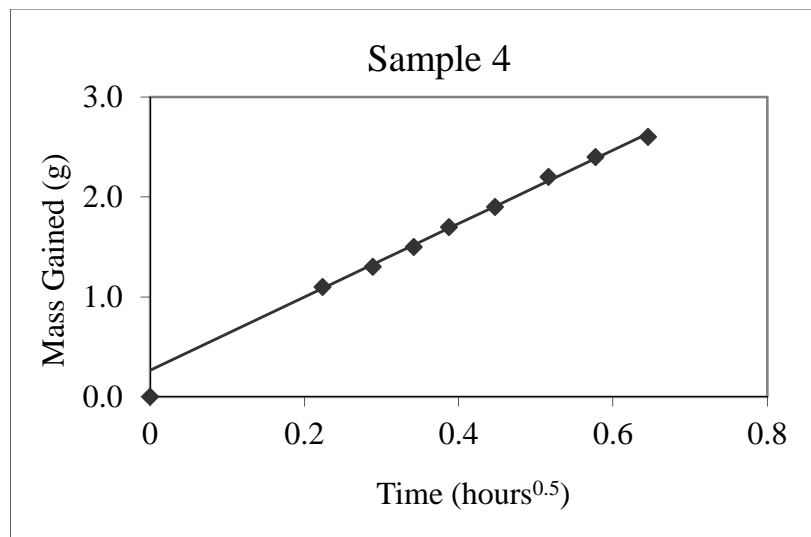
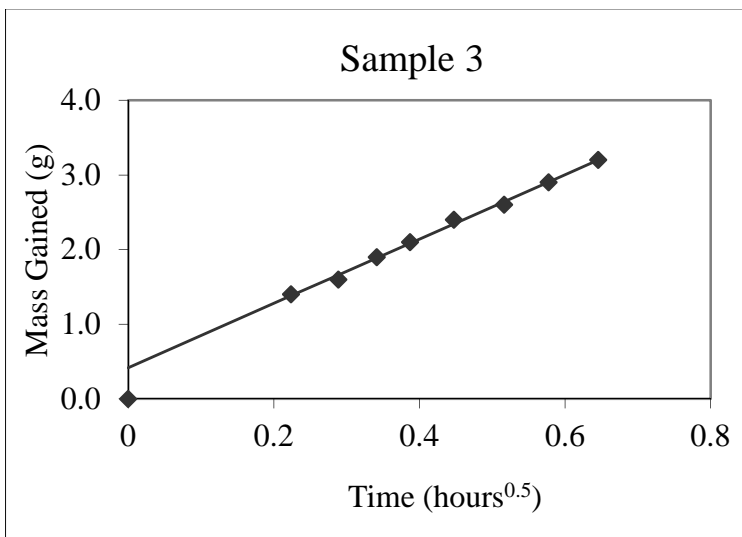
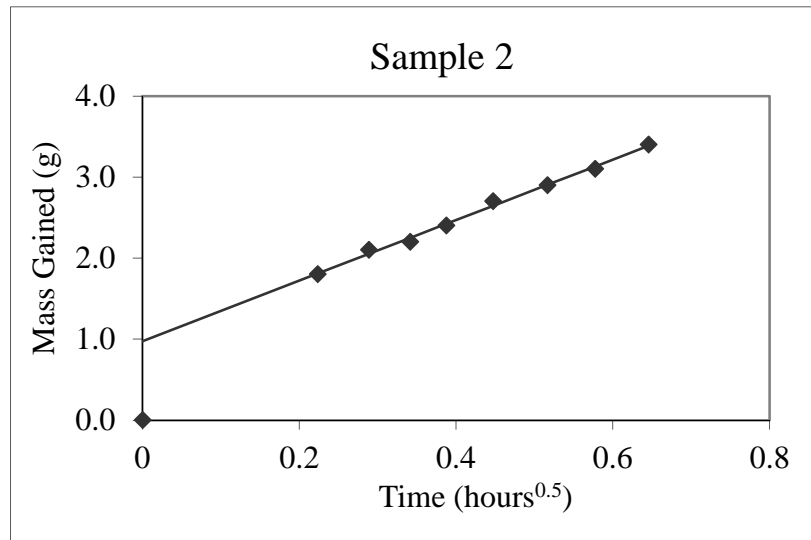
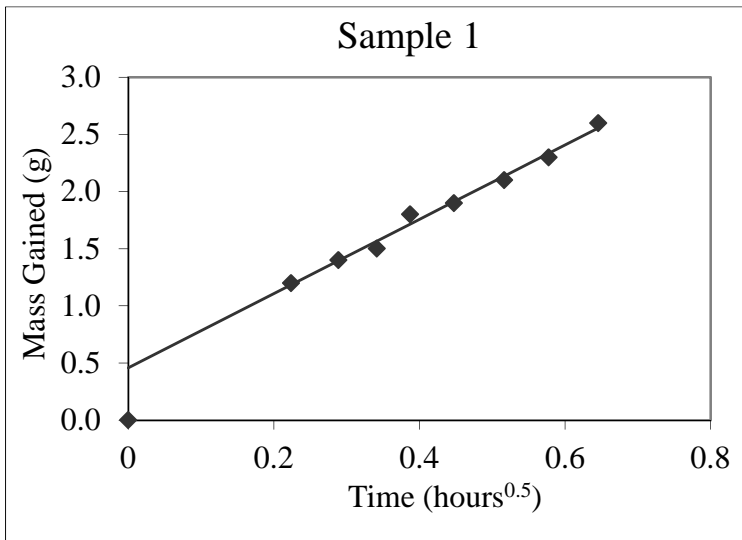
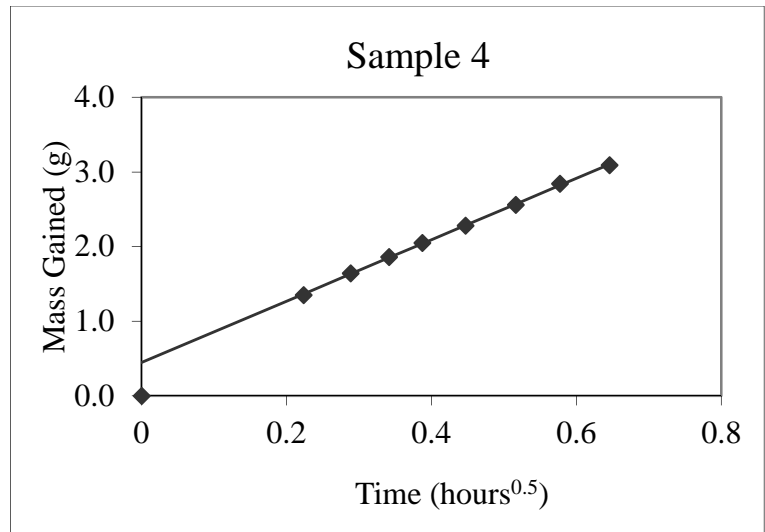
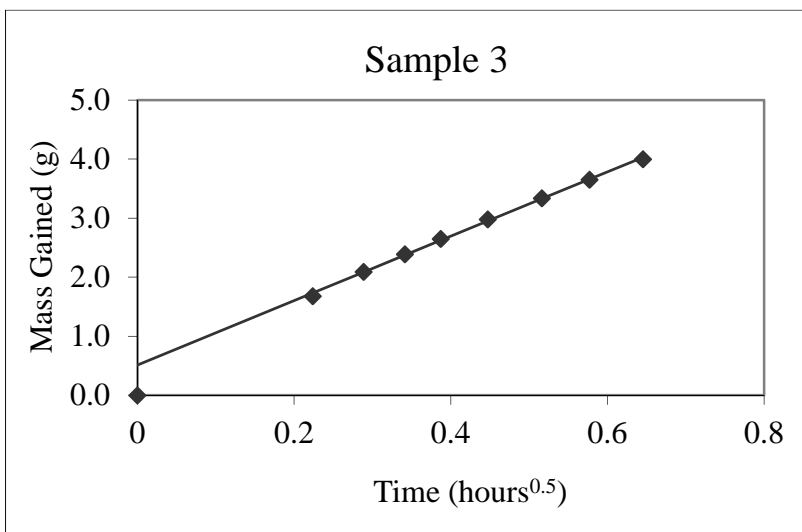
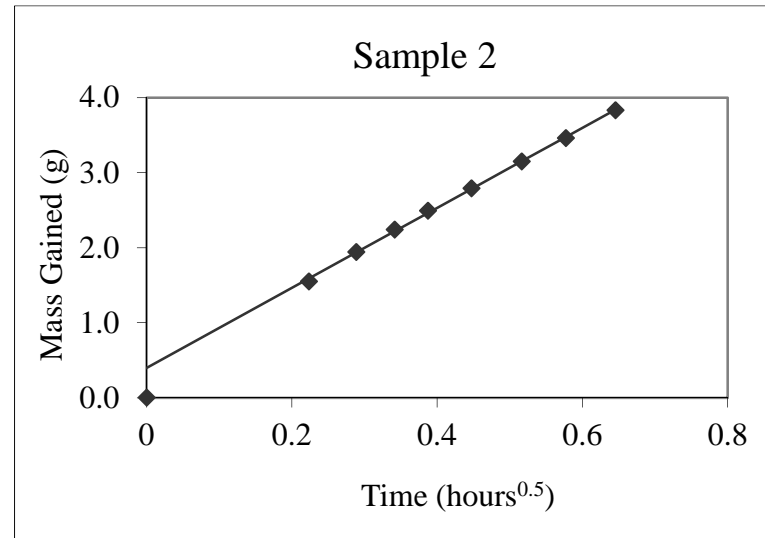
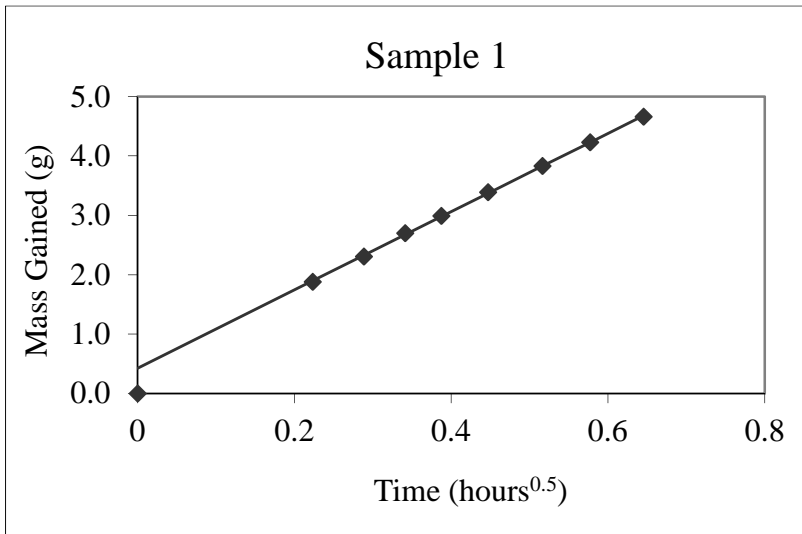


Table B11: Water Sorptivity Test for 15% Replacement

Sample ID:	15% Replacement			
Date:	10/11/2013			
Av. Sorptivity:	10.2	COV:	11.2	
Av. Porosity:	14.2	COV:	11.6	
	1A	1B	2A	2B
Diameter (mm)	68.38	68.48	68.55	68.91
Thickness (mm)	27.82	27.98	27.69	29.31
Time (min)	Mass (g)	Mass (g)	Mass (g)	Mass (g)
0	217.72	220.31	226.04	240.44
3	219.60	221.86	227.72	241.79
5	220.03	222.25	228.13	242.08
7	220.42	222.55	228.43	242.30
9	220.71	222.80	228.69	242.49
12	221.11	223.10	229.02	242.72
16	221.55	223.46	229.38	243.00
20	221.95	223.77	229.69	243.28
25	222.38	224.14	230.04	243.53
Saturated Mass (g)	234.06	235.87	239.63	253.97
R ² (Must be >0.98)	0.9997	0.9997	0.9992	0.9992
Range	3-25 min	3-25 min	3-25 min	3-25 min
Sorptivity (mm/hr ^{0.5})	11.2	9.6	11.1	8.9
Porosity (%)	16.0	15.1	13.3	12.4



Chloride Conductivity

Table B12: Chloride Conductivity Results for Control Sample

Sample 1			Sample 2		
Capillary Voltage (V)	Supply Current (mA)	Chloride Conductivity (mS/cm)	Capillary Voltage (V)	Supply Current (mA)	Chloride Conductivity (mS/cm)
7.66433	0.21171	2.28368	7.76846	0.24202	2.49049
7.39670	0.20482	2.28932	7.41128	0.23134	2.49533
7.17380	0.19891	2.29233	7.22201	0.22587	2.50022
7.02855	0.19502	2.29396	7.17297	0.22459	2.50298
6.95097	0.19306	2.29618	7.15596	0.22430	2.50577
6.91424	0.19217	2.29773	7.14726	0.22425	2.50825
6.88581	0.19151	2.29937	7.14137	0.22426	2.51042
6.87804	0.19139	2.30050	7.13627	0.22538	2.52477
6.87674	0.19146	2.30176	7.13469	0.22435	2.51379
6.88063	0.19165	2.30275	7.13355	0.22446	2.51539
6.88785	0.19193	2.30368	7.13183	0.22459	2.51745
6.89666	0.19226	2.30472	7.13080	0.22463	2.51829
6.89990	0.19244	2.30573	7.12913	0.22467	2.51936
6.89961	0.19249	2.30650	7.12752	0.22473	2.52056
6.89833	0.19254	2.30744	7.12734	0.22484	2.52182
6.92011	0.19322	2.30838	7.12667	0.22482	2.52184
6.94128	0.19386	2.30899	7.12577	0.22492	2.52332
6.94507	0.19401	2.30949	7.12545	0.22493	2.52358
6.94560	0.19409	2.31024	7.12406	0.22490	2.52366
6.95519	0.19439	2.31057	7.12404	0.22492	2.52393
6.94586	0.19420	2.31142	7.12381	0.22523	2.52752
6.93270	0.19390	2.31222	7.12349	0.22529	2.52829
6.94328	0.19426	2.31303	7.12334	0.22532	2.52863
6.94325	0.19424	2.31282	7.12256	0.22634	2.54036
6.94381	0.19424	2.31258	7.12197	0.22637	2.54089
6.94488	0.19437	2.31384	7.12260	0.22644	2.54153
6.94064	0.19426	2.31393	7.12316	0.22646	2.54152
6.93838	0.19427	2.31482	7.12295	0.22648	2.54184
6.94479	0.19445	2.31486	7.12331	0.22668	2.54391
6.95075	0.19466	2.31536	7.12310	0.22655	2.54259
6.96231	0.19504	2.31599	7.12302	0.22657	2.54274
6.95821	0.19495	2.31630	7.12244	0.22663	2.54364
6.96118	0.19511	2.31713	7.12328	0.22663	2.54336
6.95755	0.19502	2.31729	7.12568	0.22674	2.54376

6.96685	0.19532	2.31783	7.12421	0.22666	2.54339
6.96992	0.19539	2.31759	7.12342	0.22671	2.54421
6.96916	0.19538	2.31770	7.12310	0.22667	2.54393
6.97018	0.19542	2.31787	7.12399	0.22671	2.54402
6.96967	0.19547	2.31862	7.12290	0.22674	2.54473
6.97286	0.19561	2.31926	7.12425	0.22680	2.54492
6.97431	0.19570	2.31979	7.12413	0.22682	2.54518
6.97471	0.19574	2.32017	7.12165	0.22669	2.54464
6.97094	0.19582	2.32235	7.12277	0.22668	2.54407
6.96648	0.19573	2.32274	7.12244	0.22659	2.54324
6.97725	0.19601	2.32252	7.11932	0.22657	2.54406
Average:		2.31003			2.52929

Table B13: Chloride Conductivity Results for 2.5% Sample

Sample 1			Sample 2		
Capillary Voltage (V)	Supply Current (mA)	Chloride Conductivity (mS/cm)	Capillary Voltage (V)	Supply Current (mA)	Chloride Conductivity (mS/cm)
7.60628	0.21423	2.10657	7.10856	0.19901	1.91299
7.19825	0.20300	2.10932	6.93047	0.19429	1.91560
7.11079	0.20069	2.11095	6.89345	0.19334	1.91651
7.09027	0.20027	2.11261	6.88681	0.19350	1.91989
7.07671	0.20007	2.11451	6.85396	0.19292	1.92330
7.06618	0.19988	2.11573	6.83772	0.19263	1.92494
7.05198	0.19958	2.11674	6.85056	0.19306	1.92567
6.84718	0.19394	2.11849	6.88090	0.19396	1.92610
6.81033	0.19302	2.11987	6.89042	0.19425	1.92629
6.83659	0.19376	2.11978	6.92760	0.19535	1.92684
6.80872	0.19243	2.11381	6.89218	0.19448	1.92815
6.80598	0.19282	2.11894	6.71300	0.18991	1.93309
6.83406	0.19358	2.11857	6.68217	0.18867	1.92932
6.87710	0.19481	2.11877	6.72291	0.18976	1.92867
6.89294	0.19529	2.11910	6.74506	0.19059	1.93078
6.85377	0.19444	2.12191	6.79900	0.19177	1.92734
6.85025	0.19422	2.12062	6.79372	0.19199	1.93104
6.84996	0.19418	2.12024	6.74643	0.19068	1.93128
6.84767	0.19414	2.12046	6.78270	0.19188	1.93305
6.84148	0.19401	2.12101	6.80338	0.19241	1.93249
6.82806	0.19364	2.12110	6.81195	0.19269	1.93290
6.81928	0.19342	2.12140	6.75249	0.19069	1.92961

6.80135	0.19293	2.12166	6.75581	0.19090	1.93085
6.80988	0.19315	2.12145	6.77848	0.19175	1.93291
6.82240	0.19350	2.12138	6.45576	0.18264	1.93309
6.81891	0.19345	2.12187	6.63051	0.18756	1.93289
6.82346	0.19354	2.12148	6.84176	0.19340	1.93155
6.82191	0.19350	2.12148	6.85549	0.19386	1.93223
6.81720	0.19339	2.12180	6.87469	0.19443	1.93248
6.79886	0.19285	2.12154	6.87117	0.19441	1.93335
6.82766	0.19367	2.12162	6.86752	0.19427	1.93292
6.83107	0.19377	2.12157	6.88454	0.19478	1.93326
6.83108	0.19377	2.12164	6.87989	0.19468	1.93354
6.80941	0.19312	2.12126	6.89855	0.19524	1.93391
6.87770	0.19509	2.12156	6.88868	0.19506	1.93483
6.89608	0.19560	2.12146	6.87414	0.19456	1.93400
6.89048	0.19547	2.12182	6.87448	0.19455	1.93380
6.89005	0.19546	2.12183	6.85091	0.19394	1.93432
6.88918	0.19545	2.12191	6.85575	0.19406	1.93421
6.89006	0.19548	2.12201	6.87423	0.19456	1.93399
6.89167	0.19554	2.12217	6.87066	0.19460	1.93530
6.88846	0.19546	2.12223	6.89788	0.19524	1.93410
6.88758	0.19544	2.12233	6.89821	0.19532	1.93479
6.88668	0.19541	2.12231	6.89301	0.19507	1.93371
6.88654	0.19542	2.12248	6.89610	0.19520	1.93413
Average		2.11959			1.93013

Table B14: Chloride Conductivity Results for 5% Sample

Sample 1			Sample 2		
Capillary Voltage (V)	Supply Current (mA)	Chloride Conductivity (mS/cm)	Capillary Voltage (V)	Supply Current (mA)	Chloride Conductivity (mS/cm)
7.60028	0.16468	1.80448	7.15919	0.16063	1.80223
7.40144	0.16067	1.80785	6.62372	0.14936	1.81127
7.28597	0.15815	1.80768	6.81308	0.15387	1.81403
7.24083	0.15711	1.80701	6.78009	0.15330	1.81611
7.22027	0.15686	1.80932	6.76118	0.15305	1.81826
7.21069	0.15654	1.80800	6.74554	0.15282	1.81975
7.20425	0.15635	1.80742	6.58182	0.14928	1.82177
7.19732	0.15616	1.80700	6.66207	0.15113	1.82213
7.19456	0.15592	1.80482	6.67009	0.15150	1.82445

7.19170	0.15584	1.80465	6.56908	0.14922	1.82458
7.18791	0.15574	1.80449	6.51932	0.14825	1.82660
7.18635	0.15570	1.80436	6.55454	0.14920	1.82836
7.18492	0.15561	1.80370	6.52904	0.14877	1.83026
7.18343	0.15564	1.80444	6.47548	0.14784	1.83386
7.18155	0.15562	1.80468	6.42940	0.14675	1.83341
7.18210	0.15562	1.80448	6.46219	0.14735	1.83158
7.18127	0.15558	1.80423	6.50935	0.14842	1.83149
7.17977	0.15554	1.80414	6.37058	0.14539	1.83320
7.17864	0.15551	1.80413	6.53681	0.14919	1.83328
7.17938	0.15553	1.80413	6.47616	0.14795	1.83505
7.17873	0.15550	1.80393	6.48685	0.14826	1.83578
7.17801	0.15546	1.80371	6.44292	0.14736	1.83711
7.17748	0.15545	1.80374	6.38713	0.14594	1.83536
7.17719	0.15544	1.80366	6.49535	0.14876	1.83959
7.17674	0.15542	1.80354	6.49354	0.14860	1.83819
7.17606	0.15541	1.80354	6.40585	0.14675	1.84011
7.17518	0.15538	1.80352	6.47882	0.14881	1.84492
7.17479	0.15538	1.80354	6.49490	0.14919	1.84500
7.17382	0.15536	1.80357	6.50651	0.14942	1.84457
7.17308	0.15534	1.80348	6.53534	0.15032	1.84749
7.17215	0.15531	1.80347	6.55356	0.15071	1.84714
7.17191	0.15530	1.80340	6.40572	0.14742	1.84858
7.17173	0.15528	1.80321	6.44229	0.14839	1.85010
7.17146	0.15527	1.80312	6.47036	0.14895	1.84905
7.17107	0.15525	1.80297	6.59803	0.15197	1.85012
7.17067	0.15524	1.80292	6.57108	0.15153	1.85226
7.17018	0.15521	1.80270	6.63802	0.15308	1.85239
7.17020	0.15521	1.80276	6.63770	0.15315	1.85324
7.17028	0.15520	1.80257	6.59005	0.15213	1.85425
7.17011	0.15519	1.80252	6.59782	0.15260	1.85779
7.17013	0.15517	1.80231	6.63242	0.15321	1.85545
7.17044	0.15517	1.80220	6.66068	0.15390	1.85592
7.17036	0.15515	1.80199	6.66450	0.15403	1.85644
7.16929	0.15512	1.80190	6.66770	0.15416	1.85711
7.16826	0.15511	1.80209	6.66867	0.15428	1.85823
Average:		1.80416			1.83773

Table B15: Chloride Conductivity Results for 10% Sample

Sample 1			Sample 2		
Capillary Voltage (V)	Supply Current (mA)	Chloride Conductivity (mS/cm)	Capillary Voltage (V)	Supply Current (mA)	Chloride Conductivity (mS/cm)
6.90919	0.13516	1.57979	6.71930	0.13208	1.44157
6.88762	0.13437	1.57549	6.77504	0.13354	1.44552
6.85588	0.13358	1.57341	6.69024	0.13173	1.44402
6.86711	0.13368	1.57202	6.83676	0.13463	1.44416
6.87109	0.13365	1.57074	6.78482	0.13335	1.44141
6.87710	0.13354	1.56815	6.82440	0.13408	1.44085
6.87828	0.13356	1.56812	6.84722	0.13454	1.44097
6.88109	0.13344	1.56604	6.88026	0.13547	1.44402
6.88497	0.13351	1.56600	6.88811	0.13563	1.44410
6.88505	0.13335	1.56406	6.89921	0.13596	1.44523
6.89244	0.13149	1.54059	6.87089	0.13526	1.44375
6.89047	0.13141	1.54017	6.85531	0.13530	1.44745
6.89124	0.13091	1.53405	6.83614	0.13483	1.44646
6.87782	0.13319	1.56384	6.83840	0.13472	1.44484
6.88144	0.13318	1.56289	6.86194	0.13500	1.44289
6.87673	0.13296	1.56145	6.86209	0.13485	1.44116
6.86248	0.13264	1.56089	6.85577	0.13505	1.44470
6.86998	0.13275	1.56053	6.87068	0.13525	1.44372
6.86984	0.13250	1.55756	6.92676	0.13628	1.44287
6.87116	0.13246	1.55685	6.87414	0.13514	1.44175
6.85324	0.13208	1.55643	6.90279	0.13572	1.44195
6.86801	0.13226	1.55512	6.91722	0.13600	1.44187
6.87138	0.13227	1.55447	6.91477	0.13573	1.43952
6.87640	0.13227	1.55341	6.92193	0.13556	1.43621
6.88021	0.13231	1.55297	6.92480	0.13588	1.43905
6.88291	0.13229	1.55210	6.91587	0.13567	1.43870
6.88756	0.13237	1.55203	6.93526	0.13572	1.43521
6.89114	0.13241	1.55174	6.92566	0.13557	1.43560
6.89449	0.13242	1.55109	6.93616	0.13582	1.43604
6.89593	0.13240	1.55055	6.94519	0.13452	1.42045
6.89731	0.13238	1.54992	6.94266	0.13400	1.41546
6.89978	0.13206	1.54560	6.91811	0.13303	1.41026
6.90129	0.13192	1.54369	6.93165	0.13294	1.40651
6.90363	0.13191	1.54305	6.94281	0.13264	1.40111
6.90251	0.13189	1.54307	6.93822	0.13247	1.40026

6.90314	0.13191	1.54316	6.93329	0.13220	1.39839
6.90294	0.13188	1.54289	6.93788	0.13243	1.39992
6.90305	0.13182	1.54217	6.95967	0.13277	1.39906
6.90282	0.13179	1.54181	6.91645	0.13219	1.40168
6.90338	0.13179	1.54174	6.96055	0.13268	1.39794
6.90387	0.13173	1.54093	6.94225	0.13224	1.39695
6.90422	0.13173	1.54083	6.94880	0.13249	1.39833
6.90367	0.13171	1.54070	6.92928	0.13200	1.39707
6.90314	0.13168	1.54048	6.94331	0.13231	1.39756
6.90278	0.13165	1.54019	6.95477	0.13254	1.39764
Average:		1.55362			1.42787

Table B16: Chloride Conductivity Results for 15% Sample

Sample 1			Sample 2		
Capillary Voltage (V)	Supply Current (mA)	Chloride Conductivity (mS/cm)	Capillary Voltage (V)	Supply Current (mA)	Chloride Conductivity (mS/cm)
6.99804	0.12938	1.38672	7.09060	0.10687	1.18415
6.93009	0.12833	1.38903	6.94457	0.10411	1.17788
6.83125	0.12650	1.38899	6.71694	0.10509	1.22930
6.61727	0.12258	1.38948	6.76156	0.10529	1.22348
6.83422	0.12707	1.39468	6.80536	0.10579	1.22138
6.79464	0.12580	1.38869	6.81705	0.10578	1.21914
6.84022	0.12650	1.38718	6.79320	0.10564	1.22180
6.90862	0.12796	1.38933	6.85778	0.10643	1.21930
6.90183	0.12774	1.38824	6.80589	0.10564	1.21952
6.88584	0.12752	1.38913	6.83275	0.10593	1.21809
6.91054	0.12792	1.38851	6.91981	0.10714	1.21650
6.88763	0.12753	1.38880	6.88409	0.10653	1.21587
6.89605	0.12774	1.38946	6.89130	0.10662	1.21556
6.88786	0.12758	1.38936	6.89681	0.10672	1.21571
6.90363	0.12791	1.38971	6.99836	0.10819	1.21462
6.92782	0.12837	1.38990	6.88998	0.10653	1.21479
6.92415	0.12831	1.38993	6.90990	0.10669	1.21311
6.91166	0.12809	1.39003	6.91983	0.10683	1.21294
6.87747	0.12743	1.38982	6.93193	0.10700	1.21279
6.89487	0.12775	1.38975	6.94553	0.10721	1.21273
6.91218	0.12812	1.39026	6.82093	0.10524	1.21229
6.91214	0.12808	1.38990	6.85512	0.10582	1.21285

6.92252	0.12826	1.38970	6.87868	0.10615	1.21246
6.93852	0.12859	1.39013	6.89857	0.10647	1.21259
6.91408	0.12816	1.39032	6.91342	0.10667	1.21229
6.92413	0.12842	1.39116	6.93038	0.10686	1.21150
6.94792	0.12883	1.39081	6.90230	0.10643	1.21146
6.94375	0.12878	1.39105	6.88293	0.10614	1.21161
6.94129	0.12872	1.39100	6.87902	0.10608	1.21163
6.94501	0.12875	1.39055	6.89096	0.10627	1.21163
6.90841	0.12816	1.39151	6.87496	0.10601	1.21150
6.94159	0.12872	1.39092	6.86695	0.10589	1.21154
6.93691	0.12868	1.39135	6.89627	0.10636	1.21173
6.94212	0.12874	1.39104	6.91951	0.10668	1.21134
6.92874	0.12850	1.39108	6.90887	0.10659	1.21212
6.92914	0.12850	1.39105	6.94092	0.10707	1.21200
6.92422	0.12842	1.39109	6.89949	0.10646	1.21238
6.91718	0.12831	1.39132	6.89043	0.10633	1.21246
6.92289	0.12840	1.39119	6.81207	0.10510	1.21216
6.91953	0.12826	1.39038	6.95056	0.10716	1.21130
6.90603	0.12810	1.39132	6.50308	0.10074	1.21713
6.93601	0.12860	1.39074	6.50055	0.10059	1.21583
6.93410	0.12859	1.39094	6.68436	0.10360	1.21777
6.93503	0.12861	1.39099	6.63518	0.10280	1.21726
6.93756	0.12863	1.39077	6.66553	0.10326	1.21721
Average:		1.39016			1.21339

Sulphate Attack Results

Table B17: Detailed Sulphate Attack Results

	Control				2.50%				5%			
Samples	Casted	16-08	Tested	30-08	Casted	18-08	Tested	01-09	Casted	16-08	Tested	04-09
	Water Curing		Sulphate Solution		Water Curing		Sulphate Solution		Water Curing		Sulphate Solution	
	Weight	Load	Weight	Load	Weight	Load	Weight	Load	Weight	Load	Weight	Load
1	2378.7	422	2391.7	390	2400.6	394	2311.7	362	2508.8	366	2578.4	356
2	2395.5	420	2389	386	2456	395	2451.2	368	2637.8	379	2601.0	350
Average	2387.1	421	2390.35	388	2428.3	394.5	2381.45	365	2573.3	372.5	2589.7	353
	tested	27-08				29-08						
1	2428.1	515	2415.3	540	2477	470	2457	480	2345.5	453	2423.5	480
2	2450.0	517	2423.6	530	2393	460	2455	485	2436	450	2300	472
Average	2439.05	516	2419.45	535	2435	465	2456	482.5	2390.75	451.5	2361.75	476
1	2371.2	595.0	2488.6	560.0	2734.6	568.0	2411.5	542.0	2461.7	560.0	2463.0	534.0
2	2412.3	580.0	2417.4	558.0	2397.3	565.0	2403.7	550.0	2457.5	558.0	2425.5	530.0
3	2460.0	584.0	2459.5	550.0	2407.0	570.0	2476.9	545.0	2477.8	550.0	2486.9	540.0
Average	2414.5	586.3	2455.2	556.0	2513.0	567.7	2430.7	545.7	2465.7	556.0	2458.5	534.7

	10%				15%			
Samples	Casted	18-08	Tested	21-09	Casted	18-08	Tested	21-09
	Water Curing		Sulphate Solution		Water Curing		Sulphate Solution	
	Weight	Load	Weight	Load	Weight	Load	Weight	Load
1	2584.7	356	2492.7	346	2441.7	334	2417.2	326

2	2523.2	362	2484.4	346	2438	330	2427.4	320
Average	2553.95	359	2488.55	346	2439.85	332	2422.3	323
1	2584.7	404	2492.7	420	2508.8	380	2578.4	400
2	2523.2	400	2484	426	2637.8	384	2601	406
Average	2553.95	402	2488.35	423	2573.3	382	2589.7	403
1	2459.5	520.0	2558.1	516.0	2538.3	500.0	2626.2	485.0
2	2505.1	526.0	259.1	506.0	2445.6	510.0	2560.9	490.0
3	2551.5	513.0	250.5	500.0	2569.1	505.0	2485.1	505.0
Average	2505.4	519.7	1022.6	507.3	2517.7	505.0	2557.4	493.3